AJSTD

Vol. 29, No. 1, June 2012
ISSN 0217-5460

A Journal of the ASEAN Committee on Science & Technology

ASEAN JOURNAL ON SCIENCE & TECHNOLOGY FOR DEVELOPMENT

ABOUT THE ASEAN JOURNAL ON SCIENCE AND TECHNOLOGY FOR DEVELOPMENT

The ASEAN Journal on Science and Technology for Development is a refereed Journal of the ASEAN Committee on Science and Technology (ASEAN COST). It reports on science and technology policies and programmes, and research activities undertaken by COST in support of social and economic development of the ASEAN member countries.

The coverage is focused but not limited to, the main areas of activity of ASEAN COST, namely, Biotechnology, Non-Conventional Energy Research, Materials Science and Technology, Marine Sciences, Meteorology and Geophysics, Food Science and Technology, Microelectronics and Information Technology, Space Applications, and Science and Technology Policy, Infrastructure and Resources Development.

ABOUT THE ASEAN COMMITTEE ON SCIENCE AND TECHNOLOGY

The ASEAN Committee on Science and Technology was established to strengthen and enhance the capability of ASEAN in science and technology so that it can promote economic development and help achieve a high quality of life for its people. Its terms and reference are:

- to generate and promote development of scientific and technological expertise and manpower in the ASEAN region.
- to facilite and accelerate the transfer of scientific and technological development among ASEAN countries and from more advanced regions of the world to the ASEAN region.
- to provide support and assistance in the development and application of research discoveries and technological practices of endogenous origin for the common good, and in the more effective use of natural resources available in the ASEAN region and in general, and
- to provide scientific and technological support towards the implementation of existing and future ASEAN projects.

Information on the activities of ASEAN COST can be obtained at its website http://www.asnet.org

DISCLAIMER

While every effort is made to see that no inaccurate or misleading data, opinion or statement appears in the Journal, articles and advertisements in the Journal are the sole responsibility of the contributor or advertiser concerned. They do not necessarily represent the views of the editors, the editorial board nor the editorial advisory committee. The editors, the editorial board and the editoria advisory committee and their respective employees, officers and agents accept no responsibility or liability whatsoever for the consequences of any inaccurate or misleading data, opinion or statement.

Editorial Board

Publisher

Universiti Putra Malaysia Press

Contents

ASEAN J. Sc. Technol. Dev.
Volume 29(1), 2012

ASEAN J. Sci. Technol. Dev., **29(1)**, 1 – 12

Performance Evaluation of a UASB Reactor Using Dairy Wastes

A. ALI[1]*, S. KHAN[2], A. N. KHAN[2], A. ALI[1], S. A. KHAN[1] AND K. A. KHAN[1]
[1]*National University of Sciences and Technology, Islamabad (MCE-NUST), Pakistan*
[2]*University of Engineering and Technology, Peshawar*

A UASB reactor of 6-litre capacity, made of acryl material, was operated continuously for 20–22 weeks in three different phases, using actual dairy mill effluent at a constant mesophilic temperature and neutral pH. The dairy wastewater was highly alkaline, turbid and milky in colour with a bad odour. The average COD and BOD concentrations of the dairy mill effluent were observed to be 2945 mg/l and 1070 mg/l, respectively. Phase I was the start-up phase, with OLR of 0.13 g COD/l.d. SLR, effluent VFAs, effluent TSS, biogas production and methane composition observed during this phase were 1.4 g COD/g VSS.d, 1240 mg/l, 240 mg/l, 1.74 l/COD_{rem}.d, and 62%, respectively. The overall observed biomass yield was found to be equal to 0.034 g VSS/g COD_{rem}. During phase II, the optimum pH was determined to be 6.8–7.1. In the last phase, phase III, the effects of OLR and HRT were observed. The optimum OLR and HRT were observed to be 4.76 g COD/l.d and 16 h, respectively. Correspondingly the COD removal efficiency, effluent VFA and TSS concentrations, and the amount of biogas production were observed to be 78%, 770 mg/l, 300 mg/l and 2.07 l/COD_{rem}.d, respectively. The results of this study suggest that a UASB reactor is an effective tool and viable option for reducing pollution from dairy mill effluent.

Key words: Dairy mill effluent; UASB reactor; COD; biogas; anaerobic digestion, OLR, HRT, pollution; treatment efficiency; wastewater

Nomenclature

COD	Chemical oxygen demand
BOD	Biochemical oxygen demand
HRT	Hydraulic retention time
OLR	Organic loading rate
CNP	Carbon-nitrogen-phosphorus
VFA	Volatile fatty acids
TSS	Total suspended solids
SLR	Solid loading rate
UASB	Up-flow anaerobic sludge blanket

Pakistan is a water-stressed nation, where per capita water availability is decreasing very rapidly due to many reasons, such as environmental pollution and improper water management.–Furthermore, its existing water sources are also being polluted at an alarming rate due to the disposal of untreated domestic and industrial effluents into surface water sources (Pak-EPA 1999). Agricultural run-off too is a major cause of water pollution. Due to

* Corresponding author (e-mail: aliarshad08@yahoo.com)

these factors, safe drinking water is available only to a limited proportion of the population, *viz*. about 20% (PCRWR 2005).

Different physio-chemical and biological methods have been developed for waste reduction. Due to the relatively high capital cost of the physical units, their use is not much encouraged for treatment on a large scale; thus, the biological methods are mostly preferred. Biological treatment is of two main types, namely aerobic and anaerobic. For developing countries, the anaerobic process is ideal because of their lower input of energy and nutrient requirements (Bhatti *et al*. 1996, Savant *et al*. 2005). The use of anaerobic technology is widely known for its simple design, compact structure, and low operational and maintenance costs. They can be used for the treatment of a variety of domestic and industrial effluents (Lettinga *et al*. 1984).

There are several anaerobic units operating throughout the world for the treatment of various types of pollutants. Their treatment efficiency in terms of pollution reduction is highly acknowledged (Hulshoff 1986; Schellinkhout 1993). However, treatability performance of the UASB reactor, using actual highly alkaline dairy mill wastes at the mesophilic temperature range still seems to be not convincing enough because the results from available studies do not precisely indicate the effects of the organic loading rate (OLR) and the hydraulic retention time (HRT) on COD reduction and biogas yield in the kinds of wastewater studied (Orhon 1993; Ozturk 1992). Therefore, this specific study was conducted in a single-stage UASB reactor, by using actual dairy mill effluent. The main objectives of the study were to evaluate the treatability performance of the anaerobic digestion system at varying OLR and HRT, and to determine the biogas production potential of a local dairy mill.

MATERIALS AND METHODS

UASB Reactor

A UASB rector of 6-litre capacity, made of acryl material, was used in the study. The

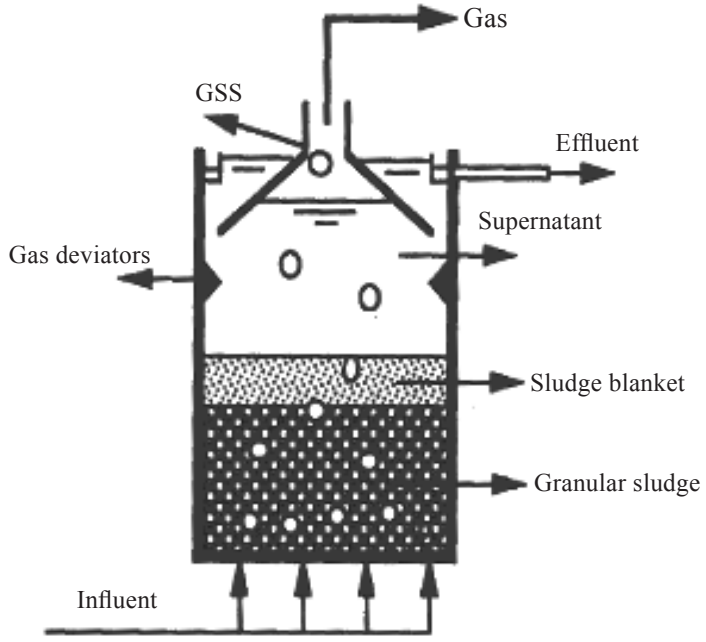

Figure. 1. Systematic diagram of a UASB reactor.

reactor was equipped with a water jacket to maintain a constant required temperature. It was also provided with a proper gas solid separator (GSS) and a mixer device to facilitate the mixing of the biomass and the substrate (Bhatti 1995). A systematic diagram of the UASB reactor is shown in *Figure 1*.

Substrate and Nutrients

Actual dairy mill effluent was used in the study as the sole carbon source for the reactor. Nitrogen and phosphorous were added in the form of $(NH_4)_2SO_4$ and KH_2PO_4, respectively, in accordance with the C:N:P ratio of 350:5:1. Trace nutrients were also added in the concentrations shown in *Table 1* (Lettinga *et al*. 1980).

Table 1. Concentrations of the trace nutrients.

Trace Nutrient	Concentration (mg/l)
$FeCl_3.6H_2O$	4.90
$CoCl_2.6H_2O$	0.30
$ZnSO_4$	0.35
$CaCl_2.2H_2O$	0.35
$CuSO_4$	0.09

Wastewater Characteristics of the Dairy Mill

The wastewater characteristics of the nearby dairy mill were studied by collecting various composite and representative samples from it. The data obtained are shown in *Table 2*. The findings indicate that the dairy mill discharged highly polluting effluent, both in terms of physic-chemical and aesthetic parameters. The samples were highly turbid and milky in colour with a bad odour. The average COD and BOD concentrations were recorded as 2945 mg/l and 1070 mg/l, respectively.

Operating Conditions of the Reactor

The UASB reactor was operated for 20–22 weeks in three different phases. In Phase I, the reactor was started up by seeding the dairy mill effluent with a granular sludge which had been developed in a laboratory-scale reactor from domestic wastes. This acclimatization phase took about 3–4 weeks. During Phase II, the optimum pH was established for the maximum treatment performance of the reactor using dairy mill effluent. This phase lasted about 5–6 weeks. Finally in Phase III of the project, the effects of the engineering parameters, such as OLR and HRT, were studied for a period of 9–10 weeks.

Monitoring and Analysis

pH, temperature, influent and effluent CODs, effluent VFA and TSS concentrations, biogas yield and methane composition were monitored regularly, i.e. 2–3 times weekly. Gas was collected over tap water saturated with NaCl.

Table 2. Wastewater characteristics of the dairy mill.

Parameter	Value	NEQS* limits
Turbidity (NTU)	1.4	–
Colour	Highly turbid/milky	–
Odour	Objectionable	–
pH	8.23	6–10
BOD (mg/l)	1070	80
COD (mg/l)	2945	150
Iron (mg/l)	0.03	–
Nitrates (mg/l)	10.09	–

*NEQS = National Environment Quality Standards

All analyses were carried out using standard analytical procedures (AWWA 2005).

RESULTS AND DISCUSSION

Phase I (Start-up of the Reactor)

The reactor was started with an influent COD concentration of 200 mg/l and at HRT of 36 h, corresponding to OLR of 0.13 g COD/l.d. The influent COD concentration was increased stepwise, in order to avoid sudden volumetric shocks to the reactor, to the level of 3000 mg/l at a constant HRT of 36 h. The final OLR during this phase was recorded as 2.0 g COD/l.d. During this phase, the average temperature and pH were observed to be 32°C and 7.0, respectively. Initially the reactor was started with OLR of 0.13 g COD/l.d, but it was increased gradually to 2.0 g COD/l.d in the last stages of Phase I. During this time period, HRT was kept constant as far as possible at 36 h.

The percentage of COD removal was observed against the influent COD during Phase I, and the treatability performance of the reactor during this phase was quite successful, being more than 80% on average, as shown in *Figure 2*. Maximum COD removal was observed on the 22nd day of operation when the influent COD concentration was about 2200 mg/l, corresponding to an OLR of 1.82 g COD/l.d. The results at this stage indicate that the acclimatization process was going on very well with the passage of time, and that the substrate and the operating conditions were helpful for the granulation process.

The time courses of SLR (g COD/g VSS.d), effluent VFA and TSS concentrations, production of biogas and methane content of the biogas during Phase I of the study are shown in Figures 3–7, respectively. The average values obtained during this phase of the study for SLR, effluent VFAs, effluent TSS, biogas production and methane composition were 1.4 g COD/g VSS.d, 1240 mg/l, 240 mg/l, 1.74 l/COD_{rem}.d and 62%, respectively. The overall observed biomass yield after about 4 weeks of the study was calculated as:

$$Y_{obs} = \sum X \text{ (total biomass produced, g VSS)} / \sum S \text{ (total substrate removed, g COD)}. \quad (1)$$

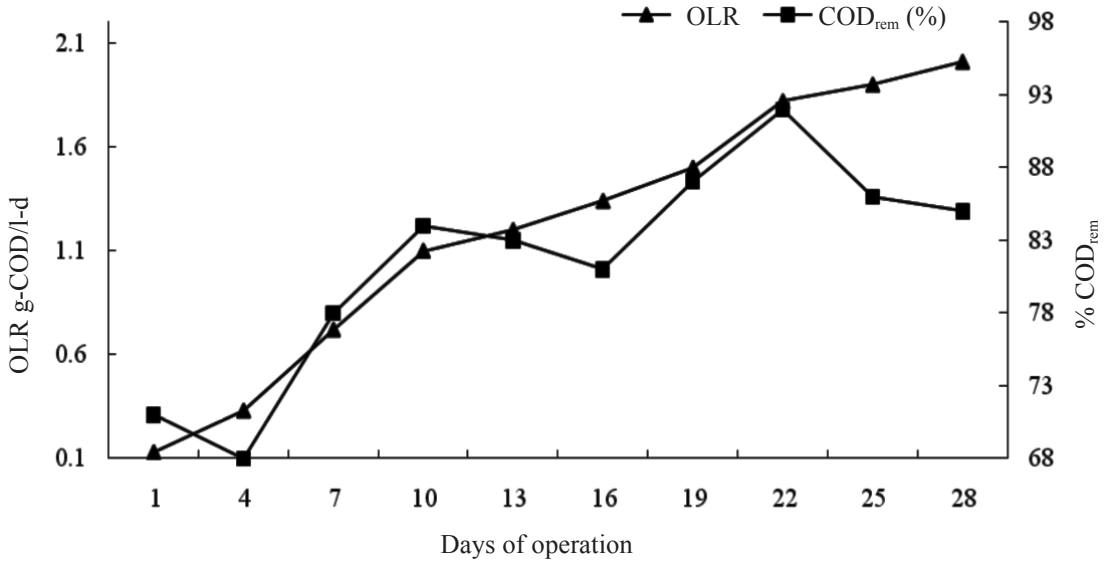

Figure 2. Time course of OLR and COD removal during Phase-I.

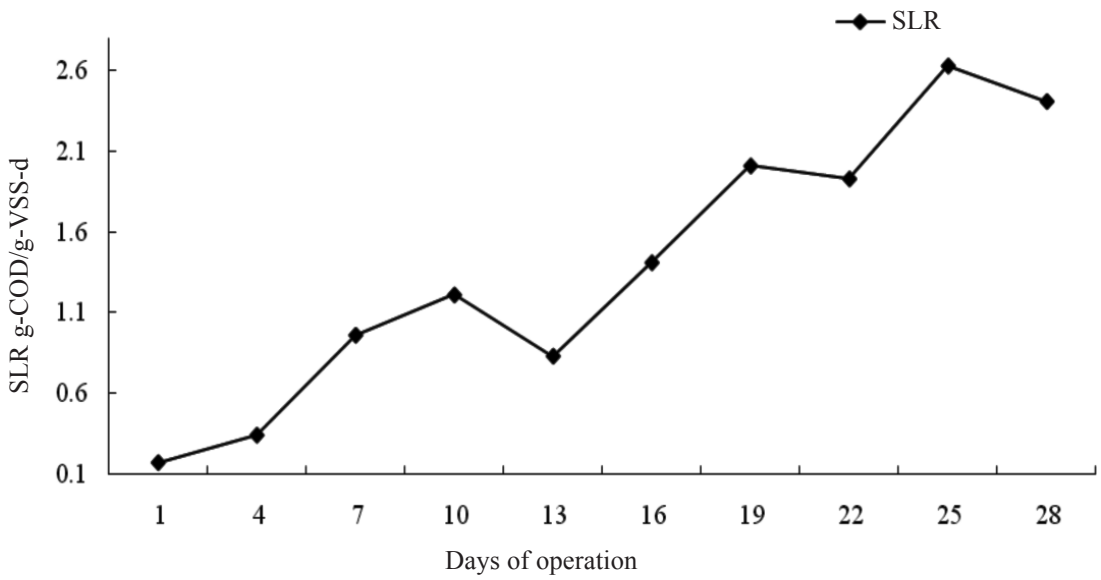

Figure 3. Time course of SLR during Phase-I.

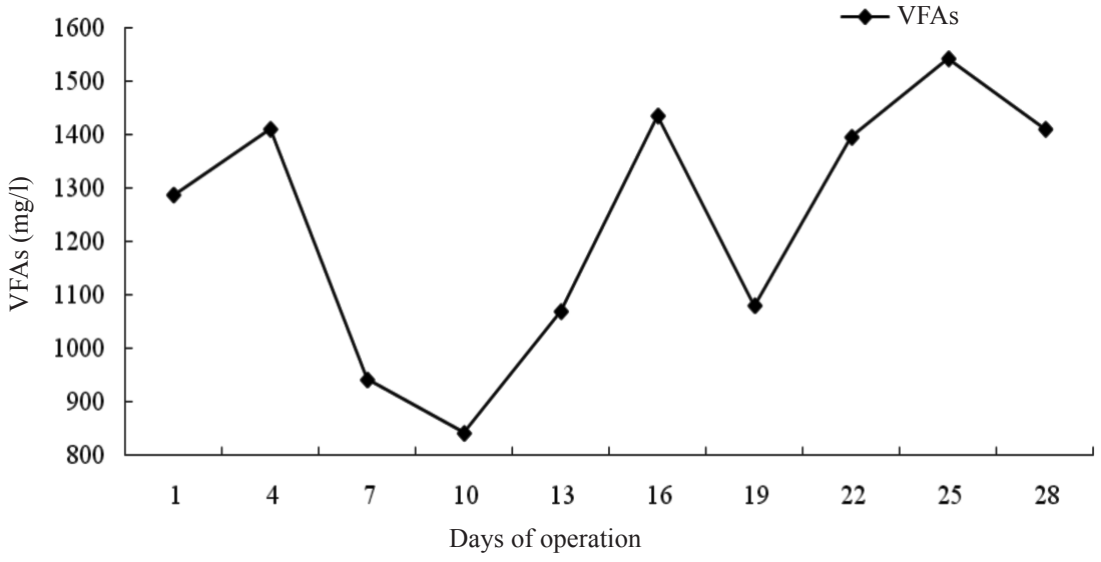

Figure 4. Time course of effluent VFAs during Phase-I.

The biomass yield was found to be equal to 0.034 g VSS/g COD_{rem}. This yield was almost one-tenth that of the conventional activated sludge process.

Phase II (Optimum pH Value for Dairy Wastes)

This phase lasted about 5–6 weeks with the main objective of determining the optimum pH

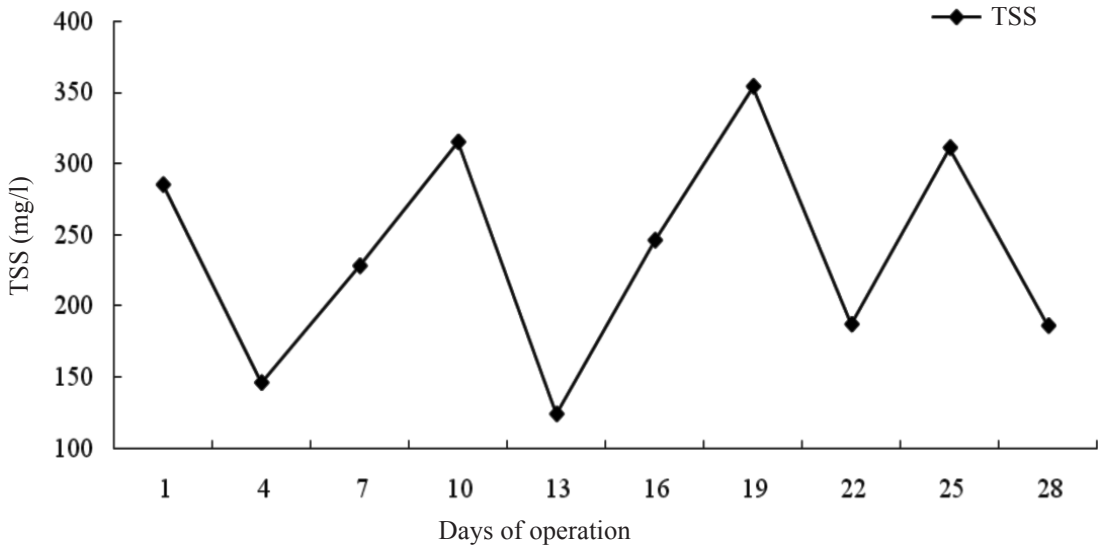

Figure 5. Time course of effluent TSS during Phase-I.

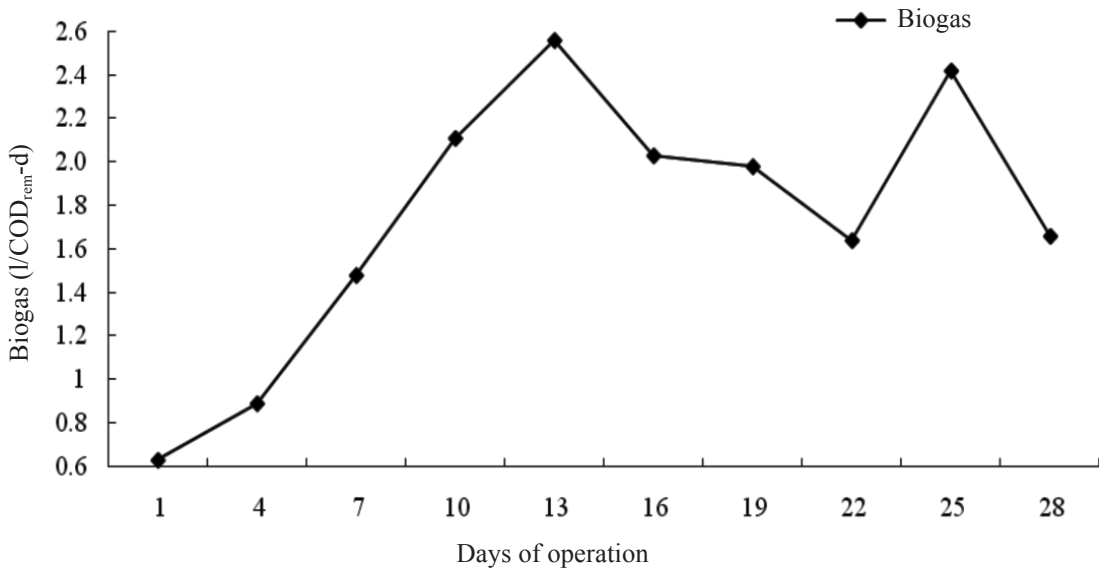

Figure 6. Time course of biogas production during Phase-I.

value for the anaerobic digestion of dairy wastes using the UASB reactor. The reactor was started with an influent COD concentration of 2200 mg/l at HRT of 36 h, corresponding to OLR of 1.82 g COD/l.d. During this phase, temperature was again kept constant at about 32°C. The pH of the reactor dropped slightly to an acidic medium in the region of pH 5.2, and this was then gradually increased by adding an external buffer solution of 0.5 M $NaHCO_3$. The buffer solution was added at a concentration of 64 ml/l to a maximum of 920 ml/l. Consequently, the pH was slowly increased from 5.2 to 8.5 as in *Figure 8*.

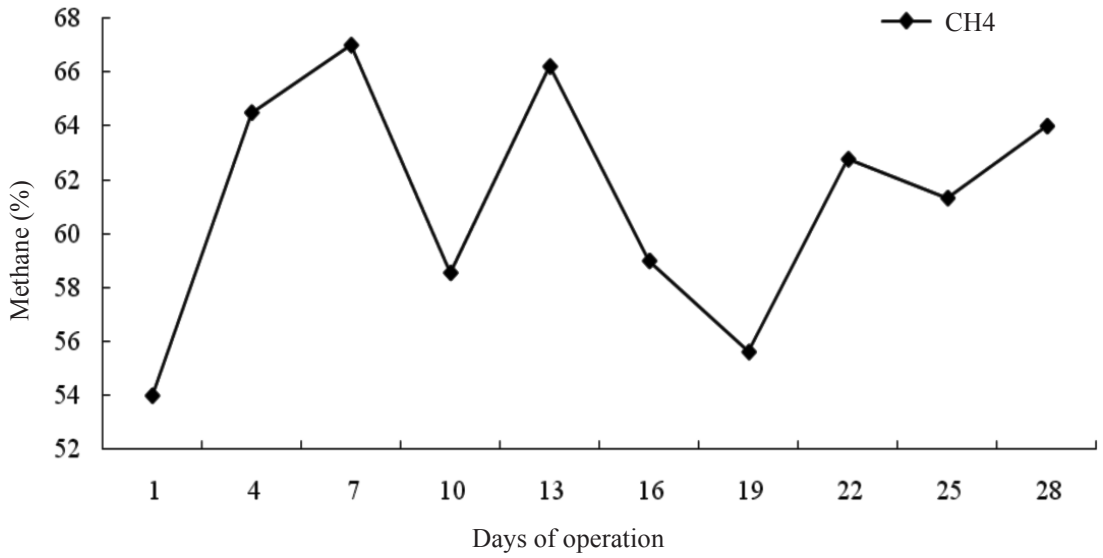

Figure 7. Time course of methane composition during Phase-I.

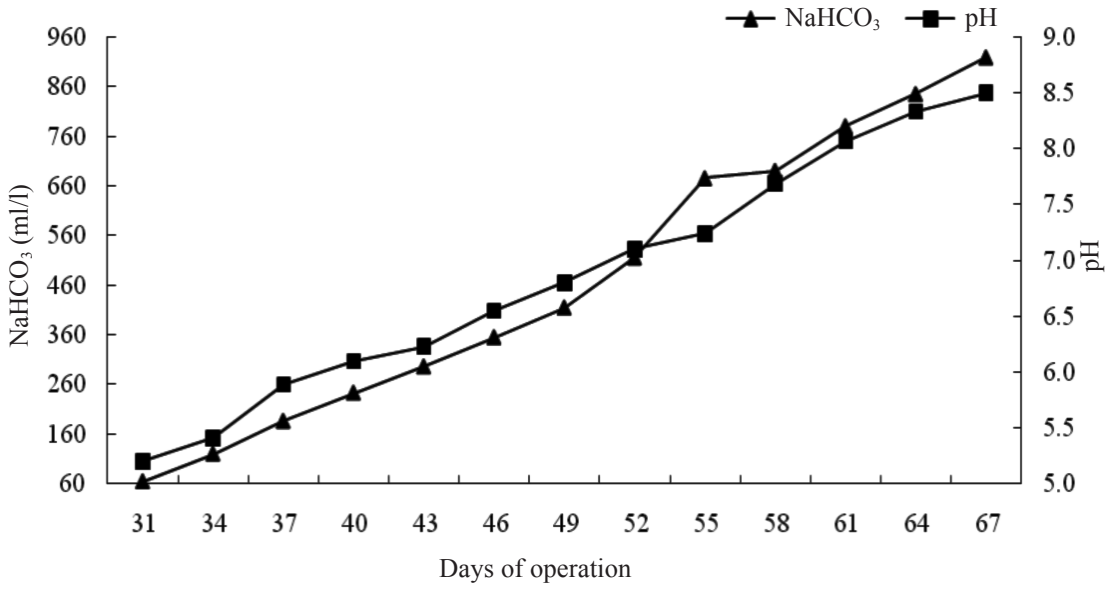

Figure 8. Time course of $NaHCO_3$ and pH during Phase-II.

The time courses of the COD removal efficiency of the reactor, effluent VFA concentration and biogas production, corresponding to the pH value during phase II of the study, are shown in *Figures 9–11*. As shown, corresponding to the pH value of 6.8–7.1, the effluent concentration of VFAs was minimum, i.e. 200 mg/l, thereby giving maximum treatability performance in terms of COD reduction at constant OLR and HRT. Corresponding to these optimum conditions, the amounts of COD reduction and biogas production were observed to be maximum, i.e. 80% and 2.94 l/COD_{rem}.d, respectively. The

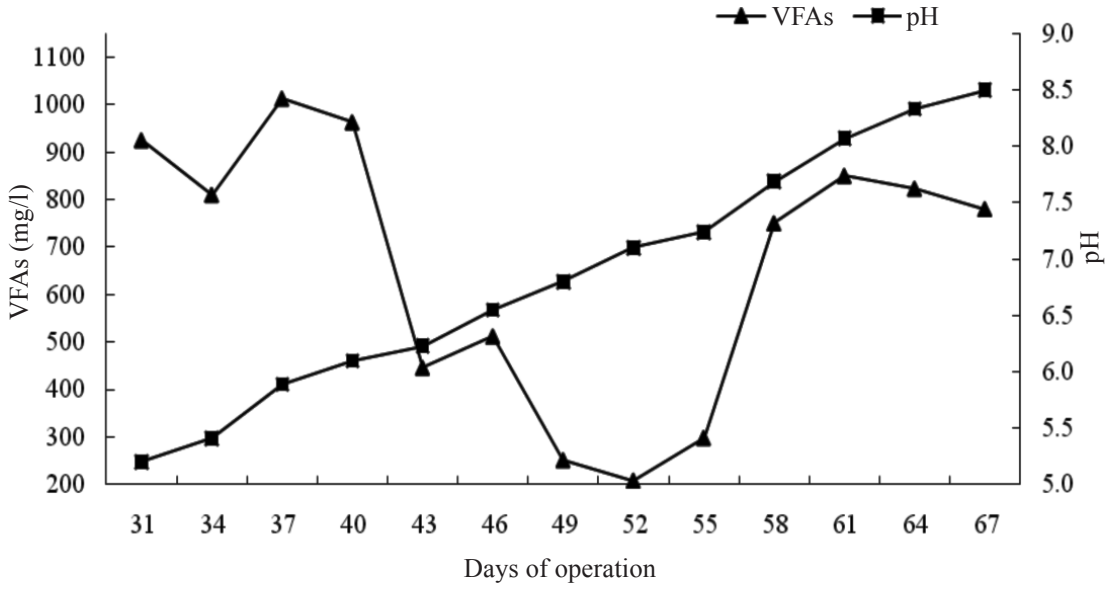

Figure 9. Time course of effluent VFAs and during Phase-II.

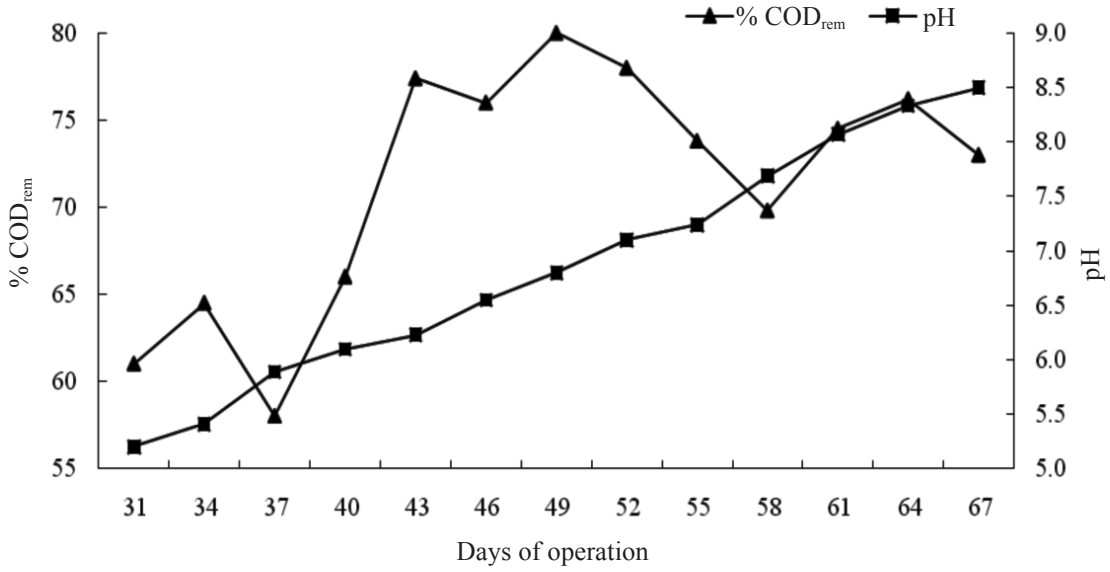

Figure 10. Time course of COD removal and pH during Phase-II.

results of this phase indicate that the optimum pH for the anaerobic degradation of dairy wastes under controlled operating conditions of OLR, HRT, temperature, etc. was 6.8–7.1, i.e. a neutral pH value.

Phase III (Effects of OLR and HRT on the Treatability Performance of the Reactor)

This phase lasted about 9–10 weeks with the major objective of determining the optimum organic loading rate and hydraulic retention

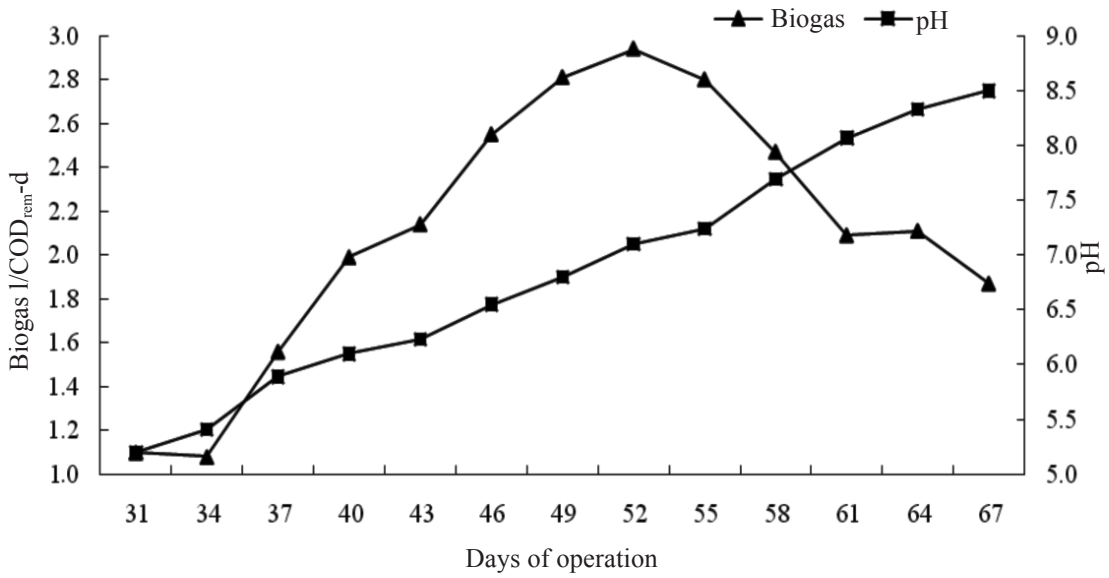

Figure 11. Time course of biogas production and pH during Phase-II.

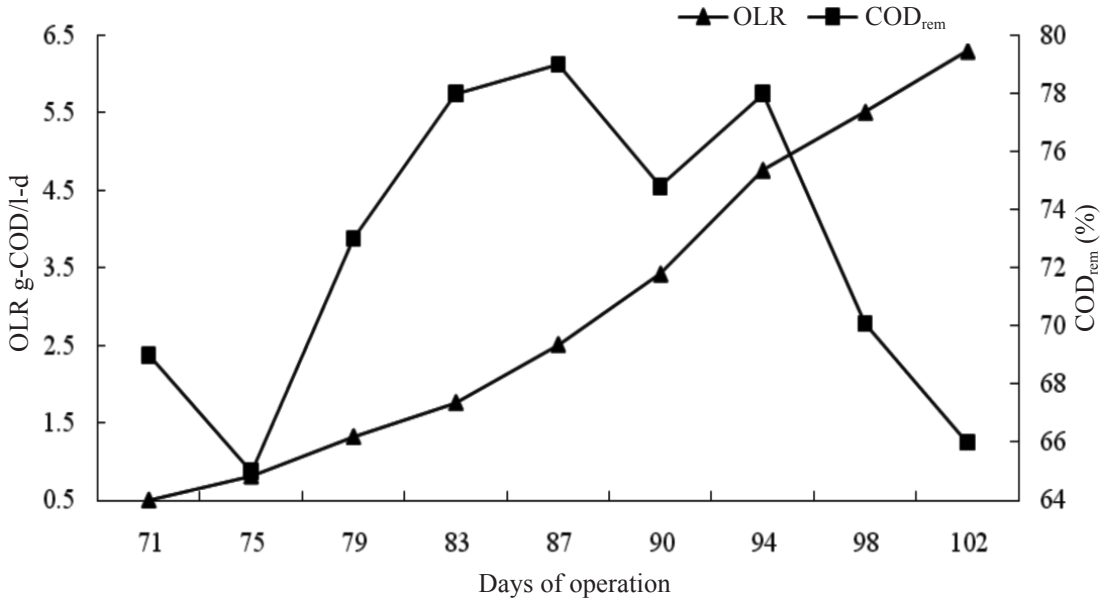

Figure 12. Time course of OLR and COD removal during Phase-III at constant OLR.

time at constant neutral pH and mesophilic temperature. The pH was controlled by adding an external buffer solution of 0.5 M $NaHCO_3$ to the feed solution at the required proportionate. Initially, HRT was kept constant at the same level of 36 h as before, and OLR was varied from 0.5 g to 6.3 g COD/l.d. Later, OLR was fixed at the optimum level of 4.76 g COD/l.d and HRT was varied from 36 h to 13 h. The time courses for COD removal efficiency of the

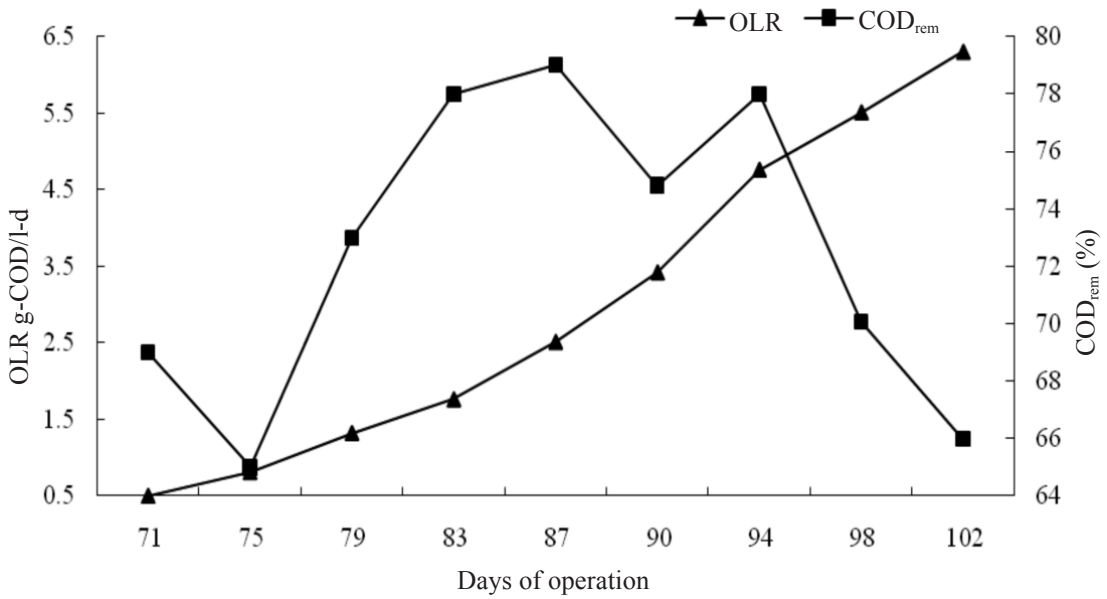

Figure 13. Time course of HRT and COD removal during Phase-III at constant OLR.

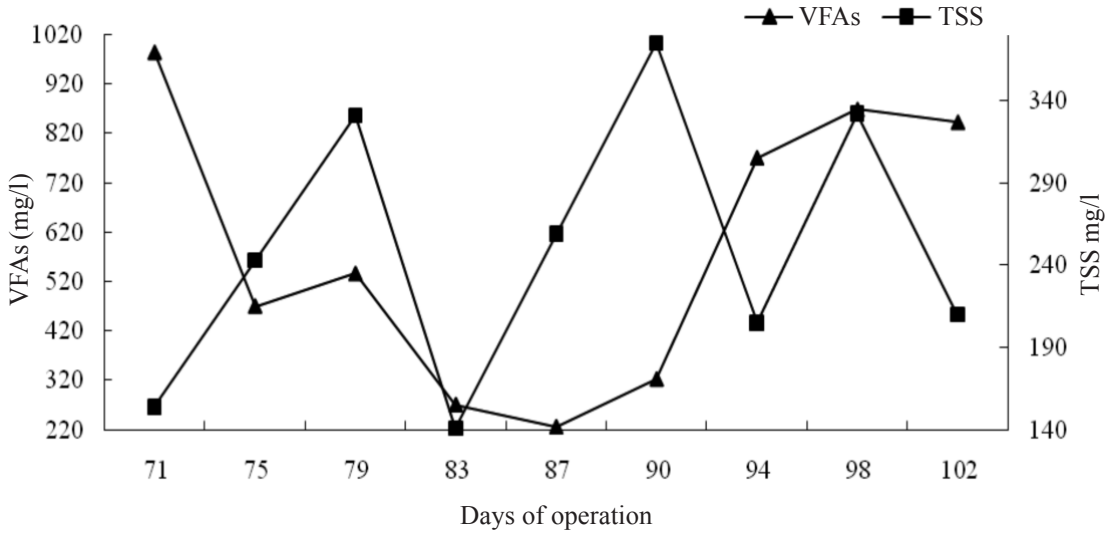

Figure 14. Time course of VFAs and TSS removal during Phase-III.

reactor, and the amounts of effluent VFAs, TSS and biogas production at varying OLR and HRT are shown in *Figures 12–15*. As may be seen, the optimum OLR and HRT were observed to be 4.76 g COD/l.d and 16 h, respectively. Corresponding to the optimum operating conditions, the COD removal efficiency of the reactor, effluent VFA and TSS concentrations, and the amount of biogas production were observed to be 78%, 770 mg/l, 300 mg/l and 2.07 l/COD_{rem}.d, respectively. A comparison of the work done in UASB reactors using different substrates is shown in *Table 3*. It is apparent that anaerobic digestion is effective not only for

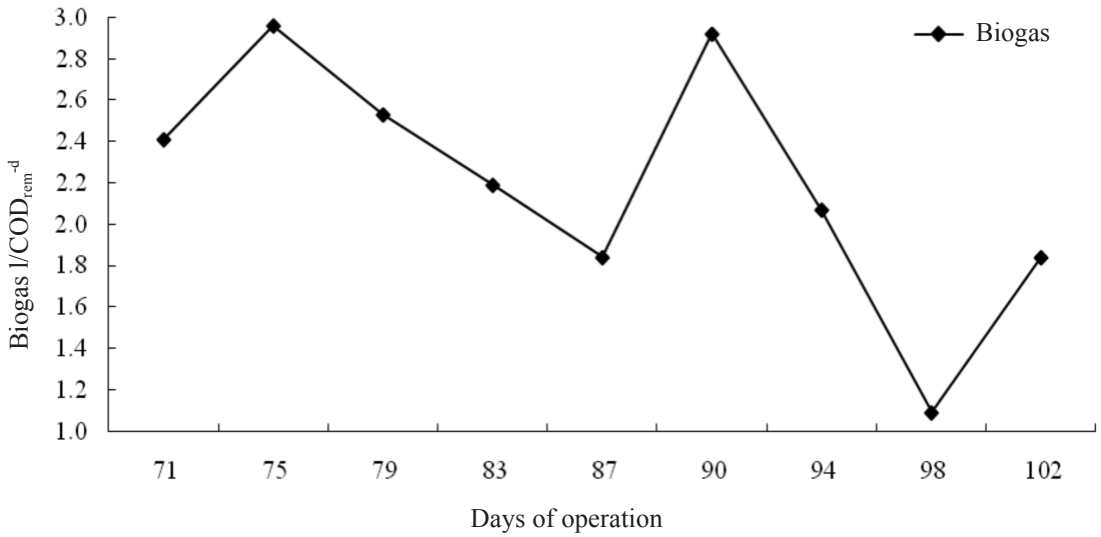

Figure 15. Time course of biogas production during Phase-III.

Table 3. Comparison of similar work done using UASB reactor.

Substrate	Operating conditions	Treatment efficiency	Biogas production	Reference
NSSC* pulping mill effluent	2.75 kg/m^3. day HRT=38 h	35% COD	0.17 m^3/kg COD$_{rem}$	Arshad *et al*. 2009
Sugar mill effluent	2.10 kg/m^3. day HRT=16 h	70% COD	0.30 L-CH_4/g COD$_{rem}$	Arshad *et al*. 2010
Textile mill effluent	2.2 kg/m^3. day HRT=20 h	80% COD	0.17 m^3/kg COD$_{rem}$	Arshad *et al*. 2011
Dairy mill effluent	4.70 kg/m^3. day HRT=16 h	78% COD	2.07 L/g COD$_{rem}$	This study

*Neutral sulphide semi-chemical

pollution reduction but is also a viable option for biogas production.

CONCLUSIONS AND RECOMMENDATIONS

The following conclusions have been acquired from this study:

- A dairy farm emits a wide variety organic-rich pollutants, which are currently disposed of directly into the open atmosphere. The wastewater characteristics of the dairy wastes indicate that they are highly turbid, alkaline and have a bad odour. The concentrations of COD, BOD, nitrates and iron are found to be 2945 mg/l, 1070 mg/l, 10.09 mg/l and 0.03 mg/l, respectively.
- The anaerobic treatment of the dairy wastes is a viable option both in terms of pollution reduction and in terms of biogas-producing potential.
- The optimum pH for the anaerobic treatment of dairy wastes is close to the neutral pH value, i.e. 6.8–7.1. The addition

of an external buffer solution of 0.5 M $NaHCO_3$ is an effective means for maintaining a neutral buffer capacity within the reactor.

- The optimum OLR and HRT for more than 78% COD reduction are 4.76 g COD/l.d and 16 h, respectively.
- At optimum operating conditions, SLR, effluent VFAs and TSS, biogas production and methane composition are observed to be 1.4 g COD/g VSS.d, 770 mg/l, 300 mg/l, 2.07 l/COD_{rem}.d and 62%, respectively.
- The overall observed biomass yield from dairy mill effluent during the process of anaerobic degradation is calculated at 0.034 g VSS/g COD_{rem}, which is almost one-tenth that of the conventional activated sludge process.

With Pakistan facing a shortage of energy, encouraging the use of such technologies can help to tackle the problem of energy crises. For this purpose, a comprehensive and long-term study is required to determine the exact behaviour of the dairy mill effluent at varying pH and temperature ranges. However, the cost of developing the UASB reactor for large- scale application needs to be reduced, and studies in this direction are required.

Date of submission: October 2011
Date of acceptance: November 2011

REFERENCES

Arshad, A, Hashim, NH, Inthikhab, AQ & Athar, S 2009, 'Treatment feasibility of NSSC pulping effluent using UASB reactor', *Journal of Water, Energy and Environment*, vol. 5, pp. 57–60.

Arshad, A, Intikhab, AQ, Tauseef, J, Hashim, NH 2010, 'Pilot plant investigation on the start-up of a UASB reactor using sugar mill effluent', *ASEAN Journal of Science and Technology for Development*, vol. 27, no. 2, pp. 61–71.

Arshad, A, Hashim, NH, Ghazala, N, Bashir, A & Kashif, AK 2011, 'Treatment assessment of the textile mills effluent using UASB reactor', *ASEAN Journal of Science and Technology for Development*, vol. 28, no. 2, pp. 139 – 150.

AWWA and WEF 2005, *Standard Methods for the examination of water and wastewater*, Washington DC, APHA Publication.

Bhatti, ZI 1995, 'Studies on the biological treatment of methanolic waste in UASB reactor', PhD Thesis, Osaka University, Japan.

Bhatti, ZI, Furukawa, K & Fujita, M 1996, 'Feasibility of methanolic wastes treatment in UASB rectors', *Water Research*, vol. 30, pp. 2559–2568.

Hulshoff, L & Lettinga, G 1986, 'New technologies for anaerobic wastewater treatment', *Water Science Technology*, vol. 18, pp. 41–53.

Lettinga, G, Velsen, LV, Zeeuw, WD, Hobma, SW & Klapwijk, A 1980, 'Use of UASB reactor for biological wastewater treatment, especially for anaerobic treatment', *Biotechnology and Bioengineering*, vol. 22, pp. 699–734.

Lettinga, G, Pol, LWH, Weigant, WM, Dezeeuw, WJ, Rinzema, A,Grin, PC, Roersma, RE & Homba, SW 1984, 'High rate anaerobic wastewater treatment using the UASB reactor under a wide range of temperature conditions', *J. Fermentation of Bioeng.*, vol. 70, no. 2, pp. 119–127.

Orhon, D, Gorgun, E, Germirli, F & Artan, N 1993, 'Bilological treatment of dairy wastewater', *Water Research*, vol. 27, pp. 625–633.

Ozturk, I, Erogulu, V, Ubay, G & Demir, I 1992, 'Hybrid UASB reactor treatment of dairy effluent', in *2nd International Symposium on Waste Management Problems in Agro-industries*, Istanbul, Turkey.

Pak-EPA Pakistan 1999, Environmental Report Draft, Environmental Technology Programme for Industries, Pak-EPA Pakistan.

Pakistan Council of Research in Water Resources, 2005, National Water Quality Report – Pakistan, PCRWR Islamabad, Pakistan.

Savant, DV, Abdul-Rahman, R & Ranadi, DR 2005, 'Anaerobic digestion of absorbable organic halides (AOX) from pulp and paper industry wastewater', *Bioresource Technology*, vol. 30, pp.30–40.

Schellinkhout, A 1993, 'UASB technology for sewage treatment: experience with a full scale plant and its applicability in Egypt', *Water Sci. Technol.*, vol. 27, no. 9, pp. 173–180.

ASEAN J. Sci. Technol. Dev., **29(1)**, 13 – 20

Bond Strength of Glued-in Rods in Malaysian Tropical Timber as Influenced by Adhesive, Diameter and Glueline Thickness

N. E. L. ZA'BA*, Z. AHMAD AND A. IBRAHIM
Institute of Infrastructure Engineering and Sustainable Management, Universiti Teknologi Mara, 40450 Shah Alam, Selangor, Malaysia

Failure in wood structure is mainly caused by improper connection design, construction (fabrication) details, or serviceability. Besides using traditional bolting methods such as nails, screws and bolts to join members, timber members also can be connected by using bonded-in joints. However, current knowledge in the use of this type of timber connection is still limited. This study investigated the performance of bonded-in pultruded rods in timber as connections by exploring the effect of a few parameters such as rod type, diameter of the rod, adhesive type and thickness of the glueline. Pull-out tests were used to characterize the strength of the bonded-in connections. From the results of this study, it was found that strength increased as glueline thickness increased, while strength decreased as the diameter of the rod increased.

Key words: Adhesive; bonded-in connection; pultruded rod; pull-out strength; timber; strength; glueline thickness

Bonded-in rods are used to connect timber members, and they have been shown to be more effective than using traditional bolting methods such as nails and screws (Joseph 1999). This type of connection has been used in timber construction for over 30 years in Europe and North America for joining and anchoring glulam members, for rock anchors, for holding down bolts in concrete (Lee *et al*. 1981), and as rods to secure wooden turbine blades (Riberholt & Spoer 1983). Bonded-in rods are also used in timber building repairs, and to strengthen the timber (Mettem & Davis 1996). The connection is made by using high strength resins to produce a concealed timber connection. Bonded-in joints using rods are known to offer improvements by reducing weight and end-splitting, eliminating very stiff connections when loaded in an axial direction, providing greater fire resistance, and also producing a neater appearance. A good compilation of existing knowledge, including lists of basic literature, can be found in the *Proceedings, PRO 22* of the *2001 RILEM Symposium on "Joints in Timber Structures"*, and in the *Proceedings of the CIB W18-Meetings* No. 28, 32, 33 and 34.

Steel rods bonded into timber elements are very efficient in introducing high forces into the timber structural members as well as in strengthening timber which is perpendicular to the grain. Bonded-in steel rods in wooden members have been investigated by numerous researchers. Most of these studies used softwood. However, there is no published work on bonded-in rods in Malaysian tropical timber. Hence, there is a need to investigate the performance of bonded-in connections using Malaysian tropical timber.

* Corresponding author (e-mail: lydia85@live.com)

Molina *et al*. (2009) conducted static and cyclic tests to determine the fatigue of steel rods connections, using two species of reforested wood, three types of commercial adhesives and at three levels of wood moisture content. The studies revealed that fatigue failure may occur in any of the materials used for the connection, i.e. steel rod, adhesive or timber species. Other than that, the fatigue behavior exhibited a visible impact, damaging mainly the steel rods and representing a potential fatigue risk for bonded-in rods used to form the connection in log-concrete composite bridge decks (Molina *et al*. 2009). The effect of spacing between the steel rods and the distance to the timber edge were tested parallel and perpendicular to the grain by Blass and Laskewitz (1999), and it was concluded that the pull-out strength of rods with the same diameter and anchoring length set perpendicular to the grain was 20%–50% higher than for rods bonded in parallel to the grain. According to Widmann *et al*. (2006), the pull-out strength is influenced by the wood density. There are also a few studies comparing the performance of threaded rods and smooth rods on the mechanical bond between the bolt and the resin. Johansson (1995) claimed that there is an advantage of threaded bolts over smooth steel rods because the latter are not effective as it is difficult to achieve sufficient adhesion between a smooth surface and the resin. Other than that, Hamad (1995) and Harvey (2003) investigated the optimization of the rib geometry of steel reinforcing bars to enable the use of shorter bonded-in lengths for a given load. Beside using steel as a general material in bonded-in joints, fibre-reinforced plastic can be used to improve resistance to corrosion which is useful in a humid or acid environment, to lower the weight of the connection, to provide easier and faster handling and installation, as well as to be more compatible with the resin and timber due to more compatible material properties. Harvey and Ansell (2000) investigated the effect of moisture content, wood type, surface preparation, type of adhesive, and glueline thickness when using glass fibre-reinforced plastic (GFRP). *Figure 1* shows the possible failure modes observed by Harvey and Ansell (2000). Number 1 is failure in the rod/adhesive interface, number 2 indicates failure in the adhesive/timber interface, number 3 shows failure in the timber close to the adhesive/timber interface, number 4 illustrates failure in the timber away from the adhesive/timber interface, while number 5 is failure in the timber also along the block.

Even with these parameters studied, the results are still considered insufficient to establish standards for the use of GFRP. Although there are standards such as Eurocode 5 which provides recommendations for bonded-in connections, the information is very limited as it does not consider the thickness of gluelines.

Several design approaches and code models have been published. By comparing these models and approaches, some discrepancy and even partial contradictions between the models, especially regarding the treatment of isolated parameters, can be found. With

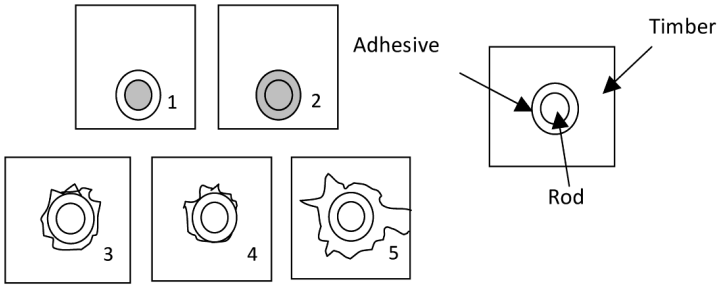

Figure 1. Possible pull-out failure modes.

this background, a small test programme was initiated to study the influence of a selection of these parameters, known or supposed to determine the pull-out strength of single, axially loaded pultruded glass fibre-reinforced plastic (GFRP) rods bonded with two types of commercial epoxy-based adhesives in timber from Kempas wood species. The tests were focussed on determining the influence of rod diameter, ϕ_{rod}, (or the corresponding drill-hole, ϕ_{hole}) and glueline thickness, h, on the pull-out strength of the glued-in rods.

Important objectives of the test programme were that it should be based on practical situations and dimensions, and that it should enable a comparison to be made with similar test series. These objectives could only be achieved by permitting certain compromises regarding the test layout. For example, although in practice the use of one single rod will not or hardly ever be the normal case, all tests described here were carried out on connections with a single rod. This is because the examination of such a connection provided a good basis to study the influence of isolated parameters. Moreover, it was possible to quantify the influence of the parameters selected for the present study on the pull-out strength of the axially loaded rods, and to propose an adequate design model.

MATERIALS AND TEST METHODS

Materials

The selected timber used in this study was from a medium hardwood species, namely, Kempas (*Koompassia malaccensis*), from strength group 2 with a density of 900 kg/m^3. This species was chosen because it is commonly used for roof trusses, and is easily available.

Glass fibre-reinforced plastic (GFRP) rods with diameters 8 and 12 mm were used with a modulus of elasticity of 150 000 N/mm^2. GFRP rods were sandpapered using coarse sand paper, and degreased with ethanol to aid bonding with the adhesive.

The adhesives used in this study were Sikadur®-30 and Morstrong. Sikadur®-30 was supplied by Sika Sdn. Bhd, Malaysia. It is a gap-filling, thixotropic and structural two-part adhesive, based on a combination of epoxy resins and a special filler, designed for use at normal temperatures between +8°C and +35°C. Morstrong, which is also a gap-filling adhesive was supplied by Morstrong Industries Sdn. Bhd.

Specimen Preparation and Test Methods

Timber specimens for the pull-out tests were prepared using timber blocks of size 100 mm × 100 mm × 60 mm by ensuring that the grain was parallel. A hole was drilled parallel to the grain with the diameter of the drilled hole being larger than the rod diameter to allow for the required glueline thickness. The specimens were left in a temperature controlled room at 28°C to avoid shrinkage prior to inserting the adhesives and rods. A gun was used for injecting the adhesive into the hole. The rod was slowly pushed in and gently rotated to squeeze out the excess adhesive without causing any air voids. An O-ring was inserted into the hole to centre the position of the rod. All the specimens were left for 10 days at room temperature for curing. Ten replicates were prepared for each treatment.

A 250-kN capacity universal testing machine (UTM) was used to conduct the pull-out tests. Axial loads were applied with a crosshead of 2 mm/min. To support and align the specimen in the pull-out test, a special jig made from stainless steel as shown in *Figure 2(b)* was used for the specimen to be gripped by the machine as shown in *Figure 2*.

Observations were made on the failure modes of the specimens to better understand the behavior of the bonded-in timber. Average shear strength, τ, at the adhesive, timber and rod interfaces was calculated by dividing the failure load by the bond area as shown in *Figure 3*, using *Equations 1* and *2*.

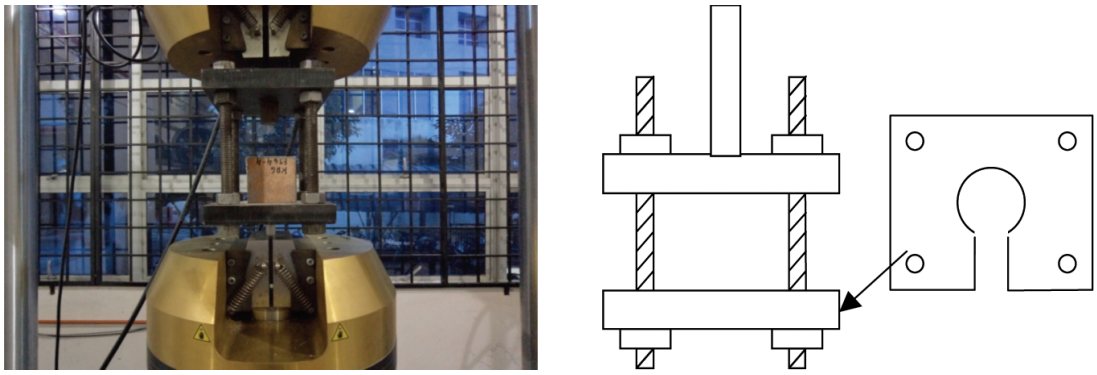

(a) (b)

Figure 2. Experimental set-up for a pull-out test: (a) pull-out specimen attached to UTM, (b) schematic diagram of the cage (jig) to hold the pull-out specimen.

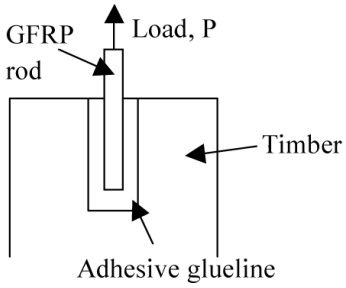

Figure 3. Schematic diagram of bonded-in rod in timber.

Adhesive-timber interface:

$$\tau_{ta} = \frac{P_{max}}{\pi \phi_{hole} L} \quad (1)$$

Rod-adhesive interface:

$$\tau_{ra} = \frac{P_{max}}{\pi \phi_{rod} L} \quad (2)$$

where, ϕ_{hole} and ϕ_{rod} are the diameters of the drilled hole and rod, respectively, and L is the rod embedment length which was 50 mm in all cases. Due to the different diameters, the bond area at the adhesive/timber interface was bigger than the bond area at the adhesive/rod interface which resulted in different strength values.

RESULTS AND DISCUSSION

Influence of Adhesive Type on the Pull-out Strength

When constructing the bonded-in connection, the strength of the joint will depend in the type of adhesive used. *Table 1* shows a summary of the pull-out strength for all the parameters studied. It can be seen that the bonded-in joints were affected by the various parameters, and that the influence was clearly visible with the 8-mm rods but not as markedly as when using 12-mm rods.

For the bonded-in joints using Sikadur with 8-mm rods, the pull-out strength increased as the glueline thickness increased. However, there was no significant difference in the pull-out strength when using Morstrong adhesive with 8-mm rods for the bonded-in joints. Comparing both the adhesives, the pull-out strength of the bonded-in joints using Sikadur was 26% higher than when using Monstrong adhesive. With Sikadur adhesive, 50% of the specimens failed at the rod/adhesive/timber interface, while Morstrong adhesive tended to fail at the rod/adhesive interface (see *Figure 3*).

The FE-modelling performed by Serrano and Gustafsson (1999) on bonded-in rods using

Table 1. Shear strength of pull-out specimens.

Adhesive type	Rod diameter (mm)	Glueline thickness (mm)	Pull-out strength		Shears strength at rod/ adhesive interface		Shear strength at adhesive/ timber interface		Failure mode *r/a, a/t, r/a/t
			P_{max} (KN)	S.D.	τ (MPa)	S.D.	τ (MPa)	S.D.	
Sikadur	8	2	17.7	0.80	11.3	0.53	7.6	0.35	100% a/t
		3	18.3	0.92	12.16	0.61	6.95	0.35	80% r/a/t, 20% a/t
		4	18.2	1.31	12.06	0.87	6.03	0.44	80% r/a/t, 20% a/t
	12	2	9.9	2.10	4.38	0.93	3.29	0.70	100% r/a/t
		3	10.0	2.21	4.43	0.98	2.95	0.65	60% r/a, 20% r/a/t, 20% a/t
		4	7.4	0.52	3.26	0.23	1.96	0.14	60% r/a, 20% r/a/t, 20% a/t
Morstrong	8	2	14.5	0.86	9.65	0.57	6.43	0.38	60% r/a/t, 40% r/a
		3	14.6	0.52	9.68	0.34	5.53	0.20	60% r/a, 40% r/a/t
		4	14.1	0.11	9.36	0.07	4.69	0.04	80% r/a, 20% r/a/t
	12	2	5.8	0.99	2.57	0.44	1.92	0.33	100% r/a
		3	4.5	0.90	1.99	0.40	1.33	0.59	100% r/a
		4	9.3	3.16	4.09	1.36	2.45	0.84	100% r/a

*Note: r/a: (Rod/adhesive failure)
a/t: (Adhesive/timber failure)
r/a/t: (Rod/adhesive/timber failure)
S.D.: (Standard deviation)

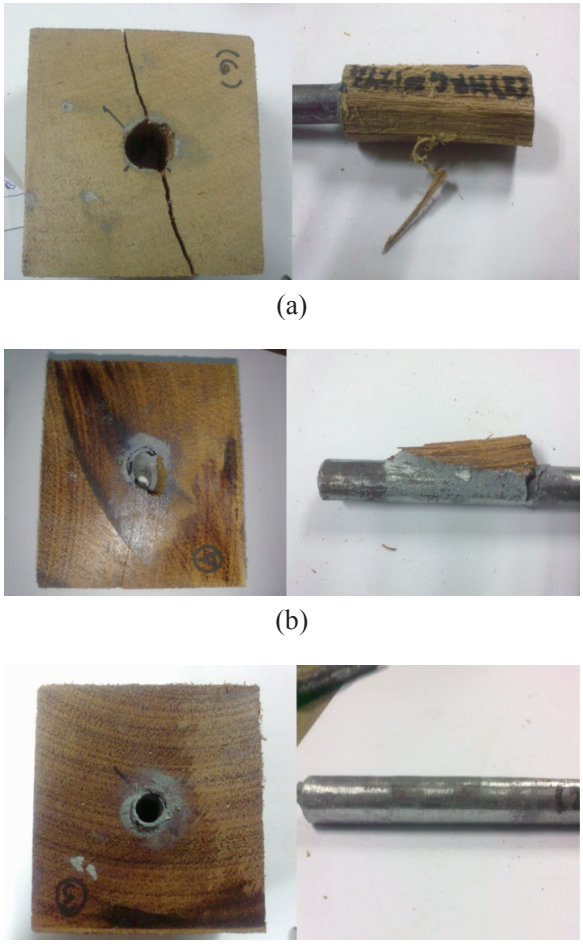

Figure 3. Bonded-in rods with different modes of failure: (a) failed in timber, (b) failed in rod/adhesive/timber interface and (c) failed in rod/adhesive interface.

ductile and brittle adhesives showed that the shear strength increased with the use of ductile adhesives with high fracture energy. Therefore, in this case, the increase in shear strength of the bonded-in rods using Sikadur as compared with Monstrong may be due to the higher fracture energy of Sikadur as this adhesive is epoxy-based with the addition of a special filler to improve toughness. An improvement in adhesive bond strength has been reported by many researchers using CTBN liquid rubber as a modifier (Bascom & Cottington 1976; Hunston *et al*. 1984; Huang & Kinloch 1993). Achary *et al*. (1991) reported a three-fold increase in lap shear strength using carboxyl terminated poly (propylene glycol) adipate as liquid rubber. Ratna and Banthia (2000) reported a two-fold increase in lap shear strength using carboxyl-terminated poly (2-ethylhexyl acrylate) (CTPEHA) as liquid rubber.

Influence of Glueline Thickness and Rod Diameter

As the tests follow a certain range of geometrical proportions in terms of rod diameter ϕ and glueline thickness h, the nominal shear strength fv is calculated assuming a constant distribution of the shear stresses over the bonded area.

Besides analysing the test results with regard to the relationship between ϕ and h, the influences of the single parameters and ϕ were studied to get an idea of their power of their influence. Regarding the influence of the glueline thickness on the pull-out strength of the rods, the relationship can be approached based on $h^{0.05}$ suggesting a relationship existed between pull-out strength and thickness of the glueline. When combining the effect of the various glueline thicknesses and diameters of the rod, the nominal shear strength of bonded-in rod can be estimated based on the following equation:

$$f_v = k_0 h^{0.05} \phi^{1/3} \quad (3)$$

Validation of *Equation 3* is not shown here. *Figure 2* shows the fitting of the model to the relationship between the pull out strength and glueline thickness at various diameters of the rod.

As the gluelines thickness increased, the failure modes changed to the rod/adhesive/timber interface from the rod/adhesive or adhesive/timber interface. In some cases, 10% of the timber blocks cracked and were completely split. As the shear stress decreased, the failure was mainly in the rod/adhesive interface. The effect of rod diameter on average peak interfacial shear stress was reflected by a decrease in shear strength of the adhesive/timber interface as rod diameter increased. The failure mode for the 8-mm rod diameter was close to the adhesive/timber interface while for the 12-mm rod diameter failure was in the rod/adhesive interface.

CONCLUSION

Pull-out tests were conducted on Kempas species with 8-mm and 12-mm diameter steel rods bonded with two types of adhesives, which were Sikadur and Morstrong. The investigation examined the influence of rod diameter and glueline thickness on the pull-out strength. The results from the experiment reveal that:

- As glueline thickness increased, the pull-out strength also increased, on condition that there was a good bond between the rod and the adhesive.
- As rod diameter increased, the shear strength of the adhesive /timber interface decreased.

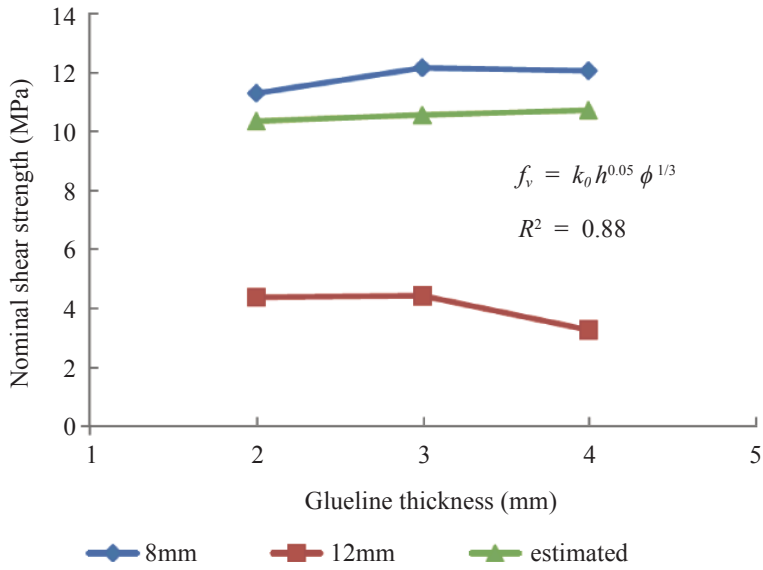

Figure 2. Design model to calculate the nominal shear strength of single, axially loaded rods in bonded-in timber connections.

- Pull-out strength using Sikadur was 26% higher than when using Morstrong adhesive, and tended to fail at the rod/adhesive/timber interface.

Date of subwmission: May 2012
Date of acceptance: June 2012

REFERENCES

Achary, PS, Gouri, C & Ramamurty, R 1991, 'Carboxyl-terminated poly(propylene glycol) adipate-modified room temperature curing epoxy adhesive for elevated temperature service environment', *Journal Applied Polymer Science,* vol. 42, pp. 743 – 752.

Bascom, WD, Cottington, RL, Jones, RL & Peyser, P 1975, 'The fracture of epoxy- and elastomer-modified epoxy polymers in bulk and as adhesives', *Journal Applied Polymer Science*, vol. 19, no. 9, pp. 2545 – 2562.

Blass, HJ & Laskewitz, B 1999, 'Effect of spacing and edge distance on the axial strength of glued-in rods', in *Proceeding CIB-W18A*, Graz, Austria.

Hamad, BS 1995, 'Bond strength improvement of reinforcing bars with specially designed rib geometries', *ACI Structural Journal (American Concrete Institute)*, vol. 92, no. 1, pp. 3 – 13.

Harvey, K & Ansell, MP 2000, 'Improved timber connections using bonded-in GFRP rods', in *Proceedings of 6th World Conference on Timber Engineering*, Whitsler, British Columbia, 31st July to 3rd August 2000, Paper P04.

Harvey, K 2003, 'Improve timber connections using bonded-in GFRP rods', *PhD thesis*, University of Bath, UK.

Huang, Y, Hunston, DL, Kinloch, AJ & Riew, CK 1993, 'Toughened plastics I', in *Advances in chemistry series, 233*, eds CK Riew & AJ Kinloch, American Chemical Society, Washington DC.

Hunston, DL, Kinloch, AJ, Shaw, SJ & Wang, SS 1984, 'Characterization of the fracture behavior of adhesive joints', in *Adhesive Joints*, ed KL Mittal, Plenum Press, New York.

Johansson, CJ 1995, 'Glued-in bolts', in *Structural timber education programme lecture, Part 1, Lecture C14*. 1st edn, ed HJ Blass, Centrum Hout, Almere, Netherlands, C14/1–C14/7.

Joseph, DR 1999, 'Flitched beams for use in domestic flooring', Final Year Research Project, Faculty of the Built Environment, University of the West of England, UK.

Lee, NK, Mayfield, B & Snell, C 1981, 'Detecting the progress of internal cracks in concrete by using embedded graphite rods', *Magazine of Concrete Research*, vol. 116, pp. 180 – 183.

Mettem, CJ, & Davis, G 1996, 'Resin bonded repair systems for structural timber', *Construction repair*, March/April, pp. 23 – 28.

Molina, JC, Calil, CJ & Carreira, MR 2009, 'Pull-out strength of axially loaded steel rods bonded in glulam at a 45° angle to the grain', in *Laboratory of wood and timber structures*, Carlos School of Engineering, University of Sao Paulo.

Ratna, D & Banthia, AK 2000, 'Toughened epoxy adhesive modified with acrylate based liquid rubber', *Polymer International*, vol. 49, no. 3, pp. 281 – 287.

Riberholt, H & Spoer, D 1983 'Design of the in-glues rods that are used for the wingblade root section on Nibemolle-B', *Series R-Denmarks Tekniske Hojskole*, Afdelingen for Baerende Konstructioner, no. 167.

Serrano, E & Gustafsson, PJ 1999, 'Influence of bondline brittleness and defects on the strength of timber finger-joints', *International Journal of Adhesion and Adhesives*, vol. 19, no. 1, pp. 9 – 17.

Widmann, R, Steiger, R & Gehri E 2006, 'Pull-out strength of axially loaded steel rods bonded in glulam perpendicular to the grain', *Material and Structures*, vol. 40, no. 8, pp. 827 – 838.

ASEAN J. Sci. Technol. Dev., **29(1)**, 21 – 28

Design and Construction of Automized Assembly Application

E. E. HTWE[1], S. HATANAKA[2] AND T. AKIYAMA[2]
[1]Mechanical Engineering Department, Mandalay Technological University, Patheingyi Township, Mandalay, Myanmar
[2]3-2-30 Itakano Higashi-yodogawaku, Osaka-shi, 533-0001, Japan

Nowadays the main stream of current automatic process and assembly is on intermittent transportation. Robot control systems can be divided into motion control and force control depending on the work. Assembly work is necessary to consider the state of force applied by detection of the force or moment on the fingers of the gripper. In this project, four groups designed and developed each one of the stages of the workpieces until the final piece was delivered; it was composed of three different workpieces. The mechanism was designed to set the shaft and fasten the screw into a vacancy in a workpiece. The machine was constructed with frame, base plate, support, gripper and workpieces by using CNC milling, turning, drilling and wirecut machine. This paper briefly describes the design analysis of a conveyor, actuator and motor control system.

Key words: Assembly; control; feeding; fastening; updown; design analysis; bearings

With the advances in electronics in recent years, industrial robots are finally coming into practical use, well supported by advanced hardware and software technology. The main considerations of this project were purpose of use, size of the object to be conveyed, the speed of the conveyance and positioning accuracy.

The project was to make a bearing assembly with two different materials. Since it had two different kinds of workpiece, two stations were needed for the machine. The first station was designed coloured workpieces, the other one designed non-colour pieces. Before reading the colour or non-colour workpiece by the colour sensor, four workpieces were placed inside the ordinary station in group one. As soon as the condition started, the first workpiece advanced on the conveyor, moving by cylinder action. After the colour sensor had read the workpiece colour, it sent a ready signal to group two.

After group two had received a ready signal from group one, the conveyor belt start to move. At the end of the conveyor, the workpiece stopped by the sensor and a gripper picked and placed it on the conveyor of group two. If work piece (1) was coloured as detected by the photo electric sensor, the first stopper's advance and work piece (1) was stopped at this station and conveyor belt stopped to move only later. Colour workpiece (2) was inserted to workpiece (1) by pneumatic cylinder.

After the pneumatic cylinder retracted, the stopper retracted and the conveyor belt started to move. After the second stopper advanced, workpiece (1) stopped at this station and sent a ready signal to group three for the screw process. After the screw process was completed, it received a ready signal from group three and the second stopper retracted, the conveyor belt moved and at the same time it sent a ready

* Corresponding author (e-mail: eieihtwe.mdy2012@gmail.com; dr.kyawsein@gmail.com; dan@kansai.interq.or.jp)

signal to group four for the rotating table and the conveyor belt to move.

If the workpiece was a non-coloured one after detection by the photo electric sensor, the second stopper advanced and a certain time later, the conveyor stopped. At this position, when workpiece (1) stopped at the second station, workpiece (2) was inserted to workpiece (1) by pneumatic cylinder. The pneumatic cylinder retracted and sent a ready signal to group three for the screw process. After the screw process was completed, a ready signal was received from group three and the second stopper retracted the conveyor belt moved. At the same time group 2 sent a ready signal to group four for the rotating table and conveyor to move. Finally, different assembly workpieces were sent to the storage stacker according to colour or non-colour workpiece, by sensor.

Automatic Machine Making Procedure

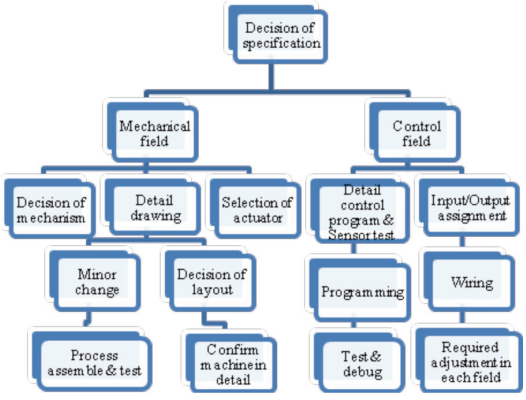

Figure 1. Flow diagram of automatic machine.

Operation and Requirement of Part List (Group 1)

This paper briefly considered how to make a section of an automatic machine to act out a sorting-out and delivery rule. It consisted of a rotary actuator, a gripper, cylinder, induction motor, belt, roller and aluminum frame.

A rotary actuator sent the workpiece to Group 2 and a gripper was used for clamping the workpiece. The cylinder pushed the workpiece to the conveyor which was driven by an induction motor. A belt was used to convey the workpiece and two rollers were used for belt rotation. All the parts mentioned above were put together and most of the frame components were machined by using the wirecut and CNC machining centre.

DESIGN ANALYSIS

First, an induction motor without brakes was selected to drive the belt conveyor. The mass of workpiece had to be identified for choosing a double acting cylinder. According to the results of cylinder tube bore, it was possible to get the stroke length for the feeder part.

Selection of the Induction Motor to Drive the Belt Conveyor

Design parameters to select the induction motor:

Mass of 1st workpiece (Aluminum) = 58 g
Mass of 2nd workpiece (Aluminum) = 3.9 g
Mass of screw(Steel) = 5.2 g
Total weight of workpiece = 67.1 g

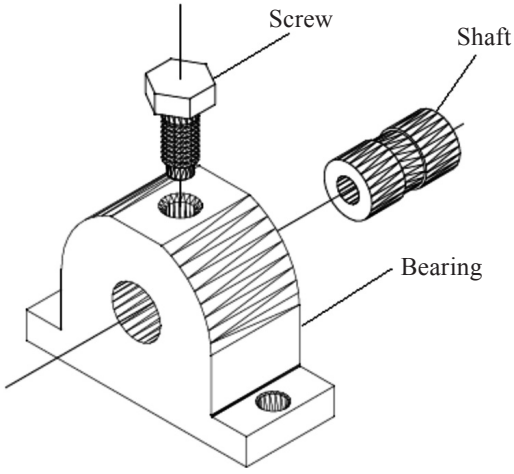

Figure 2. Bearing workpiece for assembly operation.

Flat Belt Type,

Thickness, length, width (mm): 0.9, 1100, 30

Drive pulley: Ø 40 mm

Weight: 1 kg/m^2, 33 g

Allowable stress: 4.0 kg/cm^2

Total mass of belt & workpiece: W = 100.1g

Friction coefficient of sliding surface: $\mu = 0.3$

Drum radius: D = 30 mm

Belt roller efficiency: $\eta = 0.9$

Belt speed: V =60m/sec

Gearhead transmission efficiency, $\eta_G = 0.66$

Motor power supply:

Single phase 110 V, 60 Hz

Determining the Gearhead Reduction

Ratio:

$$N_G = \frac{60V}{\pi D} \quad (1)$$

Since the rated speed for the induction motor at 60 Hz was 1200 rev/min, the gearhead reduction ratio i was calculated as follows:

$$i = 1200/N_G \quad (2)$$

The nearest available gear ratios on catalogue were 30 and 36, but 36 was selected for the speed.

Calculating the Required Torque

On a belt conveyor, maximum torque was needed to start the belt to move. To calculate the torque needed for starting, the friction force F of the sliding surface was firstly determined:

$$F = \mu W \quad (3)$$

Load torque T_L was then calculated by:

$$T_L = \frac{FD}{2\eta} \quad (4)$$

The load torque obtained was actually the load torque at the gearhead drive shaft, so that value was be converted into load torque at the motor output shaft. If the required torque at the motor output shaft was T_M :

$$T_M = \frac{T_L}{L\eta_G} \quad (5)$$

Therefore, a motor OIK1GN _ AUL was the best choice. Since the reduction ratio 36 was required, gearhead OGN 36KA was connected to the OIK1GN _AUL motor.

Choosing Double Acting Cylinder for Feeder Part

Friction $\mu = 0.28$

Operating pressure = 0.4 MPa

$$F_1 = (\mu W)_4 + (\mu W)_5 \quad (6)$$

$$F = F_1 \times 2 \text{ (For safety)} \quad (7)$$

Where, W_4, W_5 = $\dfrac{\text{Number of 1st workpiece}}{\text{Weight}}$

According to P_ O17 Graph 1, when the load factor = 0.5 and we could use 15, 30, 45, 60 stroke lengths from the catalogue for diameter 6, we selected 45 mm stroke for the feeder part. (CDJ2B6-45R-H7NWL)

For stopping workpiece (Determining the Gearhead Reduction)

Weight of stopper = 2.7 g

As a second to stop workpiece (Determining the Gearhead Reduction), we chose a double acting cylinder with stroke length 30 mm and diameter 6 mm. (CDJ2B6 –30R – H7NW)

Select a Rotary Actuator

Specifications of design parameters:

Mass of Lever, $m_1 = 0.0323$ kg

Lever's inertia, $I_1 = \frac{m_1 L^2}{3}$ (8)

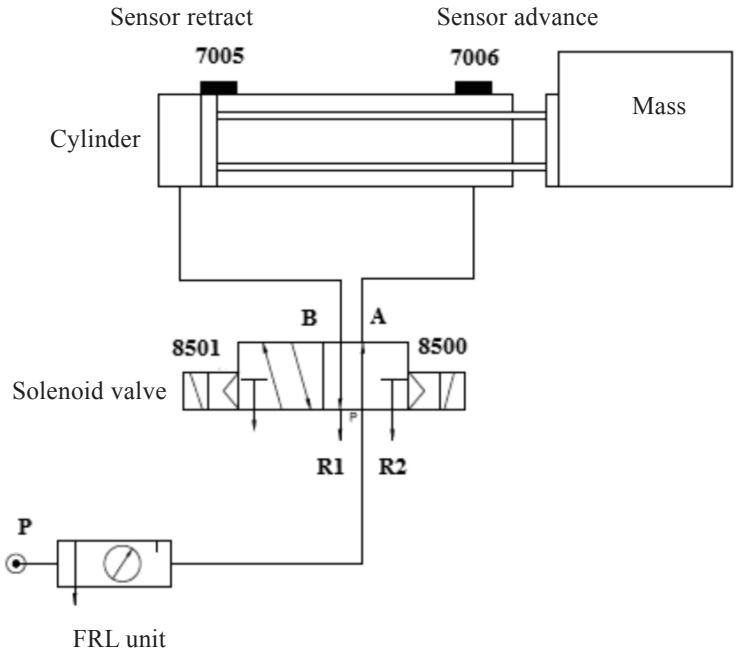

Figure 3. Pneumatic circuit for cylinder.

Gripper's inertia,

$$I_2 = m_2\left[\frac{a^2 + b^2}{12}\right] + m_2 L^2 \qquad (9)$$

Workpiece's inertia,

$$I_3 = m_3\left[\frac{a^2 + b^2}{12}\right] + m_3 L^2 \qquad (10)$$

Total inertia,

$$I = I_1 + I_2 + I_3 \qquad (11)$$

Load of inertia,

$$T_a = I\omega \qquad (12)$$

Accelerating rate,

$$\omega = \frac{2\theta}{t^2} \qquad (13)$$

For safety, it needs to consider 10 times of load of inertia. So, CDRB1BWU 20-100-D-S79L rotary actuator was satisfactory for this project.

RESULTS

For Checking Allowable Shaft Load,

Total weight of lever + gripper + workpiece,

m = 140.3 g

$F = ma$
$= 1.372\ N$

F = 1.372 N is smaller than vane style (double)

F_r = Lever Length × ($W_{\text{gripper}} + W_{\text{workpiece}}$)
= 85 × (50 + 58)
= 9180 g-mm

Load of inertia $= F_r \times 9.81 \times 10^{-6}$
$= 0.09\ N\,m$

0.0122 < 0.09 (satisfied)

So, CDRB1BWU 20-100-D-S79L rotary actuator is satisfactory for this project.

Table 1. Design results of induction motor and actuator.

Induction Motor	Result	Units
Speed at gearhead output (N_G)	38.2	Rev/min
Gearhead ratio (i)	36	–
Friction force (F)	30	g
Load torque (T_L)	500	g-mm
Torque at motor output (T_M)	42.08	g-mm
Actuator:		
Lever's inertia (I_1)	7.78×10^{-5}	Kg-m^2
Gripper's inertia (I_2)	3.65×10^{-4}	Kg-m^2
Workpiece's inertia (I_3)	4.33×10^{-4}	Kg-m^2
Load of inertia (T_a)	1.22×10^{-2}	Nm

According to the results, the load of inertia was needed to be considered at 10 times for safety and a smaller actuator was better. The shocks were considered to be at the rotating ends for selecting the rotary actuator.

PERFORMANCE TEST

There were three parts to distinguish in the mechanism which had the electric, pneumatic and electronic devices:

a. Feeder area
b. Updown area; and
c. Fastening area.

The application required low speed, concerning only the accuracy of the stroke. Due to the rotational inertia of the plates and screws, the size and capacity of the motor was small.

If a cam was used, it would be very complicate to calculate, design and construct the movement of the fastening unit. The stepping motor was a good alternative to solve such inconveniences, since the only requirement was to program the speed control and driver with the positions needed, disregarding how accurate it might be.

The fastening area had the task of fastening the screw into the main workpiece. A stepping motor was selected for the actuator for this part of the machine, it is selected because it could be driven to rotate to as many turns required to achieve the fastening process.

Assembly Operation of Automatic Machine with Different Processes

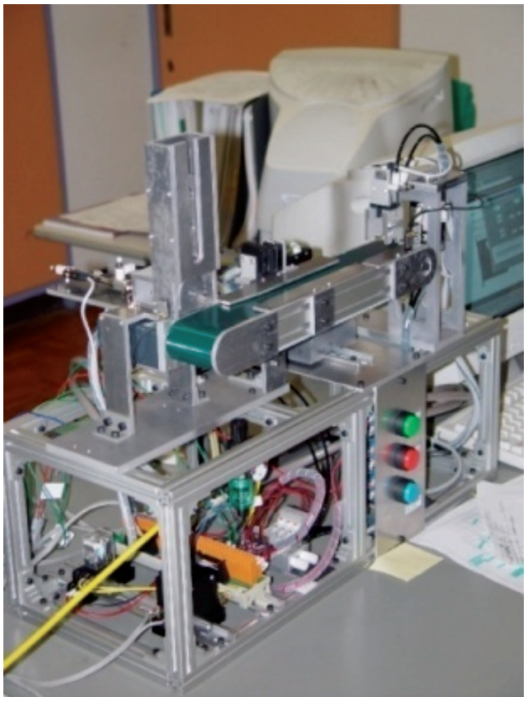

Figure 4. Feeding unit.

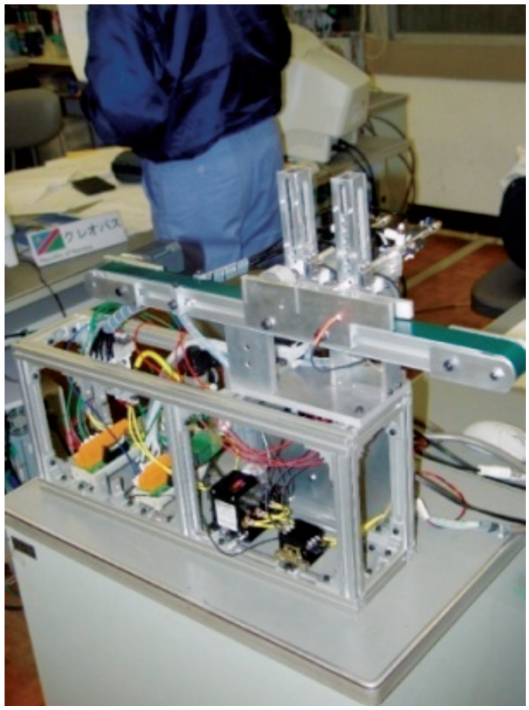

Figure 5. Colour or non-colour assembly.

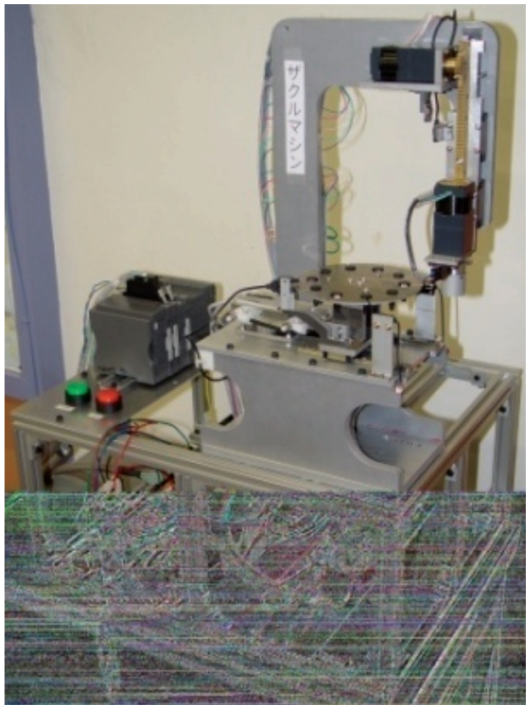

Figure 6. Updown and fastening unit.

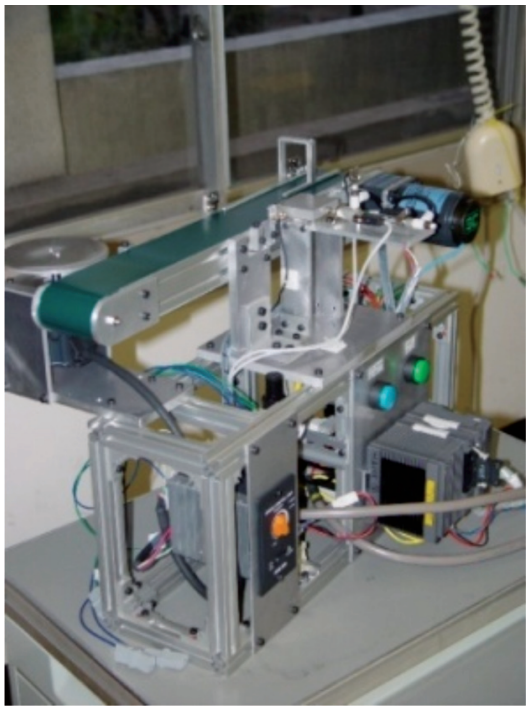

Figure 7. Colour or non-colour storage unit.

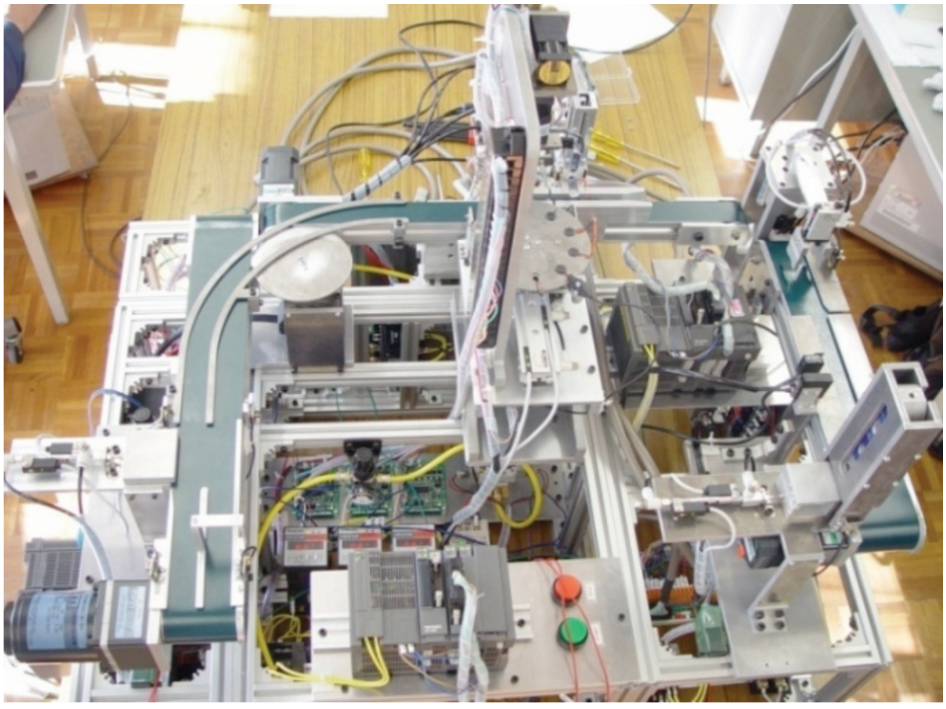

Figure 8. Bearing assembly with automatic machine.

Difficult Points on the Machine

At difficult points on Group four were guides which were in the form of arcs. They were used to determine the radius of the arc that connected the two conveyors together and they had to pass over the table at the same time.

The table was in the space of 90º that was formed by the two conveyors and it was almost equidistant to each conveyor. With the help of the Autocad, the two belt conveyors which formed a 90º angle and a 8 mm gap between two conveyors were drawn.

Input /Output Assignment (Group1)

CH	In	Out
00	Cylinder retract sensor	Cylinder retract
01	Cylinder advance sensor	Cylinder advance
02	Rotary actuator G1 side sensor	Rotary actuator G1 side
03	Rotary actuator G2 side sensor	Rotary actuator G2 side
04	Gripper open sensor	Gripper open
05	Gripper close sensor	Gripper close
06	Photoelectric sensor for workpiece	Motor on
07	Photoelectric sensor for middle position	Send signal to G2 start
08	colour sensor	Workpiece colour
09	Photoelectric sensor for end position	
10	Start button	
11	Reset button	
12	Continuous operation button	
13	Signal from G2 ready	

CONCLUSION

The machine was created using the Mechatronics field as a sorting-out and delivery machine. It consisted of a motor to move the conveyor and table, belt, frame and roller with shaft; two pair of sensors and plates for each group. Most of the parts were machined by using Autocad and wirecut. All the parts mentioned were assembled together to form the machine. The function of the machine was quite simple but it was very important for the smooth operation of the whole robot. There was no doubt that the machine would perform depending on the availability of all the components and the correct set control program.

ACKNOWLEDGEMENT

The financing of this project was provided by JICA Association and is gratefully acknowledged. The author of this paper would also like to thank members of the monitoring project advisory group: Sadao Hatanaka, Takahiro Akiyama and Kae Chogin. The author deeply thank the rector of Mandalay Technological University and her instructor Dr. Kyaw Sein, Professor of School of Mechatronic Engineering, University Malaysia Perlis (UniMap). The author is deeply grateful to her dear parents for their moral support, patience and encouragement throughout her whole life.

Date of submission: December 2011
Date of acceptance: June 2012

REFERENCES

Kobayashi, K 1994, *Mechatro 1~3,* Overseas Vocational Training Association (OVTA).

Miyamoto, K 1994, *Machining Center, Numerically Controlled Series Machine Tool*.

Akabane, N 1993, *Pneumatic Sequence Control, Series 1~3*, Polytechnic Center, Tochigi, Japan.

SMC Corporation, *PneumaticTechnology*, Shimbashi, Minato-ku, Tokyo, Japan.

Takada, Y 1994, *NC Lathe, Numerically Controlled Series Machin Tool*, Polytechnic College, Isikawa.

Kimura, Y 1996, *Programmable Logic Controller*, Toyama Polytechnic Center.

Isoyama, Y 1994, *Sequence Control*, Kimitsu Polytechnic Center.

ASEAN J. Sci. Technol. Dev., **29(1)**, 29 – 49

Implementation of a Communication Satellite Orbit Controller Design Using State Space Techniques

M. T. HLA[1]*, Y. M. LAE[2], S. L. KYAW[3] AND M. N. ZAW[4]
[1]*Department of Electronic Engineering, Mandalay Technological University, Patheingyi Township, Republic of the Union of Myanmar*
[2, 3]*Department of Electronic Engineering, Mandalay Technological University, Patheingyi Township, Republic of the Union of Myanmar*
[4]*Technological University (Maubin), Maubin, Republic of the Union of Myanmar*

This research is of great importance for controlling the altitude of a satellite, especially one used for global communications in a geo-stationary orbit. The objective of this research was to advance a design based on the modelling of an orbit controller for a satellite orbiting into a circular orbit. This encompasses a good understanding of the system's dynamics. Once a satellite is launched into a desired orbit, it never remains in this ideal orbit. The external forces present in space cause perturbations to the ideal orbit. To bring the satellite back into the desired orbit, on-board thrusters provide the in-orbit propulsion. In this research, the altitude of the satellite was controlled by a thruster fashioned by the on-board thrusters installed in the radial and tangential directions. However, dictated by the controllable prerequisite, we achieved dynamic system stabilization with the aid of two thrusters as well as one thruster. Thus, the feedback dynamic control system responded to both the two-input and the single-input cases. The model developed was effectively a linearized, normalized and state-space model. The simulation of this model was based on the MATLAB environment. The design evolved accordingly was used to revise the effect of pole placement on the controlling parameters, such as settling time, peak time, overshoot, and damping ratio of the closed-loop system. This enabled us to make predictions on the stability requirements for several dynamic systems of the type considered. The design tool thus developed was applied to an actual current communication satellite design. The design results were evaluated and recommendations completed.

Key words: orbit controller design; state space analysis; MATLAB; communication satellite; advanced control techniques; simulation; feedback dynamic control system; stability requirements

Satellites offer the unique possibility of interconnecting users, regardless of their location or distance, and providing a complete spectrum of telecommunication services regardless of bandwidth requirements (Richharia & Westbrook 2011). A satellite also needs a guidance system to make sure that it maintains the proper angle in relation to the earth. Communications satellites, weather forecasting satellites and remote-sensing satellites all have different subsystems. These spacecraft require major subsystems. They are the propulsion subsystem, thermal control subsystem, power supply subsystem, telemetry tracking and control subsystem, and altitude and orbit control subsystem. A satellite is launched into its approximate desired orbit by a large rocket, which may be carrying several satellites at the same time. Once a satellite is launched into a desired orbit, it never remains in this ideal

* Corresponding author (e-mail: kohlamyotun@gmail.com)

orbit. This is because the external forces present in space cause perturbations to the ideal orbit. The satellite then uses its own main propulsion system to go into its final orbit, correcting for any unavoidable errors from the initial launch. Once a satellite has achieved its correct orbit, auxiliary rocket engines or thrusters are used to turn the satellite to the correct orientation in relation to the earth and the sun, and to perform many small station-keeping corrections for overcoming orbital distortions. There is a large range of satellite orbits, but not all of them are of use for satellite communications (Dorf & Bishop 2011). The most commonly used orbit for fixed communications is the 24-hour geostationary orbit with an altitude of 35 786 km (Maini & Agrawal 2011). Modern satellite communication systems utilize geostationary satellites because they can provide significant advantages in achieving round-the-clock communications and tracking of the satellite. An altitude control system for a satellite vehicle within the earth's atmosphere is shown in *Figure 1*. The space satellite uses a control system to adjust its angular speed $\omega(t)$ and its angular position $\theta(t)$ for complete control of the satellite. This system requires two inputs in the radial and tangential directions to control the satellite. Thus, a state variable feedback controller is used for the altitude control system. In this research, the design of the controller utilizing state feedback is expressed. The basic principle of the feedback controller is the use of the pole placement technique that provides a unique solution.

Principles of Orbiting Satellites

The motion of natural and artificial satellites around the earth is governed by two forces. One of them is the centripetal force directed towards the centre of the earth due to the earth's gravitational force of attraction, while the other is the centrifugal force that acts outwards from the centre of the earth as shown in *Figure 2*. In the case of a satellite orbiting the earth, the satellite exerts a centrifugal force. In the absence of the earth's centripetal force, the satellite would have continued to move in a straight line at a constant speed after injection. The centripetal force directed at right angles to the satellite's velocity towards the centre of the earth transforms the straight line motion to a circular or elliptical one, depending upon the satellite's velocity. This is in accordance with Newton's third law of motion, which states that for every action there is an equal and opposite reaction (Maral 2009).

Mathematical Model

The planar motion of an orbiting satellite is considered in the inverse-square gravitational field of the earth when carrying out the mathematical modelling of the system. For simplicity's sake, the satellite is approximated to a particle of mass M_s. In the geostationary (circular) orbit, the gravitational force, which follows the universal law of gravity being equal to the required centripetal force, yields the description of the orbit. The orbit can be expressed in terms of the gravity at the orbit.

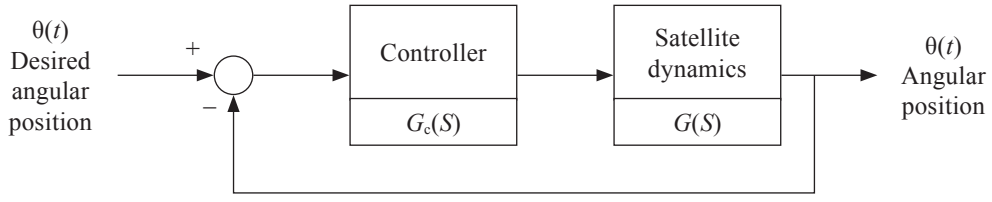

Figure 1. Block diagram of satellite altitude control.

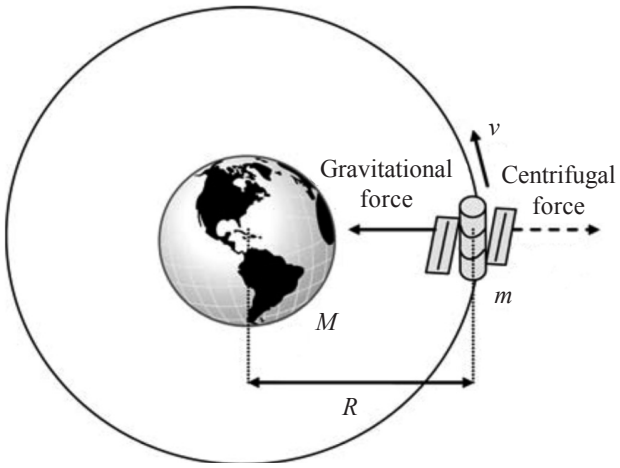

Figure.2. Two forces in orbiting earth.

The earth's varying gravitational field at varying altitudes may be written as:

$$g_{\text{orbit}} = g_{\text{surface}} \left[\frac{R_{\text{earth}}}{r} \right]^2 \tag{1}$$

$$g = g \left(\frac{R_{\text{e}}}{R_e + h} \right)^2 \tag{2}$$

where, R_e = the radius of the earth, and

h = the altitude of the satellite from the surface of the earth.

$$r(t) = R_e + h \tag{3}$$

where, $r(t)$ is the distance from the centre of the earth to the centre of the satellite.

Using Newton's third law of motion to substitute:

$$F_g = M_s g \left(\frac{R_{\text{e}}}{R_e + h} \right)^2 \tag{4}$$

we get:

$$F_g = M_s g \left(\frac{R_{\text{e}}}{r(t)} \right)^2 \tag{5}$$

This system involves a circular motion around a fixed centre, and thrusts are defined with respect to the tangential and radial directions as shown in *Figure 3*. The satellite motion is more conveniently described by its polar co-ordinates. In this situation, it is often more convenient to represent all variables in vector form with complex numbers.

The radial thrust vector is:

$$F_1 = F_1 \text{re}^{j\theta} \tag{6}$$

The tangential thrust vector is:

$$F_2 = F_2 \text{re}^{j(\theta+90)} \tag{7}$$

The gravitational force is:

$$F_g = -M_s g(R^2/r^2)\,\text{re}^{j\theta} \tag{8}$$

The inertial force vector is

$$F = Ma = M_s \frac{d^2 r}{dt^2} \tag{9}$$

Newton's second law can be expressed mathematically as follows: where ΣF is the vector sum of all the forces, M_s is the

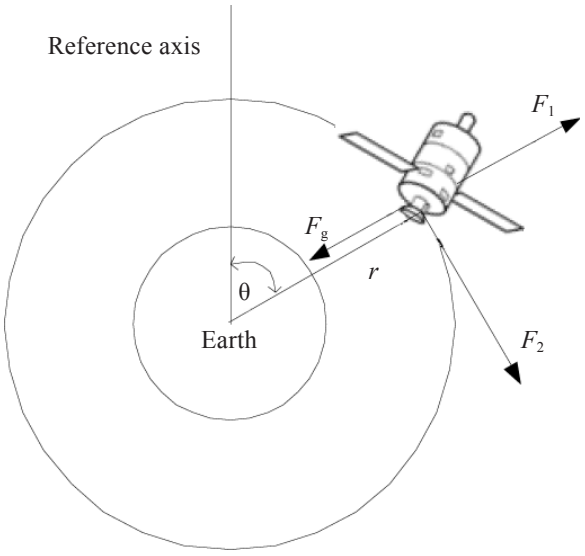

Figure 3. Circular movement of a communication satellite model (Richharia & Westbrook 2011).

mass of the satellite, and is the vector acceleration of the mass measured relative to an interval reference form.

$$\sum F = M_s \ddot{r} \tag{10}$$

$$F_1 + F_2 + F_3 = M_s \frac{d^2 r}{dt^2} = M_s \frac{d^2}{dt^2} \left[\mathrm{r(t)re}^{j\theta} \right] \tag{11}$$

Therefore,

$$F_1 e^{j\theta} + jF_2 e^{j\theta} - M_s g \left(\frac{R^2}{r^2} \right) e^{j\theta} = M_s \left[\ddot{r} e^{j\theta} - r\dot{\theta}^2 e^{j\theta} + j(r\dot{\theta} e^{j\theta} + 2\dot{\theta}\dot{r} e^{j\theta}) \right] \tag{12}$$

$$\left[F_1 - M_s g \left(\frac{R^2}{r^2} \right) e^{j\theta} \right] + jF_2 e^{j\theta} = \left[(M_s \ddot{r} - M_s r\dot{\theta}^2) e^{j\theta} + j(M_s \dot{r}\ddot{\theta} + 2M_s \dot{\theta}\dot{r}) e^{j\theta} \right] \tag{13}$$

By cancelling the common factor and equating the real part and the imaginary part, respectively, of *Equation 13*, two second-order differential equations are produced:

$$F_1 = M_s \ddot{r} - M_s r\dot{\theta}^2 + M_s g \left(\frac{R^2}{r^2} \right) \tag{14}$$

$$F_2 = M_s \dot{r}\ddot{\theta} + 2M_s \dot{\theta}\dot{r} \left(\frac{R^2}{r^2} \right) \tag{15}$$

Hence, *Equation 14* and *Equation 15* can be rewritten as follows:

$$\frac{F_1}{M_s g} = \frac{\ddot{r}}{g} - \frac{r\dot{\theta}^2}{g} + \frac{R^2}{r^2} \tag{16}$$

$$\frac{F_2}{M_s g} = \frac{r\ddot{\theta}}{g} + \frac{2\dot{\theta}\dot{r}}{g} \tag{17}$$

To simplify the numerical problem, the time, distance and force variables are normalized into dimensionless quantities.

$$\text{Let } \tau = \frac{\tau}{\left(\frac{R}{g}\right)^{1/2}} \; ; \rho = \frac{r}{R};$$

$$u_1 = \frac{F_1}{M_s g} \; ; u_1 = \frac{F_2}{M_s g} \tag{18}$$

where, τ = settling time, ρ = constant, u_1 = radial thruster force, u_2 = tangential thruster force; then:

$$u_1 = \frac{\ddot{r}}{g} - \frac{r\dot{\theta}^2}{g} + \frac{R^2}{r^2} \tag{19}$$

Further,

$$u_2 = \frac{r\ddot{\theta}}{g} + \frac{2\dot{\theta}\dot{r}}{g} \tag{20}$$

When we wish to change from the function (t) to the function (τ), we can use the following relationship:

$$r = \frac{dr(t)}{dt} = \frac{d}{d\tau}\left(\frac{g}{R}\right)^{1/2} r(\tau) \tag{21}$$

This *Equation 21* may be rewritten as:

$$\dot{r}(t) = \acute{r}\,(t) \times \left(\frac{g}{R}\right)^{1/2} \tag{22}$$

$$\ddot{r}(t) = r''(t) \times \left(\frac{g}{R}\right)^{1/2} \times \left(\frac{g}{R}\right)^{1/2}$$

$$= r''(t) \times \left(\frac{g}{R}\right) \tag{22}$$

Similarly, $\dot{\theta}(t) = \dot{\theta}(\tau) \times \left(\frac{g}{R}\right)^{1/2}$ (24)

$$\dot{\theta}^2(t) = \dot{\theta}^2(\tau)\left(\frac{g}{R}\right) \tag{25}$$

$$\acute{\theta}^2(t) = \acute{\theta}^2(\tau)\left(\frac{g}{R}\right) \tag{26}$$

By substituting *Equation 22* and *Equation 23* into *Equation 26*,

$$u_1 = \rho'' - \rho\acute{\theta}^2(\tau) + \left(\frac{1}{\rho^2}\right) \tag{27}$$

Then,

$$u_2 = 2\acute{\rho}(\tau)\acute{\theta}(\tau) + \rho\theta''(\tau) \tag{28}$$

The system of the first-order ordinary differential equations is considered. By defining the four-state variables as below, this will result in a set of differential equations.

Let $x_1 = \rho$; $x_2 = \theta$; $\dot{x}_1 = \dot{\rho} = \dot{x}_1 = \dot{\rho} = x_3$;
$\dot{x}_2 = \dot{\theta} = x_4$; $\dot{x}_3 = \ddot{\rho}$; $\dot{x}_4 = \ddot{\theta}$

$$\text{Hence, } \rho'' = u_1 + \rho\acute{\theta}^2(\tau) - \frac{1}{\rho^2} \tag{29}$$

This *Equation 27* may be rewritten as:

$$\acute{x}_3 = x_1 x_4^2 - \frac{1}{x_4^2} + u_1 \tag{30}$$

Hence, from Equation 28

$$\acute{x}_4 = -\frac{2x_3 x_4}{x_1} + \frac{1}{x_1} u_2 \tag{31}$$

Thus, a non-linear state model is obtained as given below:

$$x_1' = x_3, \dot{x}_2 = x_4 \tag{32}$$

$$x_3' = x_1 x_4^2 - \frac{1}{x_4^2} + \mathrm{u}_1 \tag{33}$$

$$x_4' = -\frac{2x_3 x_4}{x_1} + \frac{1}{x_1}\mathrm{u}_2 \tag{34}$$

Linearized System Model

A mathematical model of a geostationary communications satellite in the earth's equatorial plane was derived. It was necessary the system to have a linearized state-space model with the geostationary orbit. The non-linear state model equation can be solved by using the Jacobian matrix to obtain the linearized equation (Dorf & Bishop 2011).

The Jacobian matrix equation of:

$$f_1(x_1, x_2, x_3, x_4) = [f_1(x_1, x_2, x_3, x_4), f_1(x_1, x_2, x_3, x_4), f_1(x_1, x_2, x_3, x_4), f_1(x_1, x_2, x_3, x_4)]^T$$

is evaluated at $(x_1, x_2, x_3, x_4)^T = (0,0,0,0)^T$

$$J(0) = A = \begin{bmatrix} 0 & 0 & 1 & 0 \\ 0 & 0 & 0 & 1 \\ x_4^2 + \frac{2}{x_1^3} & 0 & 0 & 2x_1 x_4 \\ 0 & 0 & \frac{-2x_4}{x_1} & 0 \end{bmatrix} \tag{35}$$

Thus, the linearized and normalized equations of motion in the geostationary orbit are given by:

$$\begin{bmatrix} \delta x_1' \\ \delta x_2' \\ \delta x_3' \\ \delta x_4' \end{bmatrix} = \begin{bmatrix} 0 & 0 & 1 & 0 \\ 0 & 0 & 0 & 1 \\ x_4^2 + \frac{2}{x_1^3} & 0 & 0 & 2x_1 x_4 \\ 0 & 0 & \frac{-2x_4}{x_1} & 0 \end{bmatrix} \begin{bmatrix} \delta x_1 \\ \delta x_2 \\ \delta x_3 \\ \delta x_4 \end{bmatrix} + \begin{bmatrix} 0 & 0 \\ 0 & 0 \\ 1 & 0 \\ 0 & \frac{1}{x_1} \end{bmatrix} \begin{bmatrix} u_1 \\ u_2 \end{bmatrix} \tag{36}$$

Therefore, according to *Equation 36*, we can express the following:

$$x_1 = \rho = \frac{r}{R_e} = \frac{R_e + h_0}{R_e} \tag{37}$$

$$x_2 = \theta \tag{38}$$

$$x_3 = \dot{\rho} = 0 \tag{39}$$

$$x_4 = \dot{\theta} = \omega_0 \tag{40}$$

According to the above statements, the other type of state model equation is:

$$\begin{bmatrix} \delta x_1' \\ \delta x_2' \\ \delta x_3' \\ \delta x_4' \end{bmatrix} = \begin{bmatrix} 0 & 0 & 1 & 0 \\ 0 & 0 & 0 & 1 \\ \omega^2 + \dfrac{2}{\rho^3} & 0 & 0 & 2r\omega \\ 0 & 0 & \dfrac{-2\omega}{r} & 0 \end{bmatrix} \begin{bmatrix} \delta x_1 \\ \delta x_2 \\ \delta x_3 \\ \delta x_4 \end{bmatrix} + \begin{bmatrix} 0 & 0 \\ 0 & 0 \\ 1 & 0 \\ 0 & \dfrac{1}{r} \end{bmatrix} \begin{bmatrix} u_1 \\ u_2 \end{bmatrix} \tag{41}$$

Steady State Components of Two-thrust Vectors

For geometric consideration, a satellite in a stable circular orbit around the earth can be expressed as $F_{\text{gravity}}=F_{\text{centripetal}}$. From this relationship, the period of the orbit and the orbital velocity or angular velocity of the satellite can be calculated. The most commonly used satellite orbit for fixed communications is the 24-hour geostationary (circular) orbit with an altitude of 35 786 km. The satellite period of rotation around the earth is 86 157.8836 s, or 23 h, 55 min and 77 s, and the angular velocity is 15.04 degrees per hour. Once the simulation is generated, a generalized case of the satellite orbiting into a circular orbit at any altitude can be created. The altitude choice and the technique for the synchronous satellite are provided by applying the illustration of coverage area and geometric satellite orbits. Using empirical values (R_e=6378 km, h=35 786 km, r=42 164 km, g=9.8087 m/s^2), the apex angle 2α equals 17.4 degrees, while the planar angle beamwidth. Now suppose the satellite is to be maintained in a circular geostationary orbit of the earth. The steady state is maintained only by the gravitational force, so that the steady state components of two-thrust vectors are zero. To minimize energy consumption, thrusts are only applied to take transient corrective action to eliminate error.

u_1=0, u_2=0

x_3=0, x_4 (angular speed) is a constant.

Therefore, x_4 and all the remaining variables can be determined.

$$\omega = 15.04 \text{ deg/h} = \frac{\pi}{43\,200} \text{ rad per sec.}$$

This corresponds to a normalized angular speed of:

$$x_4 = (R/g)^{1/2}\omega = 0.05866$$

The satellite maintains a nominal orbit as long as there are no disturbances. If the perturbations are sufficiently small (E<<1), they may be described by a linearized system. Here, the non-linear

model and linearized model equations are both of the fourth order, and apply to situations in which not only the angular speed $x_4=(t)$ or $\omega(t)$ needs to be regulated, but also the angular position $\theta(t)$ must be accurately controlled for complete control of the satellite. So far, this all implies that the system requires two inputs in the radial and tangential directions to control the satellite. However, the system will be further checked to find out the different possibilities for controllability of the system.

In the state space equation, R_e=6378 km and h_0=35 786 km,

$$x_1 = \frac{r}{R} = \frac{R_e + h_0}{R_e} = \frac{6378 \text{ km} + 35\,786 \text{ km}}{6378 \text{ km}} = 6.6108$$

$$\omega = 15.04 \text{ deg/h} = \frac{\pi}{43\,200} \text{ rad per sec} = 7.2915 \times 10^{-5} \text{ rad/s}$$

$$\text{Normalized angular speed or } \omega = \left(\frac{R}{g}\right)^{1/2} \times 7.2915 \times 10^{-5} = 0.05873$$

$$A = \begin{bmatrix} 0 & 0 & 1 & 0 \\ 0 & 0 & 0 & 1 \\ x_4^2 + \frac{2}{x_1^3} & 0 & 0 & 2x_1x_4 \\ 0 & 0 & \frac{-2x_4}{x_1} & 0 \end{bmatrix} + \begin{bmatrix} 0 & 0 & 1 & 0 \\ 0 & 0 & 0 & 1 \\ 0.01036 & 0 & 0 & 0.7753 \\ 0 & 0 & -0.1774 & 0 \end{bmatrix} \quad (42)$$

The linearized and normalized equations of motion in the geostationary orbit are given by:

$$\begin{bmatrix} \delta x_1' \\ \delta x_2' \\ \delta x_3' \\ \delta x_4' \end{bmatrix} = \begin{bmatrix} 0 & 0 & 1 & 0 \\ 0 & 0 & 0 & 1 \\ 0.01036 & 0 & 0 & 0.7753 \\ 0 & 0 & -0.1774 & 0 \end{bmatrix} \begin{bmatrix} \delta x_1 \\ \delta x_2 \\ \delta x_3 \\ \delta x_4 \end{bmatrix} + \begin{bmatrix} 0 & 0 \\ 0 & 0 \\ 1 & 0 \\ 0 & 0.1511 \end{bmatrix} \begin{bmatrix} u_1 \\ u_2 \end{bmatrix} \quad (43)$$

Position Control with Two-thrust State Feedback

In the first case, the satellite is being controlled by radial and tangential thrusts. Then the satellite can be regulated by its angular speed $x_4(t)$ or $\omega(t)$. The angular position $\theta(t)$ must also be controlled, and it is assumed that all the four state variables are available. The multi-input state variable systems require feedback control. This feedback system can de-couple into two single-input to overcome the two-input problem as shown in *Figure 4*. Here, the state variables δx_1 and δx_3 are responsible for changing the radial position of the satellite, while the state variables δx_2 and δx_4 cause a change to the angular position of the satellite.

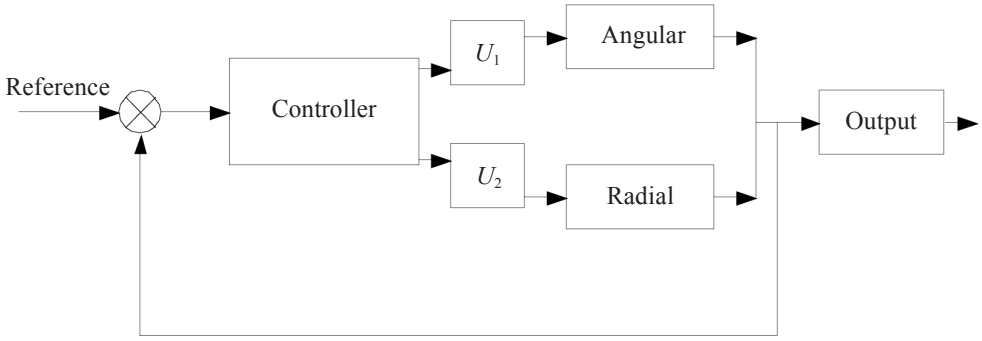

Figure 4. Decoupled two single-input feedback (Malik, Zaidi & Khushnood 2001).

While carrying out the de-coupling, the third row of matrix A from the linearized model equations can be arbitrarily changed with the state feedback applied to u_r (or u_1).

$$\begin{bmatrix} \delta x_1' \\ \delta x_2' \\ \delta x_3' \\ \delta x_4' \end{bmatrix} = \begin{bmatrix} 0 & 0 & 1 & 0 \\ 0 & 0 & 0 & 1 \\ 0.01036 & 0 & 0 & 0.7753 \\ 0 & 0 & -0.1774 & 0 \end{bmatrix} \begin{bmatrix} \delta x_1 \\ \delta x_2 \\ \delta x_3 \\ \delta x_4 \end{bmatrix} + \begin{bmatrix} 0 \\ 0 \\ 1 \\ 0 \end{bmatrix} \begin{bmatrix} u_1 \end{bmatrix} \tag{44}$$

Then, let $u_{1a} = -0.01036\delta x_1 - 0.7753\delta x_4$, putting it in the third row of the linearized model equations.

So, a single-input second-order system can be written as:

$$\delta x_1' = \delta x_3 \tag{45}$$

$$\delta x_3' = 0.01036\delta x_1 + 0.7753\delta x_4 - 0.01036\delta x_1 - 0.7753\delta x_4 \tag{46}$$

$$\delta x_3' = u_{1b} \tag{47}$$

thus, producing a single-input second-order system as in *Equation 48*.

$$\delta x_1' = \delta x_3,\ \delta x_3' = u_{1b} \tag{48}$$

Control of the radial variables is separated from the state model equation. Thus, the above second-order model equation describes the control of the angular variables. The response of the double-integrator system equation can easily be controlled to provide a desired characteristic equation.

Applying the inverse Laplace transformation on both sides of the equation:

$$y'' + 2\xi\omega_n y' + \omega_n^2 y = 0 \tag{49}$$

Let $\delta x_1 = y$, $\delta x_1' = y' = \delta x_3$, $\delta x_3' = y'' = -2\xi\omega_n y' - \omega_n^2 y$, $\delta x_3' = u_{1b} = -2\xi\omega_n y' - \omega_n^2 y$

and by selecting ξ=0.707(say) to meet the overshoot requirement, the settling time of 12 hours can expressed by:

$$\tau_s = \frac{4}{\xi\omega_n} = 53.5731 \tag{50}$$

$$\omega_n = 0.1056 \tag{51}$$

The settling time specification is then easily translated into $\omega_n = 0.1056$. The second-order model equation becomes:

$$\delta x_1' = \delta x_3 \tag{52}$$

$$\delta x_3' = -0.0115\delta x_1 - 0.1493\delta x_3 \tag{53}$$

Hence, the overall state feed law for the radial thrust is:

$$u_1 = -0.0215\delta x_1 - 0.1493\delta x_3 - 0.7753\delta x_4 \tag{54}$$

In exactly the same manner, the angular dynamics described in the second and the fourth rows of the matrix A of the state-model equation can be de-coupled with state feedback applied to the tangential thrust u_t (or u_2).

$$\begin{bmatrix} \delta x_1' \\ \delta x_2' \\ \delta x_3' \\ \delta x_4' \end{bmatrix} = \begin{bmatrix} 0 & 0 & 1 & 0 \\ 0 & 0 & 0 & 1 \\ 0.01036 & 0 & 0 & 0.7753 \\ 0 & 0 & -0.1774 & 0 \end{bmatrix} \begin{bmatrix} \delta x_1 \\ \delta x_2 \\ \delta x_3 \\ \delta x_4 \end{bmatrix} + \begin{bmatrix} 0 \\ 0 \\ 0 \\ 0.1511 \end{bmatrix} \begin{bmatrix} u_2 \end{bmatrix} \tag{55}$$

Let $u_{2a} = \frac{0.1774}{0.1511}\ \delta x_3 = 0.1774\delta x_3$, putting it in the third row of the linearized model equations.

So, a single-input second-order system can be written as:

$$\delta x_1' = \delta x_3', \ \delta x_4' = 0.1511 u_{2b} \tag{56}$$

thus, producing a single-input second-order system as in *Equation 55*

$$\delta x_1' = \delta x_3'; \ \delta x_4' = 0.1511 u_{2b} \tag{57}$$

Control of the tangential variables is separated from the state model equation. Thus, the above second-order model equation describes the control of the angular variables. The response of the double-integrator system equation can easily be controlled to provide a desired characteristic equation.

Similarly, the two-input state feedback equations are:

$$u_1 = 0.0215\delta x_1 - 0.1493\delta x_3 - 0.7753\delta x_4 \tag{58}$$

$$u_1 = 0.07379\delta x_1 - 0.1174\delta x_3 - 0.9881\delta x_4 \tag{59}$$

Therefore, the two-input state feedback control takes the form as follows:

$$u = \begin{bmatrix} -0.02151 & 0 & -0.1493 & -0.7753 \\ 0 & -0.07379 & 0.1174 & -0.9881 \end{bmatrix} \begin{bmatrix} \delta x_1' \\ \delta x_2' \\ \delta x_3' \\ \delta x_4' \end{bmatrix} \tag{60}$$

In this way, the satellite altitude can be controlled by the use of two thrusts in the radial and tangential directions which help in controlling both the angular speed $x_4(t)$ and $\omega(t)$, and the angular position $\theta(t)$ of the satellite with the application of the control parameters.

State Feedback Control of Angular Rate with the Tangential Thrust

After checking the controllability of the model equation, it was revealed that the satellite could also be controlled by only a single radial thrust by controlling the angular rate $\omega(t)$ of the satellite but with a constant non-zero offset error in the angular position $\theta(t)$. Moreover, this controlling technique can be employed in a situation where the radial thruster has failed and only the tangential thrust is applied to the MATLAB's ctrb function. This reduced model equation with the elimination of the radial thrust u_1 of the third order is shown in *Equation 40*. The 'C' matrix is essentially the required parameters that are of value from the input values.

$$\begin{bmatrix} \delta x_1' \\ \delta x_2' \\ \delta x_3' \end{bmatrix} = \begin{bmatrix} 0 & 1 & 0 \\ 0.01036 & 0 & 0.7753 \\ 0 & -0.01774 & 0 \end{bmatrix} \begin{bmatrix} 0 \\ 0 \\ 0.1512 \end{bmatrix} [\, u_2 \,] \tag{61}$$

$$y = Cx + Du,\ y = [1 \quad 0 \quad 0 \quad 0],\ D = 0 \tag{62}$$

Pole Placement Using State Feedback

This is a single-input system problem, which can be easily solved by pole placement that is able to provide a unique solution. In this situation, the three state variables are available for providing feedback. Energy efficiency consideration is one of the important factors in an aerospace system. Normally, pole placement is achieved by moving poles at least five times to the left of the s-plane compared with the dominant ones, thus making the analysis and design easier. This usually requires the use of a large control input, which is not feasible in an aerospace system. The input energy requirement can often be reduced if all the closed-loop poles are placed at about the same distance from the origin. Thus, the three poles are placed at an equal distance from the origin.

$$s_1 = \omega_n e^{j120}, s_2 = \omega_n e^{-j120}, s_3 = \omega_n e^{j180} = \omega_n, (\cos 180 + j\sin 180) = -\omega_n \quad (63)'$$

For such three-pole systems, the third pole at $s_3 = -\omega_n$ usually has an effect of lowering the overshoot and reducing the settling time. Thus, a conservative estimate of transient performance can be obtained by ignoring s_3 and considering only the effects of s_1 and s_2. For this system, the damping ratio chosen is $\xi=\cos 60=0.5$, which corresponds to 17% overshoot. This implies that the system requires a 2% settling time of 12 h, i.e. 53.53731 seconds as shown in *Equation 50* in the previous discussion can be expressed.

$$\tau_s = \frac{4}{\xi\omega_n} = 53.5731, \omega_n = 0.1495 \quad (64)$$

In this way, the state feedback gain for the third-order state model can be determined when all the closed-loop poles are placed at an equal distance from the origin, and correspond to a damping ratio of $\xi=0.5$ and $\omega_n=0.1495$. The desired characteristic equation is then $s^3+0.22395s^2+0.033435s+0.00166=0$.

For the third-order system with a close-loop transfer function, the equation is:

$$T(s) = \frac{1}{(s + \xi\omega_n)(s^2 + 2\xi\omega_n s + \omega_n^2)} \quad (65)$$

The three-state variable feedback shown in $\dot{x} = Ax + Bu$ are selected.

$$\begin{bmatrix} \delta x_1' \\ \delta x_2' \\ \delta x_3' \end{bmatrix} = \begin{bmatrix} 0 & 1 & 0 \\ 0.01036 & 0 & 0.7753 \\ 0 & -0.01774 & 0 \end{bmatrix} \begin{bmatrix} 0 \\ 0 \\ 0.1512 \end{bmatrix} [\, u_2 \,] \quad (66)$$

If the state variable matrix K is $K=[k_1\ k_2\ k_3]$, and the feedback of the state variables is $u = -Kx$, then $\dot{x} = Ax - BKx = (A - BKx)$.

The state feedback matrix is:

$$\dot{x} = \begin{bmatrix} 0 & 1 & 0 \\ 0.01036 & 0 & 0.7754 \\ 0 & -0.01774 & 0 \end{bmatrix} - \begin{bmatrix} 0 \\ 0 \\ 0.1511 \end{bmatrix} [\, k_1 \quad k_2 \quad k_3 \,] \quad (67)$$

$$\det [A - BK] = s^2 + 0.1511s^2 + (0.00345 + 0.1174)s - 0.0016k_3 + 0.1175k_1 \quad (68)$$

when comparing with the values of k, $k_1=0.0343$, $k_2=0.2553$, and $k_3=1.48$.

This shows that the pole placement requires k_1=0.0343, k_2 =0.2553, k_3=1.48. Hence, the state feedback gain for the system with the desired pole placement is:

$$K = (0.0343 \quad 0.2553 \quad 1.48) \tag{69}$$

After computing the state feedback gain vector, the close-loop transfer function is considered for steady-state tracking. The open-loop state equation is specified by the following coefficient matrices although they are in controller form.

$$A = \begin{bmatrix} 0 & 1 & 0 \\ 0.01036 & 0 & 0.7753 \\ 0 & -0.01774 & 0 \end{bmatrix}, B = \begin{bmatrix} 0 \\ 0 \\ 0.1512 \end{bmatrix}, C = [1 \quad 0 \quad 0] \tag{70}$$

The open-loop transfer function is, by inspection,

$$H(s) = \frac{0.1171s}{s^3 + 0.00339s} \tag{71}$$

The state feedback gain was computed to be K = [0.0343 0.2553 1.48]

The close-loop transfer function is:

$$C(sI - A - BK)^{-1} B = \frac{0.1171}{s^3 + 0.2236s^2 + 0.03337s + 0.00171} \tag{72}$$

Simulation Results

The mathematical model of the system and the implementation for the control system will be described below. The orbit controller is then designed for the purpose of keeping the satellite in its nominal orbit.

Checking the system stability. The impulse response curve was plotted to investigate the system's stability. The angular velocity was 0.001 rad/s, which was a 90-min orbit in *Figure 5*. This figure shows that the control input u_1 affected the output y_2, and that u_2 influenced both outputs y_1 and y_2. The impulse response kept growing which showed that the system was unstable.

Figure 6 shows the pole-zero map of the four-state variable model which established whether the system was stable or unstable. This figure shows that the system was unstable because the poles were situated on the right-hand side of the s-plane.

Figure 7 shows the impulse responses when the angular velocity was 7.3×10^{-5}. This corresponded to a 24-hour orbit (the geostationary orbit). As shown in the figure, the control input u_1 affected output y_2, and u_2 influenced both outputs y_1 and y_2. The impulse response kept

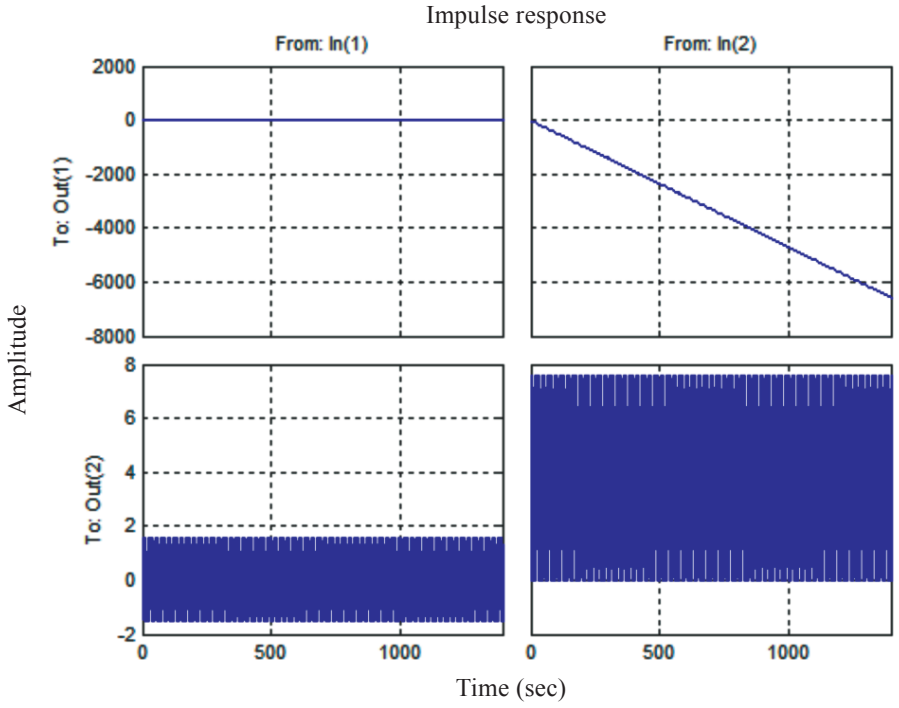

Figure 5. Impulse response of a four-state model in low earth orbit.

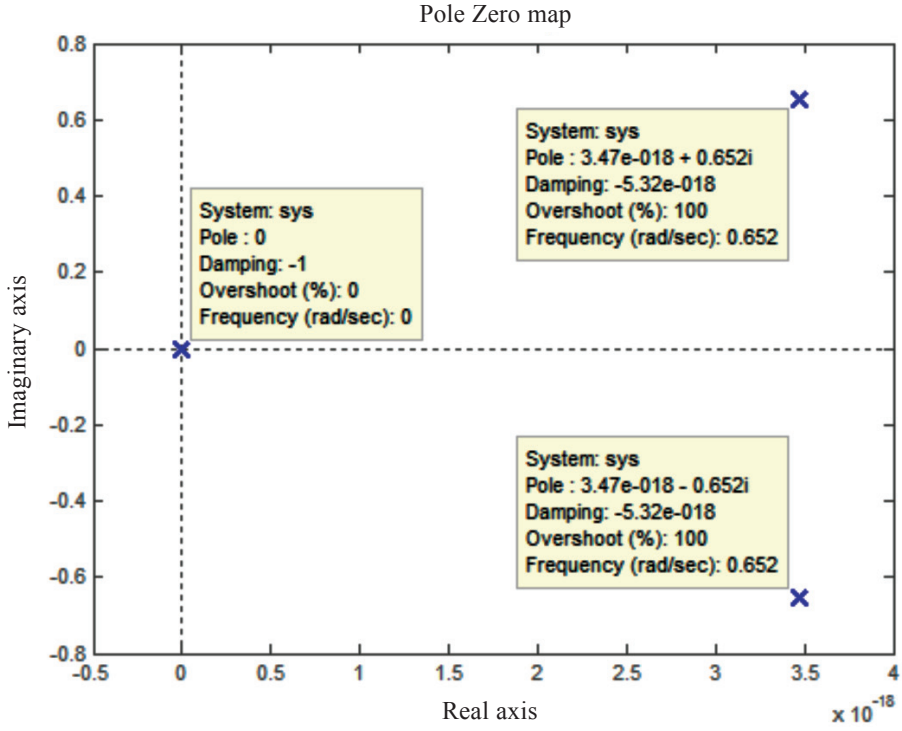

Figure 6. Pole-zero map of the four-state model in low earth orbit.

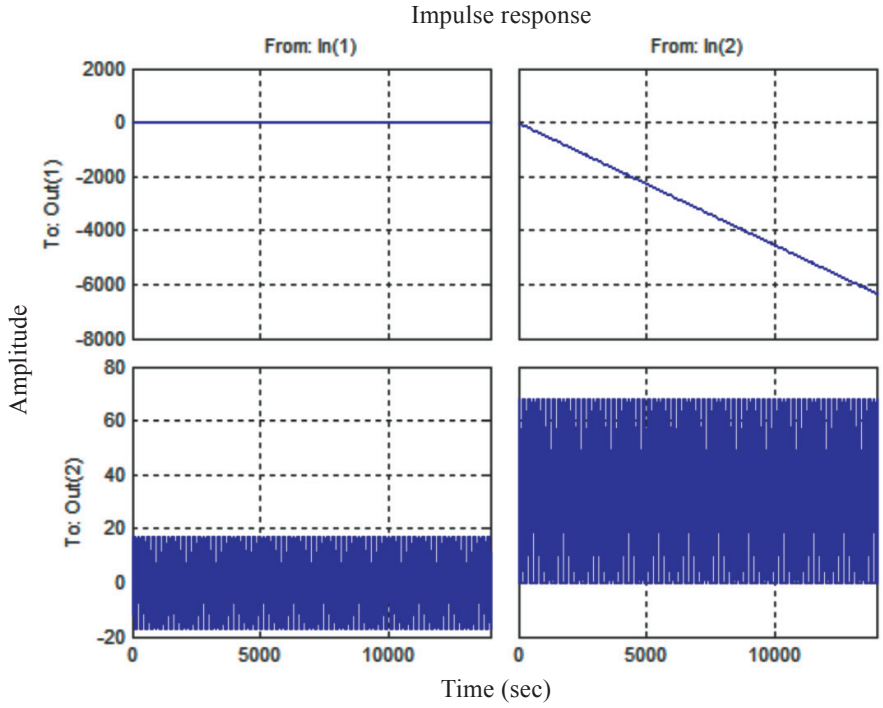

Figure 7. Impulse response of the four-state model in geostationary orbit.

growing, showing the system to be unstable. *Figure 8* shows the pole-zero map of the four-state variable model to establish whether the system was stable or unstable. As the system had repeated poles on an imaginary axis, it was marginally stable. Consequently, the system needed to be controlled so that the poles would be shifted to the left-hand side of the s-plane to ensure stability.

Checking the three-state model. *Figure 9* illustrates the pole-zero map of the three-state variable model to establish whether the system was stable or unstable. With the poles located on an imaginary axis, the system was marginally stable. Therefore, the system needed to be controlled so that the poles would be shifted to the left-hand side of the s-plane to ensure stability. As shown in *Figure 10*, the impulse responded when the angular velocity was 7.3×10^{-5}. For the three state variables, it may be seen in *Figure 10* that the input influenced the output. This system was unstable according to the impulse response. Therefore, this system was considered a close-loop system with state variable feedback.

Pole placement configuration. The desired pole location of the system was established to determine whether the state feedback controller was stable or unstable. The desired poles were located at –1, 0.0748+j0.129 and 0.0748 – 0.129. The overshoot was 16.3% and the damping ratio was 0.5 as shown in *Figure 11*. A step response was illustrated for the third-order system with a close-loop transfer function as shown in *Figure 12*. For this system, the damping ratio was chosen at ξ=0.5, which corresponded to a 17% overshoot and a settling time of 2%. This system was in a stable condition for about 80 seconds. The impulse response of the third-order system is as shown in *Figure 13*.

Initial condition of the three-state matrix. The response of the system to the given

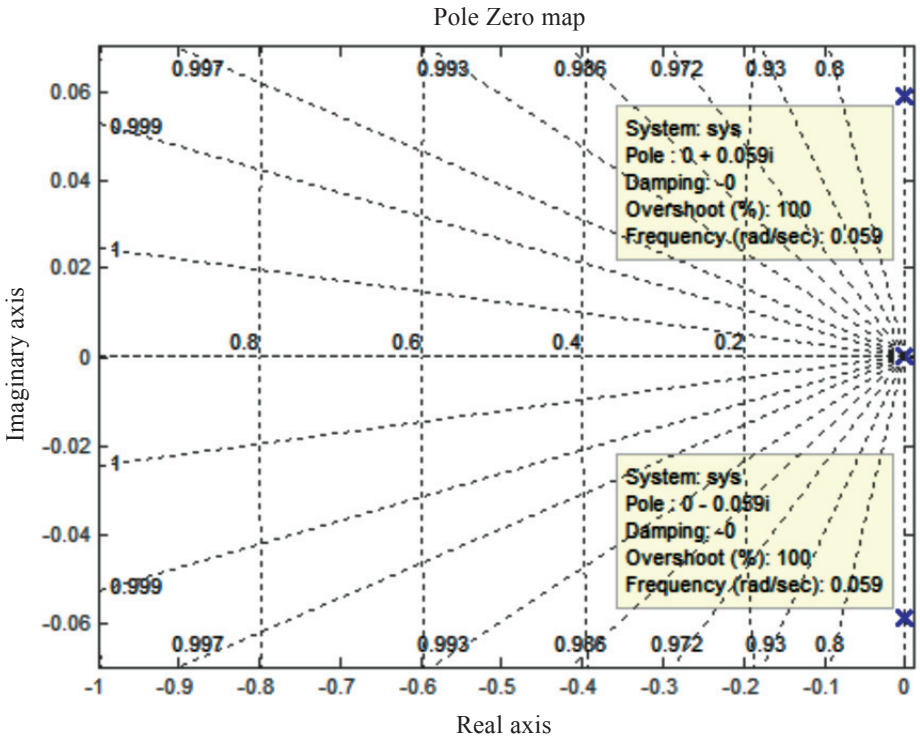

Figure 8. Pole-zero map of the four-state model in geostationary orbit.

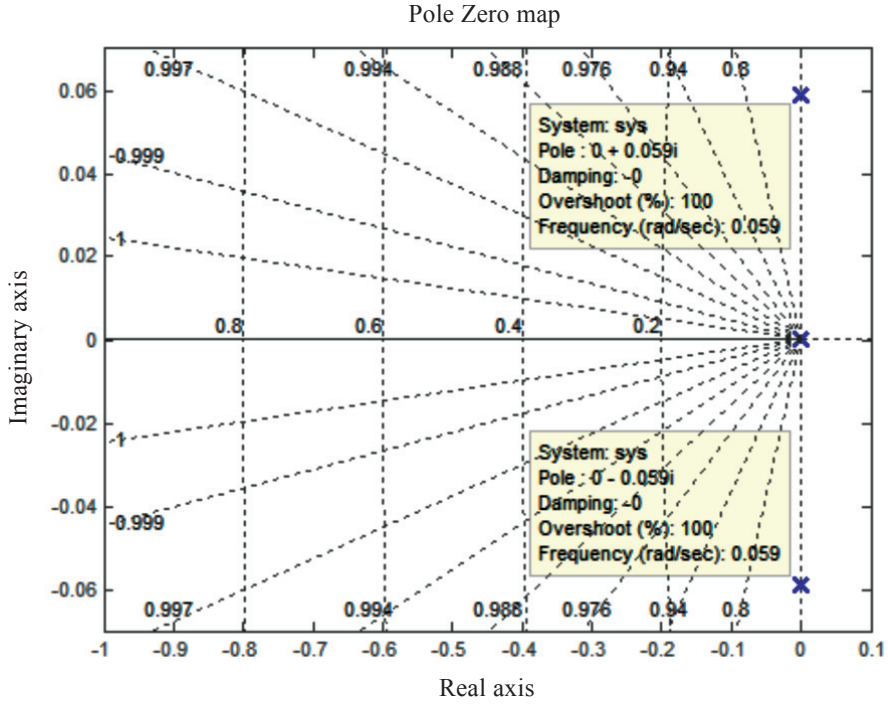

Figure 9. Impulse response of an open-loop system.

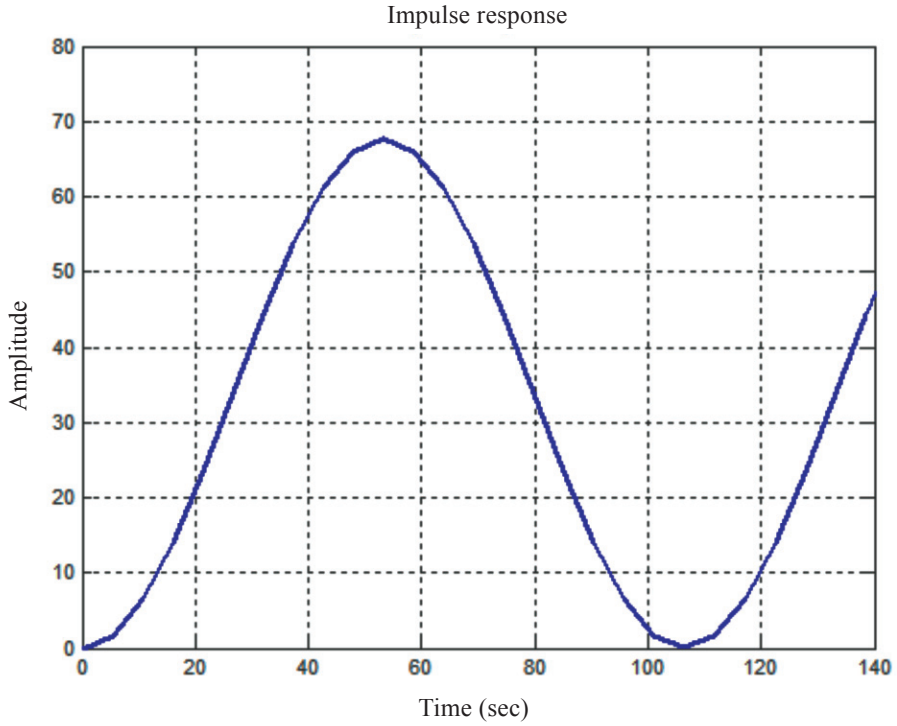

Figure 10. Step response of an open-loop system.

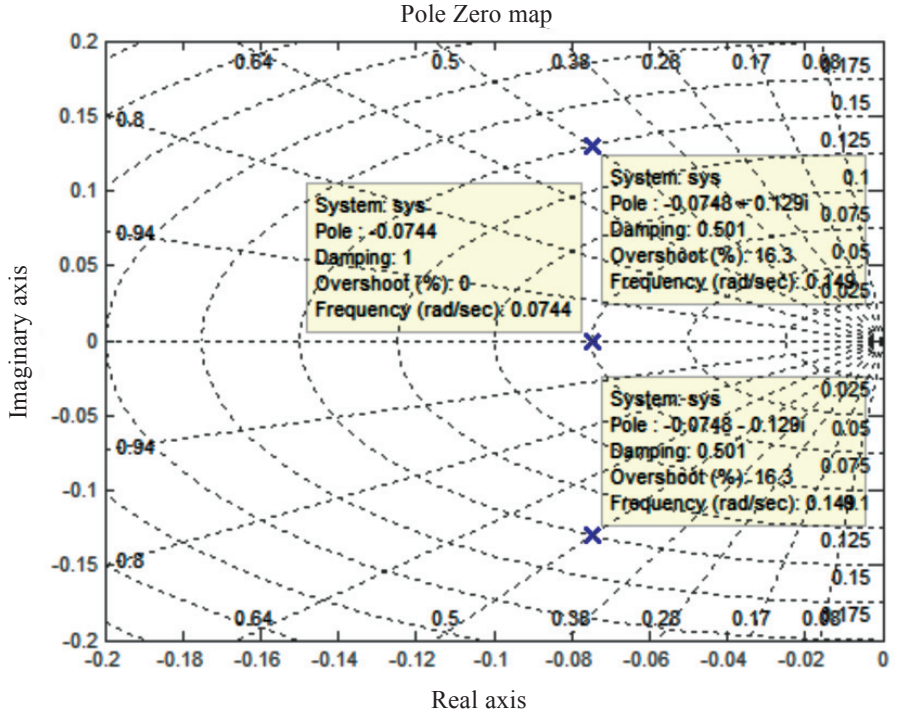

Figure 11. Pole placement configuration.

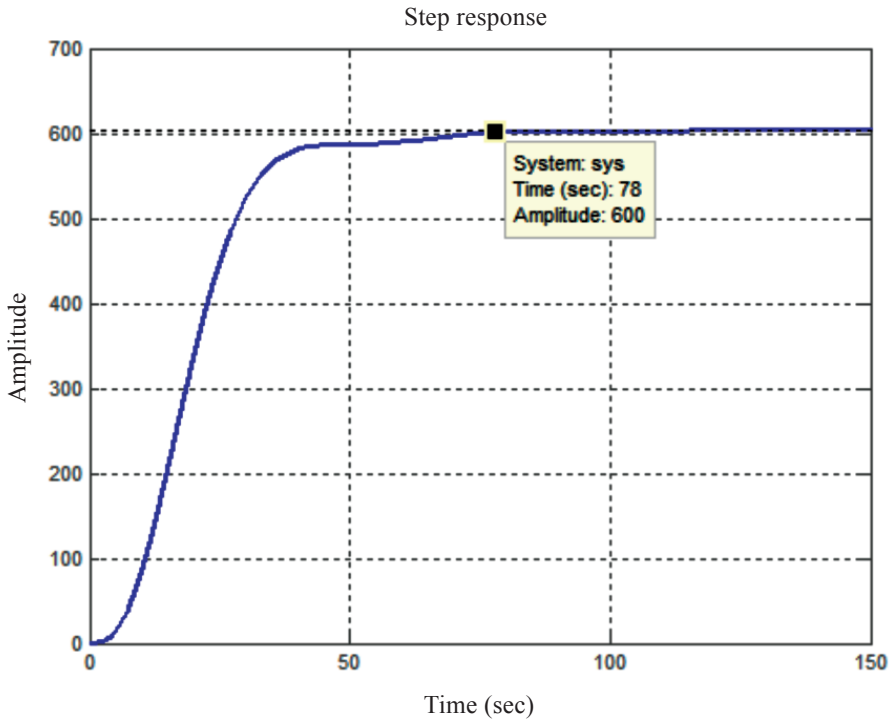

Figure 12. Step response of a state feedback controller.

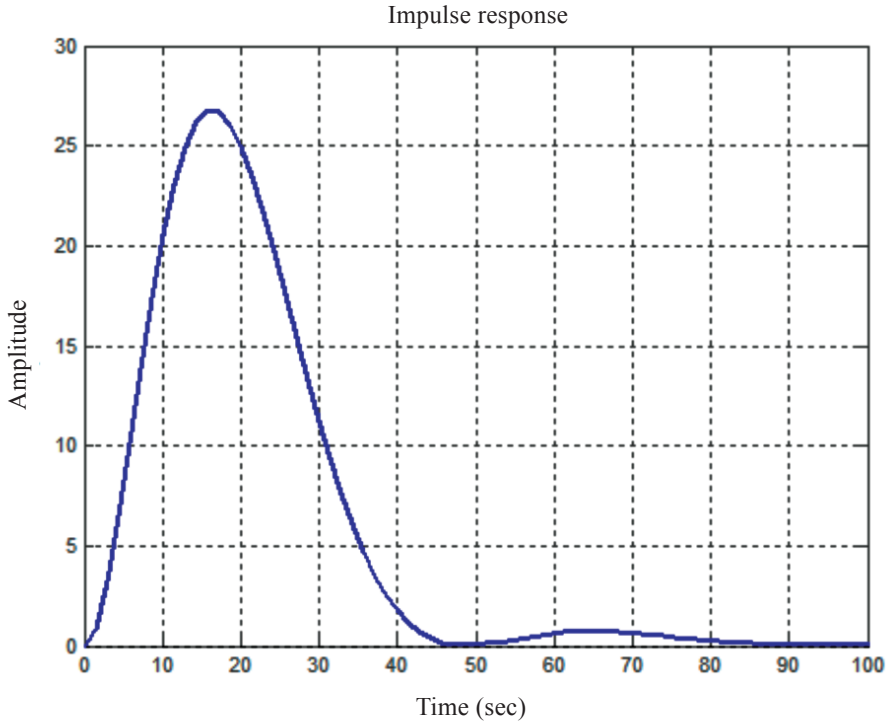

Figure 13. Impulse response of a state feedback controller.

initial condition was determined. The resulting response curves are shown in *Figure 14*. The response curves were acceptable for the system.

Linear state feedback. *Figure 15* shows the impulse response of a closed-loop system. The closed-loop system was formulated by using a state feedback control law with a gain matrix. The step response of the closed-loop system is shown in *Figure 16*. The settling time was 78.8 seconds. *Figure 17* shows the linear simulation results of the closed-loop system. The time response of continuous linear systems to arbitrary inputs was simulated.

CONCLUSION

This work was initially done to study and analyze theoretically the orbit controller for a geostationary satellite. After generating the simulation for the supposed orbit controller, it was compared with the standard design for an orbit controller. The proposed orbit controller design could be linked to a communication satellite by comparing it with the simulation approaches of the existing system. Confirmation of the supposed design was ascertained and verified by running the simulation with the parameters of the orbit controller of standard design. To implement the orbit controller of the satellite, the stable state model is needed. It should be tried with more data and parameters before the controller is chosen. For any satellite to progress from a concept to an actual orbiting satellite, properties such as stability and control derivatives, which determine the characteristics of the satellite, must be determined. This research has attempted to design an orbit controller for a satellite orbiting in a circular orbit. The purpose of the research was to create a mathematical model for the circular orbit. These data of the selected orbit were based on the current satellite technology, which includes modelling analysis. The orbit controller was established by the state space equations. The assigned poles and close-loop eigenvalues stabilized the system. The controllability of the system *via* state feedback was in an adequate condition. In situations where the plant was not controllable, using the feedback controller

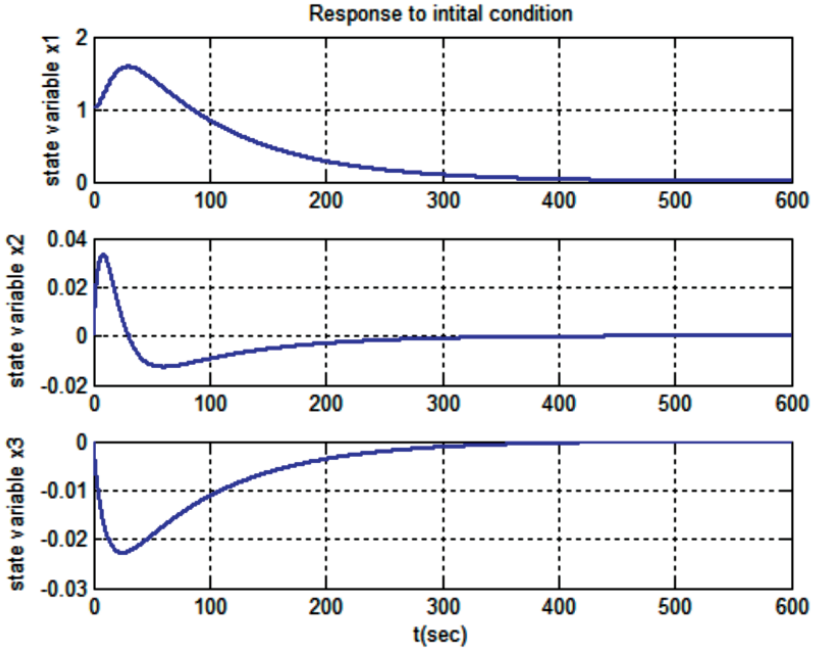

Figure 14. Response curve of the initial condition.

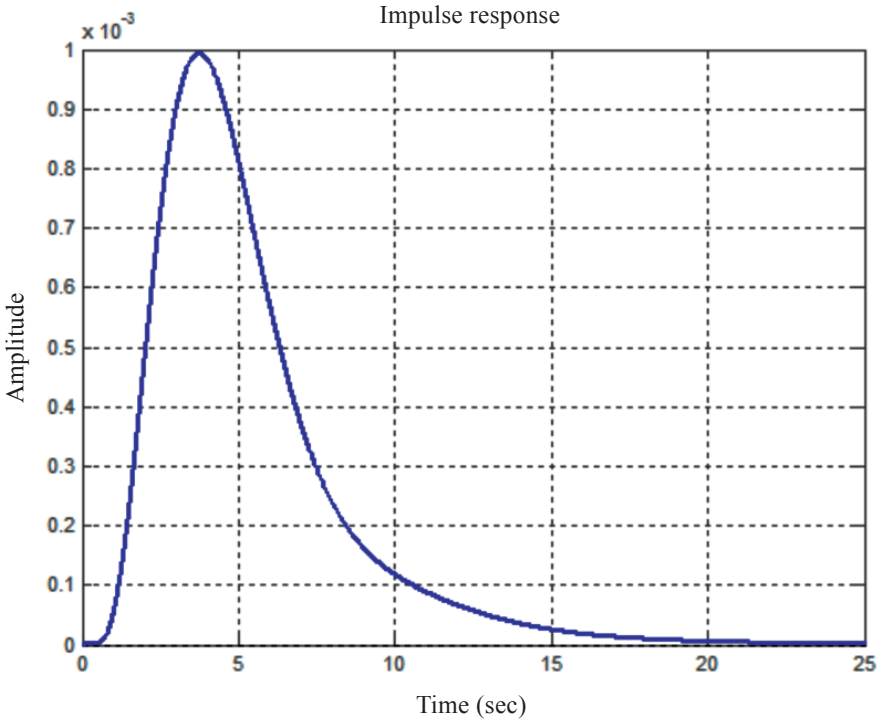

Figure 15. Impulse response of a closed-loop system.

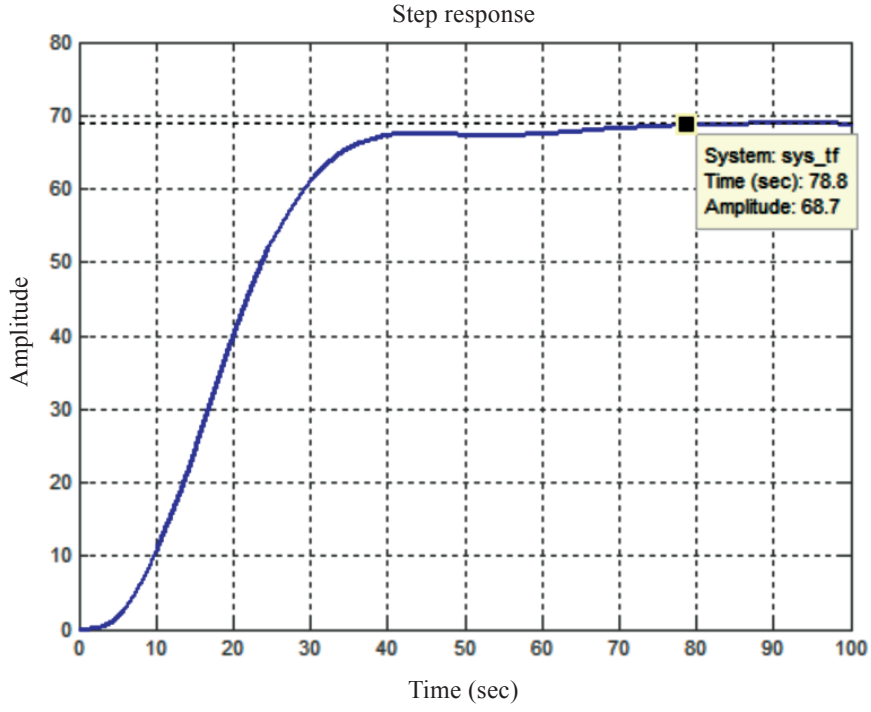

Figure 16. Step response of the closed-loop system.

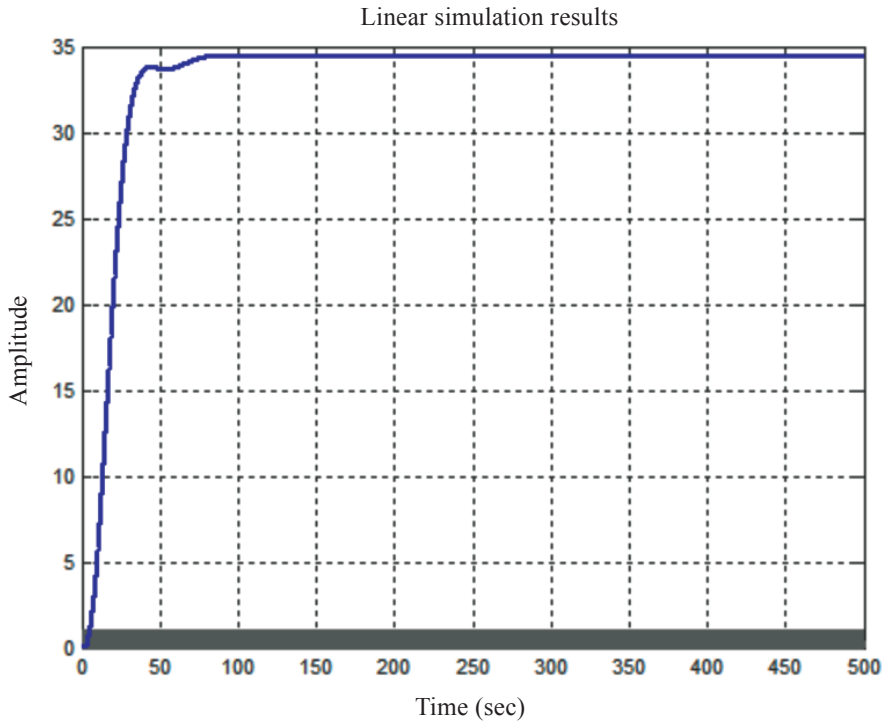

Figure 17. Linear simulation results of the closed-loop system.

can stabilize the unstable plant. In this system, the orbit controller design was considered for different possible controllable options. The response curves represented the stability of the system. The requirements of the orbit controller were designed by computing with MATLAB. It is very important to control the altitude of a satellite used for communications in a geostationary orbit. Hence this simulation program could be exploited for satellites orbiting around the earth at several altitudes to design the on-board propulsion system, and also to evaluate the amount of fuel necessary for the individual life of the satellite.

Date of submission: October 2011
Date of acceptance: June 2012

REFERENCES

Dorf, RC & Bishop, RH 2011, *Modern control systems*, 12th edn, USA.

Gu, D-W, Petkov, PH & Konstantinov, MM 2005, '*Robust control design with MATLAB'*, USA.

Maini, AK & Agrawal, V 2011, '*Satellite technology: principles and applications',* Wiley, Chichester, United Kingdom.

Malik, MA, Zaidi, GA, Aziz, I & Khushnood, S 2001, '*Modeling and simulation of an orbit controller for a communication satellite*', Pakistan.

Maral, G 2009, '*Satellite communications systems',* United Kingdom.

Richharia, M & Westbrook, LD 2011, '*Satellite systems for personal applications: concepts and technology*', United Kingdom.

ASEAN J. Sci. Technol. Dev., **29(1)**, 50 – 54

Ferromagnetic Order in the Intermetallic Alloys $LaNi_{5-x}Mg_x$

D. N. BA[1]*, L. T. TAI[1,2], N. T. TRUNG[3] AND N. T. HUY[4]
[1]*International Training Institute for Materials Science, Hanoi University of Technology, 1 Dai Co Viet, Hanoi, Vietnam*
[2]*Faculty of Physics, College of Natural Science, Vietnam National University, 334 Nguyen Trai, Hanoi, Vietnam*
[3]*Department of Radiation, Radionuclides & Reactors, Delft University of Technology, Mekelweg 15, 2629 JB Delft, Netherlands*
[4]*Hanoi Advanced School of Science and Technology, Hanoi University of Technology, 40 Ta Quang Buu, Hanoi, Vietnam*

The influences of the substitution of Ni with Mg on crystallographic and magnetic properties of the intermetallic alloys $LaNi_{5-x}Mg_x$ ($x \leq 0.4$) were investigated. The X-ray diffraction patterns showed that all samples were of single phase, and the lattice parameters, *a* and *c*, decreased slightly upon chemical doping. $LaNi_5$ is well known as an exchange-enhanced Pauli paramagnet. Interestingly, in $LaNi_{5-x}Mg_x$, the ferromagnetic order existed even with a small amount of dopants; the Curie temperature reached the value of room temperature for $x = 0.2$, and enhanced with increasing x.

Key words: hydrogen storage materials; chemical substitution; crystallographic and magnetic properties; X-ray diffraction

The intermetallic alloys of general formula RM_5 (R: rare earth or transition metal; M: transition metal) are able to store large amounts of hydrogen to form metallic hydrides, in which $LaNi_5$ can absorb or desorb more than 7H per formula unit at room temperature. Thus $LaNi_5$, which crystallizes in a hexagonal structure of $CaCu_5$ type (space group P6/mmm — (Wernick & Geller 1959; Guegan, Lartigue & Achard 1985), is a very attractive and now well known as a hydrogen storage material (Barnes *et al.* 1976; van Vucht, Kuijpers & Bruning 1970). In order to improve the hydrogen storage capacity, the stability of the hydride phase, or the alloy corrosion resistance of $LaNi_5$, the effects of replacing by other metals have been extensively studied (Kielbik *et al*. 2000; Latroche *et al*. 1995; Luo *et al*.1995; Tai *et al*. 2003; Mendelsohn, Gruen & Dwight 1977; Lartigue, Guegan & Achard 1980; Sakai *et al*. 1990). It was reported that the partial substitution of Ni with Al, Mn, and Co can improve the cycling performance and decrease the plateau pressure of hydrogen without reduction of hydrogen storage capacity (Mendelsohn, Gruen & Dwight 1977; Lartigue, Guegan & Achard, 1980), and significantly extend the cycle life (Sakai *et al.* 1990), respectively. Interestingly, upon chemical doping, the electronic structure of alloys changed leading to some new magnetic properties which however has not been fully understood. On the other hand, one of the most promising hydrogen storage materials mentioned is Mg (Jains *et al.* 2009). Mg can store large quantities of hydrogen, and is relatively inexpensive. The effects of Mg doping on Ni site was reported in sample $LaNi_{4.8}Mg_{0.2}$ (Giza *et al.* 2008). The

* Corresponding author (e-mail: damnhanba@gmail.com)

hydrogen capacity of $LaNi_{4.8}Mg_{0.2}$ is about 6.0. This suggests $LaNi_{4.8}Mg_{0.2}$ can be used as negative MH electrodes in the Ni/MH batteries. Based on researches on $LaNi_5$-based alloys, we investigated properties of the intermetallic alloys $LaNi_5$ doped with Mg. In this paper, the results of experiments on crystallographic and magnetic properties of the $LaNi_{5-x}Mg_x$ are discussed.

MATERIALS AND METHODS

A series of polycrystalline $LaNi_{5-x}Mg_x$ samples with x in the range $x \leq 0.4$ were prepared from nominal compositions by arc-melting the constituents La, Ni and Mg (all 3N purity) under high-purity argon atmosphere in a water-cooled copper crucible. A slight excess of La was added to compensate the weight loss during arc-melting process. The samples were turned over and re-melted several times to attain good homogeneity. The crystalline structure and the phase impurity of the samples at room temperature were examined by X-ray powder diffractometer, using Cu-K_α radiation. The obtained powder XRD patterns were analyzed by means of a Rietveld refinement (Rietveld 1969) procedure using X'pert High Score Plus in order to determine the type of structure and the lattice parameters. The magnetic properties of the alloys $LaNi_{5-x}Mg_x$ were measured on a Quantum Design SQUID magnetometer in magnetic fields up to 5 T and in the temperature range from 5 K and 300 K.

X-ray diffraction normally is one of useful route to examine the crystal structure and determine lattice parameters of materials. In *Figure 1*, we showed the XRD patterns of the $LaNi_{5-x}Mg_x$ system. The data confirmed that all the samples were single phase, and to be crystallized in the hexagonal $CaCu_5$-type structure. We could not detect any secondary phases within the 1% error of measurements. *Figure 2* represents the lattice parameters

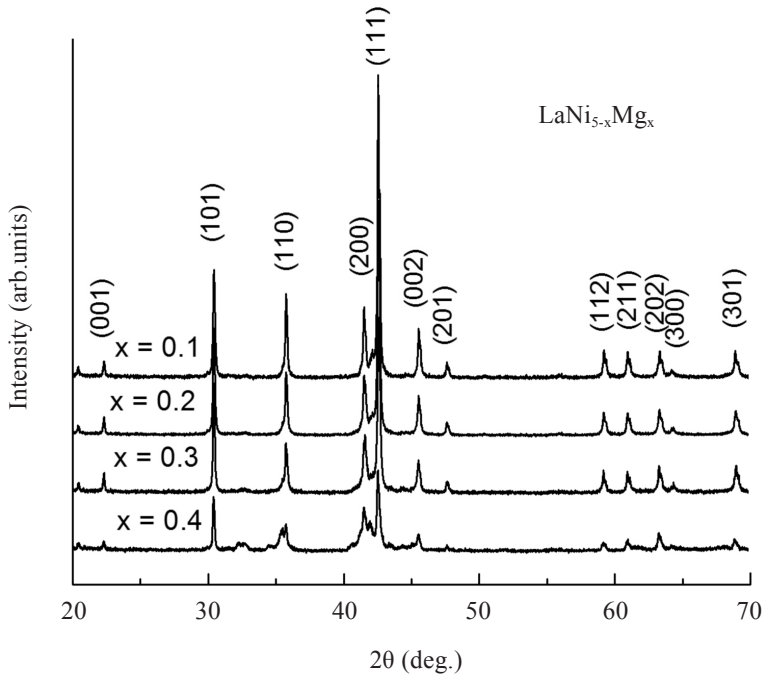

Figure 1. The XRD patterns at room temperature of the intermetallic alloys $LaNi_{5-x}Mg_x$ (with x ≤ 0.4).

determined for the samples with $x \leq 0.4$ by using the Rietveld refinement analysis, together with literature data for pure $LaNi_5$ (Tai, pers. comm., nd). Upon partial substitution of Mg for Ni, both parameters, *a* and *c*, slightly decrease, however they did not change as much as compared with those for $LaNi_5$. We realized that the obtained value for $x = 0.2$ was in good agreement with the only literature values reported (Giza *et al.* 2008). The unit cell volume $\Omega = 86.68$ Å^3 for $LaNi_5$ followed Vegard's law (Vegard 1921) and reduced linearly at a rate of 0.5112 Å^3/at.% Mg.

Figure 3 shows the applied magnetic field dependence of magnetization of $LaNi_{5-x}Mg_x$ measured at fixed temperatures between 5 K and 300 K. Here we ploted the normalized magnetization, M/M 1Tesla as a function of applied magnetic field. The data taken at $T = 5$ K is represented in *Figure 3a*. For $x = 0.1$, the $M(H)$ curve exhibited a *S*-shape charactering for a like-superparamagnetic behaviour. This suggested a hint of ferromagnetic order in samples with a small amount of doping content, Mg. In the literature, $LaNi_5$ is well known as a Pauli paramagnet via the measurements down to 1.6 K (Nasu *et al*. 1971). With increasing *x*, the ferromagnetic order was enhanced as corroborated by the the symmetric loop with visible remnant moments M_r and coercive fields H_c. The inset in *Figure 3a* displays a typical hysteresis loop of the sample with $x = 0.4$, measured at 5 K in the magnetic field of $-0.1\ T \leq B \leq 0.1$ T. The values of M_r and H_c are obtained for 0.01 μ_B/f.u. (formula unit) and 6 mT, respectively. This classified the sample as a weak ferromagnet. The values of magnetic moments at 5 Tesla were 0.02 – 0.13 μ_B for $x = 0.1 – 0.4$, respectively. For experiments carried out at higher temperatures $T = 100$ and 200 K (*Figures 3b* and *c*), for $x = 0.1$ the normalized magnetization linearly depended on the applied fields with a small slope of dM/dH, and no hysteresis effects were observed, indicating a paramagnetic state. Thus we predict that the sample with x = 0.1 has the Curie temperature T_C around 10 K. $M(H)$ curves still remain in the *S*-shape for $x > 0.1$. *Figure 3d* demonstrates

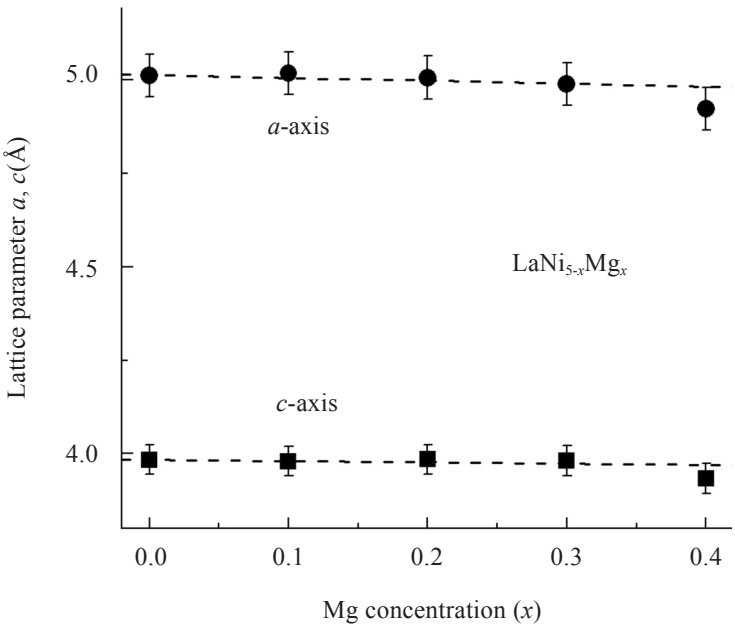

Figure 2. Lattice parameters of $LaNi_{5-x}Mg_x$ as a function of the Mg concentration x measured at room temperature. Notice: the data for x = 0 are taken from Rietveld (1965).

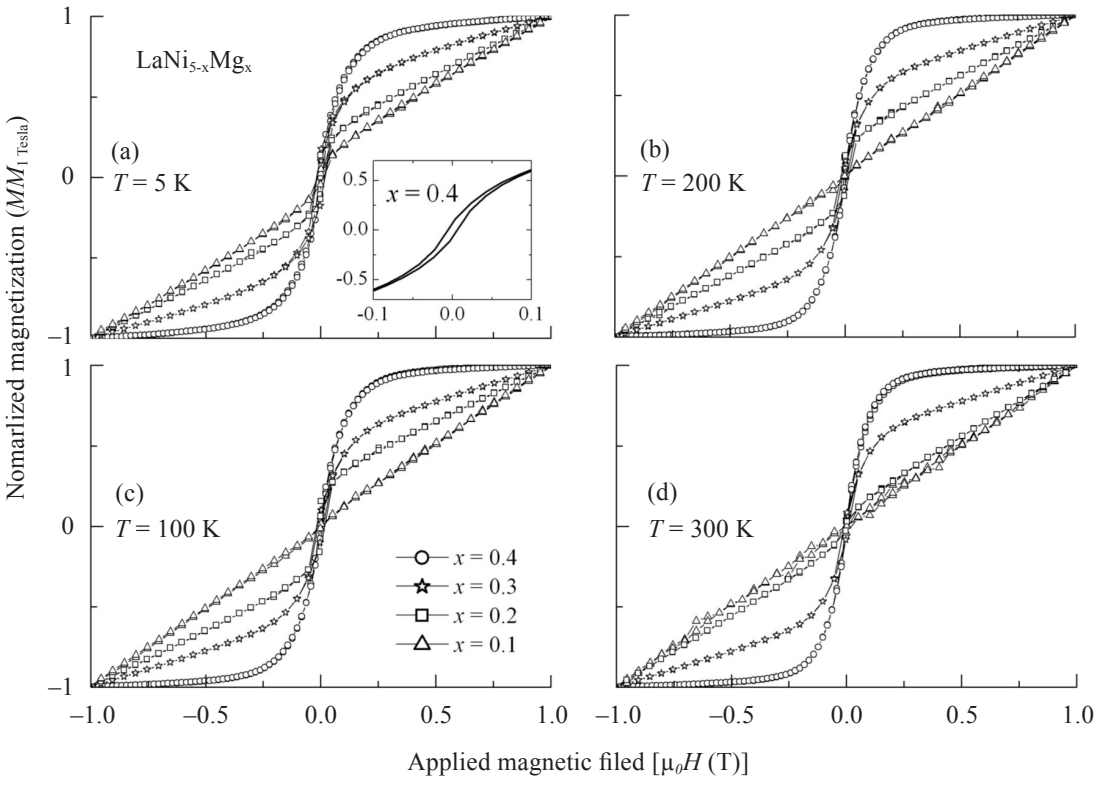

Figure 3. Magnetization vs. applied magnetic field M(H) *curves of* $LaNi_{5-x}Mg_x$ *alloys measured at different temperatures (a)* T = *5 K, (b) 100 K, (c) 200 K, and (d) 300 K. Mg concentrations are (from bottom to top)* x = *0, 0.1, 0.2, 0.3 and 0.4. Notice: the vertical axes represent the normalized magnetization (*M *divided to* M *at 1Tesla). Inset: Hysteresis loop of* $LaNi_{4.6}Mg_{0.4}$ *in a small scale of the horizontal axis measured at* T = *5 K.*

the data measured at 300 K. For x = 0.2, the magnetization trends towards a linearly variation with magnetic fields, however, the data show a small curvature through origin as a sign of a ferromagnetic component. Nevertheless, it is believed the sample has a transition from ferromagnetic to paramagnetic state near 300 K. For x = 0.3 and 0.4 samples, the magnetization data clearly reveal the existence of ferromagnetic ordering, which means the samples have T_C above 300 K.

On the study concerning the magnetic properties of $LaNi_5$-based alloys, in which Ni is partially replaced by other metals, such as Co, Mn, Fe, Al, etc., the long-range ferromagnetic ordering exists in $LaNi_{5-x}Fe_x$ alloys. The net magnetization is induced by magnetic Fe atoms, and increases with the Fe content. This is attributed to the enhanced Fe-Ni exchange interaction, and is confirmed by the increase of the Curie temperature in $LaNi_5$-$_x$Fe$_x$ (Cullity 1972; Tai *et al.* 1999; Yang *et al.* 2000). Both Fe and Ni are 3*d* electron metals, and hence their electronic structures are similar. Ni can be replaced with Mg, due to the difference in the electronic structure of the two elements. Therefore the original of ferromagnetism in $LaNi_{5-x}Mg_x$ is openly discussed. It needs more evidence from both experiments and theories (*i.e.* to calculate the total density of state (DOS) of $LaNi_{5-x}Mg_x$) to clarify this phenomenon.

CONCLUSION

In conclusion, we have investigated the crystallographic and magnetic properties of the intermetallic alloys $LaNi_{5-x}Mg_x$ ($x \leq 0.4$). The XRD patterns provided evidence of the single phase and crystallizing in the hexagonal $CaCu_5$-type structure in all the samples. The lattice parameters calculated by the Rietveld method, both *a* and *c*, slightly decreased with increasing Mg concentration. The magnetization data showed the existence of ferromagnetism and enhanced upon chemical doping. This is corroborated by the typical *S*-shape of hysteresis loops charactering specifically for weak ferromagnetic materials. The Curie temperature was suggested to be around 10 K for sample with $x = 0.1$, and rapidly to be increased up to room temperature for higher Mg concentration $x > 0.1$. For further studies, we will focus on measurements, which help to determine exactly the Curie temperature and also to determine the origin of ferromagnetism of $LaNi_{5-x}Mg_x$.

Date of submission: November 2011
Date of acceptance: January 2012

REFERENCES

Barnes, RG *et al.* 1976, *J. Less-Common Metals,* vol. 49, p. 483.

Cullity, BD 1972 *Introduction to Magnetic Materials*, Addison-Wesley, Reading, MA.

Giza, K *et al.* 2008, *Journal of Power Sources,* vol. 181, p. 38.

Guegan, AP, Lartigue, C & Achard, JC 1985, *J. Less-Common Metals,* vol. 109, p. 287.

Jain, IP, Lal, Ch. & Jain, A 2009, *Int. J. Hydrogen Energy*, in print.

Kielbik, R *et al.* 2000, *J. Alloys Compd*., vol. 298, p. 237.

Lartigue, C, Guegan, AP & Achard, JC 1980, *J. Less-Common Metals,* vol. 75, p. 23.

Latroche, M *et al.* 1995, *J. Alloys Compd*. vol. 231, p. 537.

Luo, S *et al.* 1995, *J. Alloys Compd*. vol. 231, p. 467.

Mendelsohn, MH, Gruen, DM & Dwight, AE 1977, *Nature,* vol. 269, p. 45.

Nasu, S *et al.* 1971, *J. Phys. Chem. Solids,* vol. 32, p. 2779.

Rietveld, HM 1969, *J. Appl. Cryst.,* vol. 2, p. 65.

Sakai, T *et al*. 1990, *J. Less-Common Metals,* vol. 161, p. 193.

Tai, CY *et al*. 1999, *IEEE Trans. Magn.* vol. 35, p. 3346.

Tai, LT *et al*. 2003, *J. Magn. Magn. Mater.,* vol. 262, p. 485.

Tai, LT (personal communication, n.d.).

van Vucht, JHN, Kuijpers, FA & Bruning, HCAM 1970, *Philips Res. Rep.,* vol. 25, p. 133.

Vegard, L 1921 *Z. Phys.,* vol. 5, p. 17.

Wernick, JH & Geller, S *Acta Cryst*., vol. 12, pp. 662.

Yang, JB *et al.* 2000, *Phys. Rev. B,* vol. 63, p. 014407.

ASEAN J. Sci. Technol. Dev., **29(1)**, 55 – 64

Nanoherbals in Human Healthcare: A Proposed Research and Development Roadmap I

S. AHMAD* AND U. HASHIM
Institute of Nano Electronic Engineering,
University of Malaysia Perlis, Kangar, Perlis, Malaysia

Bioactive secondary metabolites derived from herbs are examined for their suitability of conversion into nanoforms having flexible morphological controls, surface stabilizations and surface functionalization. This can lead to stable chemical conjugations based on molecular recognition for their possible applications in the form of smart pharmaceuticals, nutraceuticals, cosmaceuticals and many other related areas of human healthcare using green chemistry routes. Using the principles of nanoscience and technology in association with genomics and proteomics, an attempt has been made to decipher whether a suitable form of drug discovery and targeted drug delivery like schemes are feasible in case of such nano phytochemicals using various kinds of nanosize carriers and labelling molecules already identified in the course of investigations of contemporary single molecule drug developments. Additional efforts can clarify whether such species will be successful in the early detection of diseases based on marker molecules. Once identified, these green phytochemicals will certainly replace many hazardous chemical compounds by their environmentally friendly and sustainable forms in times to come.

Key words: Secondary metabolites; nanoherbals; drug discovery; drug delivery; phytochemicals; nutraceuticals; cosmaceuticals; genomics; proteomics; bioassays; screening

Medicines required for treating, preventing and alleviating disease symptoms constitute a major component in human healthcare system, notably mental and physical well being. Contemporary or molecular medicines can apply the findings of biomedical science research and technologies to diagnose and treat diseases through medication, surgery and other therapy. There are two types of therapies commonly used, namely traditional and contemporary system of medicine. Traditional medicine (TM) may involve a combination of systems like Indian (Ayurveda), Chinese and Arabic (Unani) medicines in addition to a variety of indigenous medicines evolved locally. TM includes both medication and non-medication based therapies. Medication therapies employ herbal medicines, animal parts and/or minerals whereas non-medication type may include acupuncture, manual and spiritual therapies. In those countries where the major healthcare system uses allopathic medicines or where TM is not a part of National Healthcare System, it is often termed as 'complementary', 'alternative' or 'non-conventional' medicine. Herbs in TM are employed in the form of their various parts or extracts including leaves, bark, berries, roots, gums, seeds, stems and flowers that have nourishing and healing properties.

Herbs have been used for human healthcare throughout human history. However, contemporary medicines in modern times belong to a broad class of physical, chemical,

* Corresponding author (e-mail: drsahmad@email.com)

biological and medical techniques that are used to describe molecular structures and mechanisms, identify fundamental molecular and genetic changes caused due to disease and develop molecular interventions to correct such anomalies. Molecular medicines, thus, employ cellular and molecular level descriptions to focus on interventions rather than holistic treatment of the patient.

Molecular medicines have succeeded well in treating large number of diseases primarily due to a better understanding of biochemical processes causing molecular level interactions in human physiology. In contrast, the present status of herbal medicines does not enjoy such support from rigorous animal and human experiments correlating each bioactive compound with specific therapeutic effects. It is known that herbs are quite effective in curing several chronic diseases. However, their precise identification is a common problem out of so many similar ones, but having different types of constituents. Systematic studies are necessary to establish their identities more precisely.

Standardization of herbal ingredients is another issue concerning the use of herbs as a dietary supplement, nutraceutical and cosmetics purposes. Geographical and environmental conditions prevailing during plantation cause large variations in bioactive constituents. These efforts need quantitative standardization for ensuring efficacy. These complexities could possibly be simplified provided therapeutic influences of each constituent was known individually and in synergy with others. Further complications add to changes occurring during their pre- and post-processing stages that may, however, become crucial in modifying bioactive compounds. In order to have the herbal preparations in reproducible form by understanding and resolving various issues, it is worthwhile to use the concepts of nanoscience and technology along with those of genomics and proteomics to resolve connected problems.

Applications of nanoscience and technology in molecular medicine are fast emerging as a new discipline of nanomedicine involving diagnosing, treating and preventing diseases and injuries, relieving pain and preserving and improving human health using molecular tools and knowledge of human physiology. It is very important to note that the materials having at least one dimension in the nanoscale exhibit significantly improved physical, chemical and biological properties due to the quantum size effect. The important contribution of nanoscience is currently being assessed extensively to convert molecular medicine into nanomedicine and target deliveries where the drug molecules are transported through nanosize carriers to the actual disease site, with the help of conjugated targeting and marker molecules. Targeted delivery of molecular medicines is currently under extensive development with reference to dose reductions, enhanced efficacies and reduced side effects.

After having observed therapeutic properties of herbal medicines in treating even incurable ailments over several thousands of years in past, it is natural to ask whether it is possible to convert them into nanoforms. In case yes, then could they possibly be considered for their targeted deliveries aiming for similar advantages as established in case of molecular medicines? An attempt has been made in this study to search for possible answers to these questions after examining various technological aspects of herbal medicines. In this quest, it is necessary to review the existing processes of nanoform conversion, surface functionalization for morphological stabilization and chemical conjugations with imaging and drug molecules/ entities. The final conversion deliveries involves the extract of single or multiple species and their active phytochemicals. Subsequently, suggestions are made for drawing a systematic plan of action for conducting future R&D. The various results reported are concerning the delivery of molecular nanomedicines have excessively been referred to while establishing

similar methodologies that are appropriate to the development of herbal medicine.

Rain forests of Malaysia and the adjoining regions offer valuable resources for nanoherbals development. Malaysia has around 12,000 species of flowering plants, of which 10% are medicinals and only a fraction of which has been screened for medicinal uses, and confined mainly to alkaloids. Systematic bioassays-based investigations remain to be carried out. Existing diverse biochemical activities of Malaysian herbs suggest valuable bioactive properties. Modifications of nanoherbals comprising a large variety of phytochemicals and traditional knowledge will be helpful in the assessment of the molecular nanomedicines.

The assessment of herbal phytochemicals for therapeutic properties of human ailments, include compounds that are appropriate for food, nutrition and cosmetic applications. Inclusion of these is advantagous as nanoformulations in food supplements, nutraceuticals and cosmetics.

HERBAL NANOFORMULATIONS

Organic, inorganic and biological nanoparticles can be prepared by a number of methods involving physical vapour deposition, colloidal solution, mechanical alloying, milling, chemical vapour deposition, sol-gel, mechanical grinding, hydrothermal, supercritical fluid, biomimetic, flame pyrolysis, laser ablation, ultrasonic, electro deposition and explosion, plasma synthesis, microwaves and precipitation techniques. Of these techniques milling, sol-gel, chemical vapour deposition and colloidal chemistry-based methods. For nanoparticles the control of shape and size by using proper surfactant, capping agents, template and self-assembly processes are important. Further development of appropriate types of surface modification techniques has rendered these nanoparticles completely dispersed in a given medium.

Self-aggregation is common in nanoparticles during storage. This may cause serious problems in therapeutic and other applications. Understanding the mechanism of self-aggregation and its prevention could be applied elsewhere as well. For example, in a number of central nervous system related diseases, protein-protein aggregation is the main cause. It is quite likely that any method developed for controlling nanoparticles aggregation may be helpful.

For extracting useful phytochemicals from the natural herbs and plants supercritical fluid extraction (SFE) using CO_2 is currently being explored as an alternative to solvents (Hartono *et al*. 2001). Supercritical CO_2 is selective in separating specific compounds without leaving unwanted residues in the extracts and is also free from the risk of thermal degradation of processed bioactive compounds due to mild temperature involved. Supercritical fluids having enhanced solvating power are highly sensitive to small changes in temperature, pressure and modification of the solvent consisting of entrainers and provide solvent-free extracts. Transport properties of supercritical fluids facilitate deeper penetration in the plant matrix and more efficient and faster extraction than with normal organic solvents.

SFE is carried out in high-pressure vessels made of materials capable of standing elevated pressure and temperature while configured in batch or continuous mode. In this process, the supercritical solvent is thoroughly mixed and allowed to stay for a while with the substance from which some specific bioactive constituent is to be extracted. The supercritical solvent saturated is allowed to reach atmospheric pressure leading to separation of the solubilised product that in turn is taken out from the separation chamber and recycle the solvent for further use. By controlling the process parameters nanosize precipitates are formed on a large scale (Hakuta *et al*. 2003). Supercritical fluid technology is also being increasingly

employed as an analytical technique for qualitative and quantitative identifications of bioactive constituents of natural products that are specifically heat sensitive (Dionisi *et al*. 1999; de Castro & Jimenez-Carmona 2000).

It has been possible to use SFE for extraction and fractionation of bioactive compounds from edible oils and fats; purification of solid matrices; separation of tocopherols and other antioxidants; clean-up of herbal medicines and food products from pesticides; detoxification of shellfish and concentration of fermentation broth, fruit juices and many others (Eggers *et al*. 2000; Lang & Wai 2001).

A large variety of alkaloids such as caffeine, morphine, emetine and pilocarpine are used in numerous medicinal products. The recovery of such alkaloids from natural herbs is important for food, pharmaceutical and cosmetic industries. For example, SFE is found to be selective indecaffeination of coffee and black tea. Recent studies have demonstrated the potential use of solvent and anti-solvent properties of CO_2 in the recovery of alkaloids like theophylline, theobromine and pilocarpine and many others (Saldaña *et al*. 2002). Similarly, cholesterol removal from meat, eggs and dairy products has been very effective using SFE process involving CO_2 alone or combined with ethane and propane as co-solvent (Greenwald 1991). Supercritical H_2O oxidation has been developed for safer destruction of toxic organic materials as a viable alternative to conventional incineration and land disposal.

Rapid expansion of supercritical solutions through very small size nozzles is currently being used for the formation of submicron size nanopowders appropriate for the formulation of drug particles, drug containing polymeric particles and solute containing liposomes (Jung & Perrut 2001, Kompellla & Koushik 2001). The supercritical anti-solvent precipitation technique is useful in the production of micron and submicron size particles with controlled particle shape, size and size distribution (Jung & Perrut 2001). Though morphologies included various kinds of shapes like spheres, rod-like and snowballs but commonly encountered ones are spherical particles. SFE is used for protein purification using fractional precipitation of protein alkaline phosphatase, insulin, lysozyme, ribonuclease, trypsin and their mixtures from dimethylsulphoxide (Reverchon *et al*. 2000).

Some of the typical extraction parameters (pressure, temperature used and percentage recoveries achieved) optimized experimentally is summarized in support of superior performance of SFE for production of different kinds of bioactive substances (Shi *et al*. 2007).

Avocade seed oil (75.8 MP, 70°C, 58.2%); paprika (55.2 MP, 50°C, 7.2%); rice bran (65.5 MP, 70°C, 19.2%); soybean (55.2 MP, 50°C, 19.4%); wheat bran (55.2 MP, 50°C, 4%); sunflower oil (32–35 MP, 40–50°C, 36%); corn germ oil (55.2 MP, 50°C, 50%); wheat germ oil (13–41 MP, 35–50°C, 98.7%); canola oil (41–62 MP, 45–70°C, 44%); carotene lutein (30–70 MP, 40°C, 90%); cardamom oil (10 MP, 40°C, 85%–95%); phospholipids (68.2 MP, 80°C); carotene (20.7 MP, 55°C); black pepper - piperine (9-15 MP, 40°C, 18%); ginger - gingeroles (30 MP, 40°C, 8.4%); palm oil cartenoid (20–30 MP, 45–55°C, 7%); tomato lycopene (17–28 MP, 40–80 °C); peppermint/ spearmint - menthol (6–18 MP, 24–43°C, 76%); chilli oil (30 MP, 40°C); coriander oil (15 MP, 50°C; 0.61%); thai sweet tamrind antioxidant (10–30 MP, 35°–80°C) and fish oil (15 MP, 50°C).

Most of the phytochemicals from the plants are not water soluble because of the absence of ionic bonds, but are easily soluble in organic solvents like alcohols, hexanes, dioxanes, acids, ethers, methylene chloride, trichloroethylene and acitonitrile. Sequential extractions using a number of organic solvents in specific order are generally employed in their extractions. Plant materials are ground, shredded, chopped,

pulverized, compacted or macerated to allow the solvents to properly penetrate inside the mass. However, the pressurized low polarity water extraction method has been developed as another variant to reduce the cost of organic solvents. For example a subcritical state of water is achieved by heating it to 374°C at 22.1 MP for reducing the associated viscosity, surface tension, polarity and dissociation constant and thus making it similar to a number of organic solvents. Using this kind of subcritical water is another alternative to hydrodistillation (Cacace & Mazza 2007) having significant benefits in terms of higher selectivity, better cleanliness, speed and cost reduction as compared to other extraction processes including SFE. Some of the examples using subcritical water extraction process are listed here. These are: clove oil (125°C – 250°C, 2.4 MP – 17 MP); fennel oil (50°C – 200°C, 2 MP); peppermint fragrance (50°C – 200°C, 6 MP); raspberry, bilberry, chokeberry (110°C – 160°C) and whole flaxseed (100°C – 160°C, 5 MP).

HERBALS IN HUMAN HEALTHCARE

Several plant species have been in use as medicines, sources of food and nutrition, flavouring agents, spices and cosmetics since long. Different plant parts like roots, stems, branches, leaves, flowers, fruits and seeds as extracts, powder or coarse mixtures are frequently involved. The herbs are relatively more effective and safer than synthetic molecules employed in the form of molecular medicines. Detailed studies are being pursued on phytochemicals present in such plants and their influence on human physiology. Characteristic features of these herbs include antioxidants, anti-inflammatory, antimicrobial, antidepressant, sedative, antiallergic and many other properties. Some of the findings published are briefly discussed below.

Herbal Pharmaceuticals

Pharmaceuticals are the substances for curing, preventing, or recognizing diseases and relieving pains through their applications. Using herbs to treat disease has been very common among the non-industrialized societies of the world. A number of traditions have dominated the practice of herbal medicines; and include — the 'classical' herbal medicine system based on Greek and Roman sources; Siddha and Ayurvedic medicine systems from India, Chinese herbal medicine and Unani-Tibb medicine of Graeko-Arab origin. Many of the currently used contemporary pharmaceuticals have been long known in form of herbal remedies, and include opium, aspirin, digitalis and quinine to name a few. The World Health Organization (WHO) has estimated that 80% of the world's population presently uses herbal medicine as a part of primary health care. In comparison to the expensive molecular medicines, herbal medicines are grown from seed or gathered from nature as low cost alternative.

Three vital aspects of herbal medicine research namely phytochemistry; pharmacognosy and horticulture are currently being pursued. In phytochemistry, herbs are characterized for their bioactive compounds that are fractionated and analyzed structurally. Pharmacognosy involves their bioactivity assays, identification of action modes and related target sites. In addition to these mentioned analytical investigations, horticultural studies aim for optimal plant growth techniques that are most appropriate for their cultivations. This has special significance as many of the medicinal plants are harvested in the wild and conditions for their cultivation are still very poorly understood. Random cultivations of the medicinal plants lead to wide variations in the plant qualities, resulting in improper choice of raw materials for herbal medicines. Concerning plant physiology, extensive scope exists for basic research on medicinal herbs and phytochemicals.

Medicinal plants contain primary and secondary metabolites. The primary metabolites

are carbohydrates, lipids, proteins, heme, chlorophyll and nucleic acids and responsible for building and maintaining plant cells (Wink & Schimmer 1999). Secondary metabolites are generally plant specific as they are not involved in common plant metabolism as such but provide defense capabilities against damages caused by plant eating animals, pathogens, inter-plant competition besides facilitating the process of pollination (Wink & Schimmer 1999). They also provide resistance against environmental stresses arising due to change in temperature, water availability, light/UV exposure and mineral nutrients. Recent studies have shown that secondary metabolites provide plant growth regulation, modulation of gene expression and signal transduction. Some of them that provide cytotoxicity against pathogens. Similarly, those having defenses against damage are effective as anti-depressant, sedative, muscle relaxant and anesthetic due to their interactions with the central nervous system. Typical characteristics of these metabolites are the result of ecological evolution through interactions with molecular targets influencing cells, tissues and physiological functions in competing with micro-organisms, plants, and animals (Wink & Schimmer 1999). Some of them resemble endogenous metabolites, ligands, hormones, signal transduction molecules, or neurotransmitters and have medicinal effects due to their potential target sites in central nervous and endocrine systems.

Contrary to the single chemical synthetic pharmaceuticals, many phytochemicals cause synergistic actions involving several other chemical compounds acting at single or multiple target sites associated with a physiological process. This could possibly be put to use in eliminating side effects associated with the use of a single compound. Multiple chemicals acting in synergy has its origin in the functional role of secondary metabolites in promoting plant survival. For example, the role of secondary metabolites as defense chemicals affecting multiple target sites would reduce the chances of these organisms developing resistance (Wink & Schimmer 1999).

Some examples of medicinal herbs are cited that have been considered for their therapeutic applications even in the USA, Europe and elsewhere. This includes *Ginseng, St John's Wort, Gingko Biloba, Kava and Echinacea sp*., and their medicinal properties have been recently reviewed (Briskin 2000).

Ginseng is a de-stressing tonic that raises the physical and mental capabilities (Schulz *et al*. 1998), showing immuno-stimulatory effect in humans (Schulz *et al*. 1998; WHO 1999; Blumenthal *et al*. 2000). The large number of triterpene saponins, collectively called ginsenosides (Huang 1999) are responsible for its medicinal properties. Experimental studies indicate that they involve the hypothalamus-pituitary-adrenal axis by influencing serum levels of adrenocorticotropic hormone and corticosterone (Huang 1999).

St. John's Wort is currently very popular for treating depression (Schulz *et al*. 1998). The aerial portion of the plant is harvested after flowering and then used for preparing alcohol/aqueous extract (Schulz *et al*. 1998; Blumenthal *et al*. 2000). Hypericin and pseudohypericin are predominant components and is standardized according to hypericin content (Schulz *et al*. 1998). Napthodianthrones in St. John's Wort is influenced by environmental factors such as light and mineral nutrients. Hypericin and pseudohypericin contribute towards the antidepressant action.

Ginkgo has been in use for thousands of years in Chinese medicine (Huang 1999). Modern formulations use acetone extract of the leaves instead of seeds (Schulz *et al*. 1998). Clinical studies show that Ginkgo improves peripheral and cerebrovascular circulation (Schulz *et al*. 1998; Huang 1999; Blumenthal *et al*. 2000). Ginkgo is also effective in

improving cognitive decline due to vascular insufficiency dementia in elderly patients (Schulz *et al*. 1998; Blumenthal *et al*. 2000) besides its use in tinnitus, vertigo and improving circulation in the legs (Schulz *et al*. 1998).

Kava is known for treating anxiety, nervous tension, agitation and insomnia patients. Clinical studies have revealed its sedative properties to be comparable to that of benzodiazapines but with no physical or psychological dependence (Singh & Blumenthal 1997; Schulz *et al*. 1998). The medicinal properties of Kava are attributed to styrylpyrones that influence several neurotransmitter systems including those involving Gln, GABA, dopamine, and serotonin (Schulz *et al*. 1998). Recent studies show that kavapyrone present in roots are influenced by environmental factors e.g. it increases with irrigation and mineral nutrient supplements and decreases with shading (Lebot *et al*. 1999).

Various parts of *Echinacea purpurea* are used for wound healing, infection and rattle snake bites (World Health Organization 1999; Blumenthal *et al*. 2000). Current interest lies in using this plant for colds, flu-like and respiratory infections (Schulz *et al*. 1998; WHO, 1999). *Echinacea* extracts modulate the immune system including stimulation of phagocytic activity of lymphocytes, fibroblasts for new tissue production, increased respiration and elevated leukocytes mobility (Schulz *et al*. 1998; WHO, 1999). *Echinacea* extract is effective in inhibiting tissues and bacterial hyaluronidase and is found active in infections and preventing spread to other body parts (WHO 1999).

Nutraceuticals

Various food ingredients have strong links with human health and their deficiencies cause various diseases (Ali *et al*. 2009). The protective effects of flax oil tocotrienols, turmeric curcuminoids, carrot carotenoids, vegetable and fruit flavonoids, fatty acids in sea foods, garlic allyl sulfides and mushroom/cereal glucans are a few examples of nutraceuticals. Certain ingredients of saturated fats e.g. sphingolipids, conjugated linolenic acid and monounsaturated fatty acids are effective in controlling carcinogenesis, immuno-modulation and lipid profile respectively (Ali *et al*. 2009). Nuts lower cholesterol because of the proper ratio of polyunsaturated versus saturated fatty acids present there in addition to excess of monounsaturated fatty acids (MUFA). Recent advances in nutritional immunology, awareness of low calories food and stimulating actions of phytochemicals on neuronal diseases show promise as functional foods and in the industrial sectors (Ali *et al*. 2009).

A constant supply of dietary nutrients is needed to support human immune systems and recovery of immune suppression triggered by inflammatory response against invasion by foreign body. Excess fat decreases the immune response and is considered to be immuno-suppressive. A large variety of nutrients consisting of polyunsaturated fatty acids, glutamine, arginine, sulfur-containing amino acids and nucleotides (Mantzioris *et al*. 2000) and compounds like carotenoids, flavonoids, catechins, curcuminoids, tannins and fibers; fatty acids and conjugated linolenic acids are vital for healing organ failure in critical illness (Thies *et al*. 2001).

Due to obesity problems, there is a search for suitable fat replacements in foods without compromising the tastes. Carbohydrate substitutes are popular due to functional properties like thickening, bulking and pasting agents in various forms such as gum, pectins and cellulose that form hydrocolloids enhancing viscosity and texture (Ang 2001). Starches are good fat substitutes. Maltodextrin, dextrin, polydextrose, insulin and fibers are frequently used in place of fats (Malkki 2001). Carbohydrate and protein-based substitutes are preferred in bakery, meat, mayonnaise, cheese

spreads, butter, and margarine. Since proteins are good emulsifying, foaming, gelling and water absorbing substances, they are preferred as fat substitutes in a variety of foods. For example, milk, egg, whey and soy proteins are processed by gelation, aggregation and cross linking to make them fat replacements (Kulozic *et al*. 2003). Whey lactoglobulin is modified by hot aggregation and thermal fractionation to make it a fat substitute (Orlein *et al*. 2006). Proteases and transglutaminases mimic fats by enzymatic modification of certain proteins (Kunst 2003). Some fatty acid esters are very good fat-based substitutes. There are two types of lipid analogs having almost zero calorie properties: (a) carbon chain fatty acids; and (b) sucrose, or some mono-saccharides to replace glycerol back bone to hold the fatty acids.

Around 4000 flavonoids exist in fruits, vegetables, nuts, cereals, legumes, spices, tea and coffee. Flavonoids are good antioxidant besides helping in chelating metal ions and forming complexes with bioactive proteins such as enzymes, especially those involved in generation of free radicals (Majzisova & Kuchta 2001).

Carotenoids like carotene, zeaxanthin; lutein, canthaxanthin, astaxanthin and lycopene resist infections. Low density lipids (LDL) lycopene prevents oxidative damage in proteins and lipids and thus prevent atherogenesis and carcinogenesis. Curcumin is a well known anti-oxidant, anti-inflammatory and anti-tumor compound (Gao *et al*. 2004) besides reducing nitric oxide and is effective in colitis (Ukil *et al*. 2003) and allergy (Kurup & Barrios 2008).

A large variety of vegetables are effective in chronic diseases as they minimize reactive oxygen species and inflammatory biomarkers (Athar & Bokhari 2006). Mixed vegetable soup reduces homocysteine in blood thereby improves bioavailability of cartenoids including other nutrients (Paterson *et al*. 2006). Berries activate immune response by increasing the number of macrophages in blood that provides strong defense as spleen phagocytes (Chao *et al*. 2004).

Bioactive chemicals in apple, citrus fruit, guava and berries control disorders through antinitrosation, inhibiting DNA adducts biosynthesis and facilitating protective enzymes activity as glutathione transferase (Craig 1999). Foods containing folate, biotin, niacin, catechins and flavonoids are effective against cancer (Oommen *et al*. 2005). Guava leaf extract prevents diabetic complications (Wu *et al*. 2009).

Vitamin C is reactive oxygen species scavenger eliminating endothelial dysfunction (Feldman *et al*. 2001) besides causing secretion of nitric oxide and regulating vasodilatation responsible for diseases like cancer, diabetes, obesity, renal disorder and coronary arterial diseases. It is an antioxidant neutralizing reactive oxygen species in chronic diseases. It improves the phenomena of inflammatory endothelium dependent vasodialation (Korantzopoulos & Galaris 2003).

Spices and nuts from clove, cumin seeds, turmeric, onion, garlic, fennel, fenugreek, nutmeg, mace and many others are rich in nutraceuticals. Garlic lowers LDL and enhances HDL, and allicin/ajoene in it inhibits nitric oxide synthase by reducing protein/mRNA and promoting vasodilatation. Strong immune-modulating characteristics of garlic enhance proliferation of T-lymphocytes and augment the response of delayed hypersensitivity. Aged garlic extract is a promising immune modifier with homeostasis balance and particularly useful in Sarcoma and lung cancer (Kyo *et al*. 2001). Both oil and water soluble garlic compounds reduce dementia and coronary diseases (Borek 2006) whereas garlic oil prevents blood coagulation even in diabetic patients (Ohaeri & Adoga 2006). Garlic aqueous extract affects cell cycle and viability of hepatoma cells (De Martino *et al*. 2006).

β-glucan in cereals is currently used as fat replacement (Woods & Navder 2006). Cereal brans are antioxidant (Serpen *et al*. 2008). Oats are rich in β-glucans that have good water retention; gelling and hydrocolloid-forming properties appropriate for fat replacement besides cholesterol lowering (Lee *et al*. 2009). Their presence in yeast cell, fungi, bacteria and cereal modulate the immune system to improve body defense (Volman *et al*. 2008). Fibers in gums, pectins, celluloses, hemicellaloses, tannins and phytates are often used in food supplements. Mushroom glycans form polysaccharides with glucose, galactose, mannose, xylose, arabinose, fucose, ribose and glucouronic acid while conjugating with proteins or peptides show antitumor activity (Zhang *et al*. 2007).

Date of submission: May 2012
Date of acceptance: June 2012

REFERENCES

Ali, R, Athar, M, Abdullah, U, Abidi, SA & Qayyum, M 2009, *African Journal of Biotechnology*, vol. 8, no. 6, pp. 891–898.

Ang, JF 2001, *Cereal food world*, vol. 46, pp. 107–111.

Athar, M & Bokhari, TZ, 2006, *J. Vegetable Sci.,* vol. 12, pp. 27–38.

Blumenthal *et al.* 2000, *Herbal medicine: Expanded commission e. monographs,* Integrative Medicine Communications, Boston.

Briskin, DP 2000, *Plant Physiology*, vol. 124, pp. 507–514.

Borek, C 2006, *J. Nutr.,* vol. 136, no. 3, pp. 810S–812S.

Cacace, JE & Mazza, G, 2007, 'Pressurized low polarity water extraction of biologically active compounds from plant products', in *Functional food ingredients and nutraceuticals processing technologies*, eds Shi, Taylor & Francis, Boca Ratan.

Chao, S, Schreuder, M, Young, G, Nakaoka, K, Moyes, L & Oberg, C, 2004, *J. Am. Nutraceut. Assoc.,* vol. 7, pp. 32–38.

Craig, WJ 1999, *Am. J. Clin. Nutr.,* vol. 70, pp. 491S–499S.

De Castro, MDL & Jimenez-Carmona, MM 2000, *Trac-Trends in Analytical Chemistry*, vol. 19, pp 223–228.

De Martino, A, Filomeni, G, Aquilano, K, Ciriolo MR & Rotilio G, 2006, *J. Nutr. Biochem.*, vol. 17, pp. 742–749.

Dionisi, F *et al*. 1999, *J. Food Sci.*, vol. 64, pp. 612–615.

Eggers, R *et al.*, 2000, *Brazilian J. of Chemical Engineering*, vol. 17, pp. 329–334.

Feldman, C, Anderson, R, Theron, AJ, Steel, HC, Rensburg, CEJ, Cole, PJ & Wilson, R 2001, *Eur. Respir. J.,* vol. 18, pp. 122–129.

Gao, X, Kuo, J, Jiang, H, Deeb, D, Liu, Y, Divine, G, Chapman, RA, Dulchavsky, SA & Gautam, SC 2004, *Biochem. Pharmacol.,* vol. 68, pp. 51–61.

Greenwald, CG, 1991, 'Overview of fat and cholesterol reduction technologies', in *Fat and cholesterol reduced foods: technologies and strategies*, Chap. 3, Advances in Applied Biotechnology Series, eds, C Haberstroh & CE Morris, Gulf Pub. Co, The Woodlands, Texas, USA, vol. 12, pp. 21–32.

Hakuta, Y, Hayashi, H & Arai, K 2003, *Current Opinion Solid State & Material Science*, vol. 7, pp. 341–351.

Hartono *et al.* 2001, *Chem. Eng. Science*, vol. 56, pp. 6949–6958.

Huang, KC 1999, *Pharmacology of chinese herbs*. CRC Press, Boca Raton, FL.

Jung, J & Perrut, M 2001, *J. Supercritical Fluids*, vol. 20, pp. 179–219.

Kompella, UB & Koushik, K 2001, *Critical Reviews in therapeutic Drug Carrier Systems*, vol. 18, pp. 173–199.

Korantzopoulos, P & Galaris, D 2003, *J. Clin. Basic Cardiol*., vol. 6, pp. 3–6.

Kulozik, U, Tolkach, A, Bulca, S & Hinrichs, J 2003, *Int. Dairy J.,* vol. 13, pp. 621–630.

Kunst, T 2003, in *Handbook of food enzymology*, eds JR Whitaker, AG Voragen, DWS Wong, Marcel Dekker, New York, pp. 221–236.

Kurup, VP & Barrios, CS 2008, *Mole. Nutr. Food Res*., vol. 52, pp. 1031–1039.

Kyo, E, Uda, N, Kasuga, S & Itakura, Y, 2001 *J. Nutr.,* vol. 131, pp. 1075–1079.

Lang, QY & Wai, CM 2001, *Talanta,* vol. 53, pp. 771–782.

Lebot, V, *et al*. 1999, *Econ. Bot.,* vol. 53, pp. 407–418.

Lee, S, Inglett, GE, Palmquist, D & Warner, K 2009, *LWT — Food sci. technol*., vol. 42, pp. 350–357.

Majzisova, G & Kuchta, M 2001, *Physiol. Res.*, vol. 50, pp. 529–535.

Malkki, Y 2001, *Cereal Food World,* vol. 46, pp. 196–199.

Mantzioris, E, Cleland, LC, Gibson, RA, Neumann, MA, Demasi, M & James, MJ 2000, *Am. J. Clin. Nutr.*, vol. 72, pp. 42–48.

Ohaeri, OC & Adoga, GI 2006, *Biosci. Rep.,* vol. 26, pp. 1–6.

Oommen, AM, Griffin, JB, Sarath, G & Zempleni, J 2005, *J. Nutr. Biochem*., vol. 16, pp. 74–77.

Orlien, V, Pedersen, HB, Knudsen, C & Skibsted, LH 2006, *Milchwissenschaft*., vol. 61, pp. 3–6.

Paterson, E, Gordon, MH, Niwat, C, George, TW, Parr, L, Waroonphan, S & Lovegrove, JA 2006, *J. Nutr*., vol. 136, pp. 2849–2855.

Reverchon, E *et al*. 2000, *J. Supercritical Fluids,* vol. 17, pp. 239–248.

Saldaña, MDA *et al.* 2002, *J. Supercritical Fluids*, vol. 22, pp. 119–127.

Schulz, V *et al.* 1998, *Rational phytotherapy: a physician's guide to herbal medicine,* Springer-Verlag, Berlin.

Serpen, A, Gökmen, V, Pellegrini, N & Fogliano, V 2008, *J. Cereal Sci.*, vol. 48, pp. 816–820.

Shi, J, Kassama, LS & Kakuda, Y 2007, 'Supercritical fluid technology for extraction of bioactive components', in *Functional food ingredients and nutraceuticals processing technologies*, eds Shi John, Taylor & Francis, Boca Ratan.

Singh, YN & Blumenthal, M 1997, *Herbalgram,* vol. 39, pp. 33–55.

Thies, F, Nebe-von-Caron, G, Powell, JR, Yaqoob, P, Newsholme, EA & Calder, PC 2001, *Am. J. Clin. Nutr*., vol. 73, pp. 539–548.

Ukil, A, Maity, S, Karmakar, S, Datta, N, Vedasiromoni JR & Das, PK 2003, *Br. J. Pharmacol*., vol. 139, pp. 20–218.

Volman, JJ, Ramakers, JD & Plat, J 2008, *Physiol. Behavior*, vol. 94, pp. 276–284.

Wink, M & Schimmer, O 1999, 'Modes of action of defensive secondary metabolites', in *Functions of plant secondary metabolites and their exploitation in biotechnology*, ed M Wink, CRC Press, Boca Raton, FL, pp. 17–112.

World Health Organization 1999, *Monographs on selected medicinal plants*, vol. 1, World Health Organization, Geneva.

Wood, E & Navder, KP 2006, *J. Am. Diet. Assoc*., vol. 106, no. 1, pp. A55.

Wu, JW, Hsieh, CL, Wang, HY & Chen, HY 2009, *Food Chem*., vol. 113: pp. 78–84.

Zhang, M, Cui, SW, Cheung, PCK & Wang, Q 2007, *Trends Food Sci. Technol*., vol. 18, pp. 4–19.

ASEAN J. Sci. Technol. Dev., **29(1)**, 65 – 75

Nanoherbals in Human Healthcare: A Proposed Research and Development Roadmap II

S. AHMAD* AND U. HASHIM
Institute of Nano Electronic Engineering (INEE),
University of Malaysia Perlis (UniMAP), Kangar, Perlis, Malaysia

(Abstract and key words are found in page 55 of this issue)

Cosmetics, Cosmeceuticals and Nutricosmetics

It is useful to clarify terminological differences that are frequently encountered. For example, cosmetics enhance the appearance or odor of the human body and consist of skin-care creams, lotions, powders, perfumes, lipsticks, finger/toe nail polish, eye/facial makeup, permanent waves, colored contact lenses, hair colors, sprays and gels; deodorants, baby products, bath oils, bubble baths, bath salts, butters and many other types of products. Cosmeceuticals are combinations of cosmetics plus pharmaceuticals such as anti-aging creams and moisturizers with bioactive ingredients having drug-like properties. On the other hand, nutricosmetics are the nutritional supplements which support the function and structure of the skin. The difference between the two lies in the delivery of cosmecuticals and nutricosmetics. Cosmeceuticals such as creams, lotions, and ointments are for external use whereas nutricosmetics are administered orally.

A fairly large number of plant derived compounds are currently being used in modern cosmetics industries. Most of these useful compounds have been highlighted by Mufti and Macchio (2009). Some typical phytochemicals are included here to highlight the importance of species in modern cosmetics.

A polysaccharide from oats is shown to be active in collagen production, fibroblast stimulation and protection against UVA/UVB damage besides improving the tensile strength of hair and significantly reduced breakage due to bleaching (Mufti & Macchio 2009; Somerset Cosmetic Company). Another plant-derived carbohydrate from konjac plant containing mannose and glucose — is an extensin of a plant-derived glycoprotein similar to animal-derived collagen and is used as a genuine replacement.

A new lip therapy based on palmitoyl oligopeptide showed excellent moisturizing properties. Pectin derived from carbohydrates backbone with monosaccharide side chains commonly found in vegetables and fruits, especially citrus fruit and apples; form a low residue gel useful in coloured cosmetics because of its compatibility with the pigments used (Mufti & Macchio 2009).

An important group of compounds like saponins, flavanols and tannins are extensively used in cosmetics. Saponins are water-soluble amorphous colloidal glycosides derived from licorice and yucca that produce froth in stirred solution are widely used as natural emulsifiers in cosmetics (Mufti & Macchio 2009; Somerset Cosmetic Company). Licorice extract is used

* Corresponding author (e-mail: drsahmad@email.com)

as skin whitener and powerful antioxidant comparable to the enzyme dismutase, found in some vegetables, mushrooms, soy beans and spinach. Potassium and zinc salts of glycyrrhetinic acid are used as anti-inflammatory substance causing soothing action in sensitive skins (Mufti & Macchio 2009). Tannins are natural plant polyphenols extracted from the bark of chestnut, nutgall, oak, sumac leaves, hemlock, coffee, tea and walnuts and are used as metal ion chelator, a protein precipitant and a biological antioxidant (Mufti & Macchio 2009).

Flavonoids are water soluble plant pigments from fruits, vegetables, nuts and seeds besides being found in ginkgo biloba, St. John's wort and pycnogenol. Wine and bilberry contain anthocyanidins while flavanones are found in citrus fruits and cherries contain sufficient catechins glycoside. The flavonoids glycosides are used in cosmetics as antioxidant and anti-inflammatory compounds. Flavonoid rutin, derived from buckwheat, protects the blood vessels from fragility and improves microcirculation at the sub epidermal level (Somerset Cosmetic Company; Mufti & Macchio 2009). Similarly, arbutin flavonoids, derived from the leaves of the ericaceae and rosaceae are used as a natural whitening agent in cosmetics. Soy isoflavonese are active against skin cancer according to some studies. Grape seed extract, containing flavonoids anti-oxidant, is comparable to soy extract containing isoflavones. Profound influence of flavonoids in cosmetics has been due to substantial increase in blood circulation at the sub epidermal level and an improvement of intra-cellular membrane exchanges of micronutrients (Mufti & Macchio 2009). They also improve venous insufficiency and capillary fragility resulting in increased oxygen supply to the cells and overall improvement of skin's texture and appearance.

Proteins, amino acids and peptides are widely incorporated into hair and skin care products to provide excellent conditioning, moisturizing and filmogenic actions (Mufti & Macchio 2009; Somerset Cosmetic Company). However, proteins from animal sources are replaced with those of marine and vegetable origin in cosmetics. On skin and hair, the hydrolyzed protein molecule exhibits extraordinary water binding and texturizing properties. It also reduces the split ends of damaged hair and induces superior gloss. Hygroscopic amino acids are mostly used in skin care products for their water-binding properties, as well as their improved elasticity, silky feel and skin firming effects. Enzyme hydrolysates and amino acids are moisturizers that penetrate the stratum corneum, epidermis and some dermal layers. On the contrary, higher molecular weight proteins do not penetrate significantly into the epidermis and remain on the surface of stratum corneum providing skin tightening or smoothing action (Mufti & Macchio 2009). The natural wheat protein, hydrolyzed wheat protein, whole oats, hydrolyzed wheat protein polysiloxane and polyvinylpyrrolidone copolymers are just a few of the higher proteins that are used in cosmetics for their beneficial actions (Mufti & Macchio 2009; Somerset Cosmetic Company).

Lipids covalently link with carbohydrates to form glycolipids and proteins forming lipoproteins and are used as emollients, moisturizers, viscosity modifiers, body builders, binders, emulsifiers for pleasant feel and above all as formula stabilizers (Mufti & Macchio 2009). There are five major classes of lipids - neutral lipids, phospholipids, sterols, waxes and glycolipids (Mufti & Macchio 2009). Stearic, palmitic, myristic, oleic, linoleic and linolenic acids are common ingredients in modern cosmetics. Biomimetic phospholipid complexes derived from some vegetable oils offer unique features for topical delivery and skin conditioning effects.

Cholesterol is widely used as water in oil emulsifier holding substantial moisture on the skin. New avocado sterols having an 80% active component with lubricious emollient action on

the skin are used in place of animal-derived lanolin. Squalene, a sterol precursor found in plants, is also used widely in cosmetics as an emollient (Mufti & Macchio 2009). Beeswax and vegetable derivatives are frequently used in cosmetics while silicone modified waxes improve feel and stability considerably. Ceramides fatty acids replenish moisture due to their water-binding capacity and help making skin soft and supple (Mufti & Macchio 2009; Somerset Cosmetic Company).

Plant exudates including naturally occurring balsams, gums, oleoresins and resins, though insoluble in water and soluble in alcohol, often soften under heat are frequently used in cosmetics as binders and formula stabilizers (Mufti & Macchio 2009). Seaweeds and algae are rich natural sources of essential amino acids, polyphenol glycosides, minerals, water soluble vitamins and trace elements. In color cosmetics, some iron oxide pigments are replaced with ground green, red, blue, brown and yellow algae. All these materials have strong antioxidant action (Mufti & Macchio 2009).

Delivery Systems

Pharmaceutical delivery systems consist of formulations and devices that deliver therapeutic agents to the desired body locations and/or provide timely release of therapeutic agents. Drug delivery systems combine polymer science, pharmaceutics, bioconjugate chemistry and molecular biology while aiming to control drug pharmaco-kinetics/dynamics, non-specific toxicity, immuno-genicity and biorecognition in the search for an improved efficacy (European Technology Platform on Nanomedicine, 2005). It is important to note that drug delivery and targeting systems minimize drug degradation and loss, prevent harmful side effects and increase the availability of the drug at disease sites. Drug carriers include micro and nanoparticles, micro and nano capsules, lipoproteins, liposomes, and micelles that are engineered to react to stimuli, slowly degrade being site specific. Targeting mechanisms could be either passive or active. For example, preferential accumulation of chemotherapeutic agents in solid tumours due to differences in vascularisation of the tumour tissues compared to healthy tissues is known as passive targeting whereas in active targeting chemical 'decoration' of drug carrier surface with molecules enabling them to be selectively attached to diseased cells.

Controlled drug release is equally important for therapeutic success and it could be sustained or pulsatile type. Sustained release may involve diffusion based drug release from polymer or by degradation over a period of time whereas pulsatile release mimics a process similar to insulin production in body. This is facilitated by using drug conjugated polymers that respond to specific stimuli like — exposure to light or other source of radiation, changes in pH or temperature.

Most of the medicines are currently administered parenterally, but there is a clear-cut preference for other routes like — oral, pulmonary or transdermal. Crossing of existing biological barriers by such large molecules is a challenging task that requires better understanding of macromolecular transport. However, any success attained would profoundly change the way nanotechnology based drugs are put to use in future. The oral route would require the precise knowledge of nanoformulations crossing the gastrointestinal tract epithelium overcoming enzymatic and permeability barriers. Similarly, pulmonary delivery is another method that should focus on aerodynamic characteristics of delivery systems and their ability to deliver drugs with improved bioavailability. Non-invasive pulmonary delivery involves extremely large surface area for drug absorption, thin alveolar epithelium, permitting rapid absorption and absence of first-pass metabolism and thus needs special attention for developing nanostructured

systems. Especially in case of central nervous system diseases, the targeted delivery capable of crossing blood-brain barrier should be examined more in detail. Rational and high throughput screening methods for technologies to transport molecular species through biological barriers and target one or many specific locations is considered as an important issue to study in future.

Nano-Devices — Targeted Delivery

Ongoing activities of developing devices like programmable nanoneedles, nanofluidic components and assemblies, nanobiosensors for detecting the presence of therapeutic agents in body fluid combined with targeted delivery are extremely useful and should continue in future. Delivery systems could also be a part of biomedical devices for implantation or surgical tools that could provide real benefits for the patient. In future, more emphasis will be (European Technology Platform on Nanomedicine 2005; Nanomedicine — Nanotechnology for Health 2006) on sustainable and pulsatile biochemical releases; micro-electro-mechanical systems/nano-electro-mechanical systems (MEMS/NEMS) devices for controlled temporal and sequential multiple drug releases; gels, patches and sensor based devices; implantable biochips/ microfluidic devices; pill on a chip based technology; polymersome and liposome smart carriers; physical stimuli sensitive carriers and nanodevices comprising of metabolite sensor combined feedback based release mechanisms.

Carriers in targeted deliveries provide mechanisms to improve effectiveness of the macromolecules. A successful carrier system demonstrates optimal loading and release properties, long shelf-life and low toxicity. Colloidal and micellar solutions, vesicle and liquid crystal dispersions and a variety of nanoparticulate dispersions consisting of particles of 10 nm – 500 nm diameter show great promise as described in brief here (European Technology Platform on Nanomedicine 2005; Nanomedicine — Nanotechnology for Health 2006).

Micelle is a spherical or rod shaped molecular aggregate in a solution consisting of 10–100 surface active molecules. Hydrophilic and hydrophobic parts orient according to their interaction with the surrounding solvent. Bioactive compounds are encapsulated in a core surrounded by a hydrophilic shell protecting the contents and transporting at concentrations exceeding their intrinsic water solubility. It is possible to select the outer shell composition such that it escapes detection by reticulo-endothelial system avoiding early elimination from the blood circulation. Micellar size, shape and chemical conjugations are easy to control to improve not only their stability but even their movements to selectively target a broad range of disease cells.

Liposomes are closed lipid vesicles surrounding an aqueous interior, appropriate to encapsulate exogenous materials for their ultimate delivery into the cells. These vesicles have one or more number of lipid bi-layers wherein molecular compounds are encapsulated and solubilised. Incorporation of size selective channel proteins in the liposome membrane converts them into size specific filters permitting diffusion of small solutes like ions, nutrients and antibiotics. Molecular compounds encapsulated in nanosize liposome structures with channel proteins are completely protected from premature degradation. However, the molecular compounds diffuse through channels driven by the concentration gradient between interior and exterior of the nanostructure.

Dendrimers are branched species of nanometre size macromolecules comprising of a central core, branching and terminal functional groups. Core chemistry determines the solubilising properties of the cavity within dendrimer whereas external chemical groups decide overall solubility and chemical

behaviour. It is also possible to attach linkers to the external dendrimer surface which enable them to bind to a specific site while its stability and protection from phagocytes is achieved by surface functionalizing them with entities like polyethylene glycol chains.

Amorphous and crystalline nanoparticles having spherical or capsule like shapes can adsorb and/or encapsulate molecular compounds thus protecting them against chemical and enzymatic reactions. In a nanocapsule, the molecular compounds are confined to a cavity surrounded by a polymeric membrane while in nanospheres the compound is uniformly dispersed in a matrix. In recent years, biodegradable polymeric nanoparticles are becoming more popular in controlled release of molecular compounds in targeting particular organs/tissues in various forms like DNA carriers in gene therapy and oral deliveries of proteins, peptides and genes. Hydrogels — a three-dimensional polymer network that swells without dissolving in water are used to regulate molecular compound release in reservoir based carriers in swelling controlled release devices. Hydrogels could be intelligent and stimuli sensitive systems capable of modulating compound release in response to changes in parameters like pH, temperature, ionic strength, electric field, specific analyte concentration gradient.

Molecular imprinted polymer or plastic antibody is another nanostructure that is formed in presence of a molecule which is removed later on leaving complementary cavities behind. Such polymers show chemical affinity for the original molecule and this could be used in biosensors, synthesizing catalysts and molecular separations. The behaviour is similar to that of antibodies or enzymes. These polymeric molecules may be employed in realizing a number of delivery modes e.g. rate programmed delivery where compound diffusion follows some specific rate profile; activation mediated compound delivery where the release is activated by some physical, chemical or biochemical process and feedback-regulated delivery where the release is regulated by the concentration of a triggering agent that is activated by the compound concentration in the body. Chemical conjugation of peptides and proteins with synthetic polymers is an efficient way of improving the control of nanostructures prepared from synthetic polymers for targeted delivery. Chemical conjugations of synthetic polymers to peptides or proteins can be used to reduce toxicity, prevent immunogenic or antigenic side reactions besides enhancing blood circulation time and improving drug solubility. Synthetic polymers and peptide conjugates can act as antibodies to specific epitopes and prevent random distribution of bioactive compounds throughout the patient's body by active targeting. Functionalization of synthetic polymers and peptides from extracellular protein matrix is an efficient way to mediate cell adhesion. However, the ability of the cationic peptides to complex DNA and oligonucleotides offers possibility of developing non-viral vectors for gene delivery.

Subcutaneous injection of liquid formulation producing solid structures are attractive *in situ* implants for non-oral applications because they are less invasive and painful compared to conventional implants. These implants deliver molecular compounds locally or systemically over prolonged periods of time extending to several months. This may be used for minimizing side effects by providing constant compound profiles especially important for delivering proteins with narrow therapeutic indices. Such systems are relatively simple and cost effective to manufacture.

Different Administration Routes

The success or failure of using a drug is influenced by choosing the way it is administered and therefore a delivery route can be decided by considering patient acceptability, drug solubility, ability to target the disease locations

and effectiveness in dealing with the specific disease (Nanomedicine — Nanotechnology for Health 2006; European Technology Platform on Nanomedicine 2005).

The most important drug delivery route is through the mouth. Though increasing number of protein and peptide-based drugs offer huge potential for most effective therapeutics but they do not easily cross mucosal surfaces and biological membranes and are easily degraded, prone to rapid clearance in the liver and other body tissues and require precise dosing. Presently, protein drugs are administered by injection but this route is less patient friendly and also poses problems of oscillating blood drug concentrations. Despite gastrointestinal tract-related problems in the stomach, enzymatic degradation throughout the gastrointestinal tract and bacterial fermentation in the colon, the peroral route is still the most sought after one as it offers maximum convenience, cost effectiveness and manufacturing cost reductions.

Parenteral deliveries comprising of intravenous, intramuscular or subcutaneous administrations are common in general patient care. Nanosize liposomes are administered intravenously these days. Nanoscale drug/compound carriers show great promises for improving delivery through nasal and sublingual routes that avoid first-pass metabolism and for difficult access ocular, brain and articular cavities. Peptides and vaccines are delivered systemically using nasal route through drug macromolecule and nanoparticle conjugates. In addition, a colloidal drug carrier is better option for improving the ocular drug deliveries.

Pulmonary delivery is carried out via aerosols, metered dose inhaler, dry powder inhalers and nebulizers that may contain liposomes, micelles, nanoparticles and dendrimers. Pulmonary delivery research is driven by its potential for successful protein and peptide drug delivery, promise of an effective gene delivery and need for replacing chlorofluorocarbon propellants in inhalers. This delivery provides local targeting for the treatment of respiratory diseases. However, success of protein drug pulmonary delivery is reduced by proteases in the lung that lower bioavailability and by barrier between capillary blood and alveolar air.

Non-invasive transdermal drug delivery avoids gastrointestinal irritation, metabolism, variations in delivery rates and interference due to the presence of food and is also suitable for unconscious patients. However, there are limitations of slow penetration rates, lack of dosage flexibility and/or precision and a restriction to relatively low dosage drugs.

Trans tissue local deliveries are fixed in resected tissues during surgery for giving better pharmacological effect and minimizing systemic and administration associated toxicities. This includes — drug/compound loaded gels that are formed *in-situ* and adhere to resected tissues releasing drugs/compounds, proteins or gene encoding adenoviruses; antibody fixed gels that form a barrier on a target tissue that could prevent cytokines permeation into that tissue; cell-based delivery that involves a gene transduced oral mucosal epithelial cell-implanted sheet; device directed delivery — a rechargeable drug infusion device that can be attached to the resected sites.

In gene delivery, a challenging task in treatment of genetic disorders, plasmid DNA is introduced into the target cells. It needs to be transcribed and the genetic information ultimately translated into the corresponding protein. The gene delivery system needs to target the desired cells, transported through the cell membrane, taken up and degraded in the endolysosomes and plasmid DNA intracellularly transported to the nucleus.

Delivery and Multitasking Medicines

Delivery consists of nanosize elements for carrying the therapeutic and biologically active compound to the desired locations. In this context, nanotechnology not only offers possibility of pharmaceuticals deliveries or other therapeutic agents, but also utilities for diagnostics and regenerative medicine (European Technology Platform on Nanomedicine 2005; Nanomedicine — Nanotechnology for Health 2006). For example, larger therapeutic systems like nanoherbals provide far more scope for diversity and complexity that makes their understanding still more challenging and their delivery more difficult. However, these larger systems do possess unique power to take care of more number of diseases such as in case of natural medicines. Such a combination of diagnosis, targeted delivery and regenerative medicine systems would therefore be ultimately capable of handling multiple tasks and even combine functions like diagnosis and therapy together — leading to a completely new paradigm of human health care. Nanoherbals could be better choice in this context as compared to simple molecular compounds of modern medicine.

Delivery systems combining a much wider range of physical and chemical functional properties of nanomaterials, components and devices together are required to be developed in the near future for general (European Technology Platform on Nanomedicine 2005; Nanomedicine — Nanotechnology for Health 2006). List of such materials are components and devices would involve — liposomes, micelles and micro-emulsions; liquid and nanocrystals; antibodies and biochemical conjugates; natural proteins; polymer and bio-conjugates; biodegradable nanoparticles and nanocapsules; virus like gene delivery system; nucleic acid or mimetic deliveries; vaccine delivery and synthetic biomimetic devices and systems. These entities should preferably be derived from herbal sources as well. Novel developments in these areas should focus on measuring efficacy and safety by conducting *in vitro* and *in vivo* experiments that may include the following aspects related to namely — polymersomes; prodrug therapy; smart and stimuli responsive drugs; *in vivo* imaging; systems localising and imaging agents and self-assembly based systems. Drug metabolism, pharmaco-kinetic and toxicological properties of such comprehensive systems of compounds, materials and devices should be carried out in detail using the methods approved by statutory bodies before they are put to clinical applications.

The process of recognising disease-specific molecules that are located either in the target cell membrane or in specific compartments within the cell is of very critical significance and importance in exercise. Any effort to enhance this function and reduce production costs is always welcome . The identification of such molecules can be carried out by using rational design, high throughput screening and even a combining the two. The important research (European Technology Platform on Nanomedicine 2005; Nanomedicine — Nanotechnology for Health 2006) areas in this context could be related to the development of newer targeting agents; intracellular specific compartment targeting and multiple target approaches.

Proper delivery will be possible only in case there is deeper understanding of the interactions of the involved nanostructures within the human body. This can be facilitated by conducting in-vitro, *ex vivo* and *in vivo* experiments. Very little information is available in public domain on how these nanomedicines are transported and eliminated *in vivo*, and what the serious consequences are such as immunogenicity. Important areas (European Technology Platform on Nanomedicine 2005; Nanomedicine —

Nanotechnology for Health 2006) to be considered would certainly include fundamental studies of interaction of nanostructures with plasma proteins and relation between protein adsorption and removal of nanostructures; cell absorption of nanostructures; nanostructure cell uptake and recycling; nanostructures trans-endocytosis; nanostructures endosomal escapes; nanostructure safety evaluation; *in vivo* carrier biodistribution and degradation and smart and intelligent nanostructures for biomedical applications.

R&D Priorities — Drug/Compound Delivery Development Programme

Nanoparticles have already been used in drug delivery systems with success but nanoparticulate delivery systems especially involving nanoherbals have still greater potentials for many newer applications including anti-tumour, gene, AIDS and radio therapy, protein delivery, antibiotics, virostatics, vaccines and as vesicles to cross over the blood-brain barrier (European Technology Platform on Nanomedicine 2005). Nanoparticles offer advantages regarding targeting, delivery and release and with their additional potential to combine diagnosis and therapy. These techniques are emerging as a major tool in multitasking nanomedicines (European Technology Platform on Nanomedicine 2005). The main hurdles faced are related to improving their stability in the biological environment, influencing the bio-distribution of active compounds, improving drug/compound loading, targeting, transport, release and interaction with existing biological barriers. Nanoparticle cytotoxicity and their degradation products are still not very well known and further improvements in biocompatibility are of major concern in future.

Some efforts were made in converting a number of herbal extracts into nanoforms using water soluble encapsulating shells (Ahmad *et al*. 2008; Islam & Ahmad 2008). When applied to cell lines and animal disease models in rats there was clear evidence of significant dose reduction associated with almost complete cure of the diseases like liver cirrhosis and brain cell damage due to ischemia. Detailed histopathological tests carried out on trial animal organs (Islam & Ahmad 2008) confirmed the changes in concentrations of the involved bio molecules taking place during treatment in the affected organs involved. This observation compares very well with those in case of traditional Chinese medicine tested elsewhere (Kang 2008) for treating liver fibrosis and cirrhosis in rat models following herbogenomic approach.

Keeping in view the existing competence level in R&D in contemporary nanomedicines (Nanomedicine — Nanotechnology for Health 2006; European Technology Platform on Nanomedicine 2005) future developments may involve research activities in areas such as delivery of large and highly localized quantities of drugs/compounds; release profile controls; development of better biocompatible, biodegradable and nontoxic nanomaterials; biomimetic polymers and nanotubes based architecture; molecular self-assembly; search for newer functions like — active targeting, on command delivery, intelligent release / bio-responsive trigger devices, self-regulated smart deliveries; intracellular delivery through virus like structures; development of Improved nanoparticle based implants; MEMS/NEMS based nanoparticle and multi reservoir release systems; nanoparticles based tissue engineering consisting of cytokines delivery for controlling cellular growth, differentiation and stimulate regeneration; biodegradable layered implant coatings and polymeric therapeutic peptide and proteins carriers to name specifically in this context.

Nanoherbal Development Roadmap — A Proposal

R&D activities in the area of molecular medicines and related technologies have been going on for more than hundred years and

with the advent of nanoscience and technology the pace has been accelerated further with better understanding of the related processes involved at atomic and molecular levels. Intelligent and smart nanomaterials synthesis is currently being attempted using organic, inorganic and biological macromolecules and their chemical conjugates, to handle various problems related to the development of nanomedicines as mentioned above (Nanomedicine — Nanotechnology for Health 2006). Having acquired enough expertise and advanced capabilities in this context world wide, in past few decades in the area of nanomedicines and related technologies, it has been possible to foresee the possible growth of R&D and then predict some kind of roadmap on the same lines as it has been described in an elegant document prepared as European Technology Platform, Strategic Research Agenda for Nanomedicines, November 2006 (Nanomedicine — Nanotechnology for Health 2006).

Considering natural medicines derived out of herbal species as a rich source of phytochemicals in abundance, it is quite logical to consider some kind of development plans for nanoherbal medicines as a collection of pharmaceuticals, nutraceuticals and nutricosmetics running almost on the similar lines as it is seen in the case of molecular medicines. Of course, the situation in herbal medicines is far more complex than simple molecular structures involved in modern medicines and therefore the pace of progress in case of nanoherbal medicines is certainly going to take more time to mature for their clinical applications as compared to those of molecular medicines highlighted in the above referred roadmap. But, on the other hand, the rigors of the animal and human trial experiments are expected to be rather simplified as most of the ingredients are generally approved by FDA in form of food supplements. For qualifying as a standard pharmaceutical, nutraceutical and nutricosmetic compound, the related product development must go through the standard route of standardization, quality control and good manufacturing practices. All other advantages of the enabling technologies developed in connection with nanomedicines are expected to be applicable with nanoherbal medicines once applied with proper care. For example, in targeted delivery the carrier itself may be chosen as one of the herbal nanoforms instead of using much simpler nanostructured material with an eye on multitasking already pointed out as the next stage development of targeted deliveries of nanomedicines. Similarly, though far more complex but better understanding of nanostructured material interaction with human body and its organs will certainly enable us the use of nanoherbals to go through their *in vitro* and *in vivo* studies for various clinical trials at a later stage.

TIME LINE OF DEVELOPMENT

Nanoherbal Pharmaceuticals

- 1 – 2 years
  - Design of herbal pharmaceutical nanoparticles - nanoherbals
  - Structural Stabilization - plant derived macromolecules
  - Green Chemistry Synthesis - laboratory scale production - SFE
- 3 – 5 years
  - *In vitro* and *in vivo* barrier crossing abilities experiments
  - Disease model animal experiments
  - Surface functionalization of nanoherbals — targeted delivery applications
- Beyond 5 years
  - Clinical trials involving models of cardiovascular diseases, cancer, musculoskeletal and inflammatory diseases, neurodegenerative diseases, diabetes and infectious diseases

Nanoherbal Nutraceuticals

- 1 – 2 years
  - Design of herbal nutraceutical nanoparticles - nanoherbals
  - Structural Stabilization - plant derived macromolecules
  - Green Chemistry Synthesis - laboratory scale production - SFE
- 3 – 5 years
  - *In vitro* and *in vivo* barrier crossing abilities experiments
  - Disease model animal experiments
  - Surface functionalization of nanoherbal nutraceuticals — targeted delivery applications
- Beyond 5 years
  - Clinical trials for establishing anti-cholesterol, anti-oxidation, anti-inflammation and bone protection processes.

Nanoherbal Nutricosmetics

- 1 – 2 years
  - Design of herbal nutricosmetics nanoparticles — nanoherbals
  - Structural Stabilization of plant derived macromolecules
  - Green Chemistry Synthesis - laboratory scale production - SFE
- 3 – 5 years
  - *In vitro* and *in vivo* barrier crossing abilities experiments
  - Animal model experiments
  - Surface functionalization of nanoherbal nutricosmetics — targeted delivery applications
- Beyond 5 years
  - Clinical trials of properties like anti-aging, anti-wrinkle, anti-inflammatory skin diseases.

Enabling Technologies

- 1 – 2 years
  - Nanoherbal particle synthesis - high pressure homogenization, nano-emulsification, nano-precipitation, SFE, hydrothermal and fluidized bed reactions
  - *In vitro* models - transport through membranes and tissues. Better understanding of interaction of nanoherbals with human body and organs.
  - Study of nanoherbals metabolism and pharmaco-kinetics
  - Better delivery routes — oral, transdermal and pulmonary deliveries.
  - Novel targeting entities involving natural herbal species.
- 3 – 5 years
  - Blood-brain barrier crossing deliveries of nanoherbal species.
  - Manufacturing cost reduction — nanoherbal materials and devices.
  - Immunogenicity prediction model.

CONCLUSION

Nanoherbals in the form of pharmaceuticals, nutraceuticals, food supplements and nutricosmetics have immense potential for their use in human healthcare related systems in future. Development of their targeted deliveries will not only reduce the consumptions of raw materials by several orders of magnitude but even enhance efficacies while reducing the unwanted side effects quite significantly. Using green chemistry-based processes like

SFE and other for preparing nanoherbals will reduce the burden on environmental pollutions arising mainly due to discharge of effluents heavily loaded with a variety of organic and inorganic solvents. Phytochemical compounds derived from plants based nano-carriers, improved targeting molecules and further development of multitasking in targeted delivery; imaging and molecular level detection of molecular markers and other related functions will enhance the scope of their applications with additional advantages of biocompatible processes employed. Handling of chronic diseases as well as life style based ailments will possibly be better managed by combining the strength of molecular medicines with those of nanoherbals integrated in various forms proposed. Biotechnological developments to modify the genetic make up of individual herbs will certainly be used to get the right kind of phytochemical constituents without much dependence on environmental variations. Genetic engineering approach of minimizing the prevalent variations in phytochemicals in a given species will make the process of standardization more under control. The proposed roadmap for carrying out the research studies in coming times may be used as a guideline for planning activities in an interdisciplinary manner by involving expertises from different but related fields. Basic scientific studies supported by engineering and technological aspects of using the outcome of fundamental studies will be put to more effective uses in developing the useful applications possible in different fields. The chances of having significant contributions from the systematic pursuit of R&D carried out in Malaysia involving a variety of herbs from the local rainforests is expected to be much brighter. It is sincerely hoped that commensurate support from the Government extended to the R&D and academic institutions will catalyse the entire effort to pick up momentum in near future. International and National collaboration will be essential and beneficial to fill in the gaps in the comprehensive plan of advanced studies envisaged as very briefly highlighted in the proposed roadmap in this work. Proper networking and sharing of new knowledge acquired by the participating teams of experts working together on a continued basis will be necessary to contribute positively in the important task of improving the situation regarding availability of ensuring affordable human health care on a global level.

ACKNOWLEDGEMENTS

The authors are extremely thankful to Prof Kamrudin Hussin, Vice-Chancellor, University of Malaysia Perlis, for his constant encouragement throughout. Prof Zul Azhar Zahid Jamal, Prof Sazali Yaacob and Dr Rusli Abd. Hamid are acknowledged for their kind support to the authors for conducting this kind of futuristic study in the University.

Date of submission: May 2012
Date of acceptance: June 2012

REFERENCES

Ahmad, S, Samim, M, Islam, F & Jalees, F 2008, 'Development of herbal Nanomedicines in Jamia Hamdard', in *First Intl. Conf. on Nanotechnology, King Abdul Aziz University, Jeddah, KSA, 14–18 June.*

European Technology Platform on Nanomedicine, Nanotechnology for Health 2005, 'Vision paper and basis for a strategic research agenda for nanomedicine', September 2005, <http://www.cordis.lu/nanotechnology/nanomedicine.htm>.

Islam, F & Ahmad, S 2008, unpublished report.

Kang, YJ 2008, 'Herbogenomics: from traditional chinese medicine to novel therapeutics – minireview', *Exp. Biol. Med.,* vol. 233; pp. 1059–1065.

Mufti, J & Macchio, R 2009, 'R&D in the cosmetic age', <http://www.happi.com/>.

Nanomedicine — Nanotechnology for Health 2006, 'European technology platform, strategic research agenda for nanomedicines', <http://cordis.europa.eu/nanotechnology/nanomedicine.htm>.

Somerset Cosmetic Company, LLC, P.O. Box 3372, Renton, WA 98056, <www.makingcosmetics.com>.

CONTRIBUTIONS TO THE JOURNAL

Contributions from academics, policy makers, research personnel and managers in public institutions as well as those in private organizations and industry are welcome. However, it is required that manuscripts submitted to the Journal should not have been published and will not be simultaneously submitted or published elsewhere. Research papers must also be factual and original.

Contributions to the Journal will normally include original research work, papers on science and technology policy, and technical notes and communications. As the Journal is a prime source in information on science and technology for development, contributions that fall within the following areas are particularly welcome:

- Science and technology policy
- Original research work; and
- Technical notes and communications.

MANUSCRIPT PREPARATION

Manuscripts should be prepared in Microsoft Word 6.0 and above. Two copies of the manuscripts on A4-size paper and a soft copy on cd should be provided. The manuscript should not exceed 5000 words and specialist terminology and footnotes should be avoided. Each paper should be provided with an abstract of about 150 words, reporting concisely on the purpose and result of the paper. All papers will be published in English. The names(s) of the authors(s) should only appear on the title page which will be detached from the paper before the referees comments are invited.

Mathematical analysis and statistical data should be placed in appendices whenever possible. Numbered tables, figures and illustrations should have their intended position in the printed text clearly indicated. Photographs in black and white should be printed on glossy paper or scanned into text at the intended position. For illustrations, the original and one copy should be provided, if the illustration is not scanned into the text. Similarly, line drawings should either be provided in soft copy or be in a form suitable for reproduction, in Indian ink, with lettering, etc., completed.

References, or citing, should follow the Harvard author-date system. The in-text reference should contain: the author's or editor's family name (or organization responsible); year of publication; page number if appropriate and where available. The bibliography at the end of the article should be arranged alphabetically. Authors are responsible for checking and accuracy of all references.

The Editor-in-Chief reserves the right to adjust the style to certain standards of uniformity. All articles should be directed to:

Emeritus Prof Md Ikram Mohd Said
Editor-in-Chief
School of Chemical Sciences and Food Technology
Faculty of Science and Technology, Universiti Kebangsaan Malaysia
43600 UKM Bangi, Selangor D.E.
(e-mail:kiamco65@gmail.com; kiam@ukm.my)

Manuscripts are accepted for publication on the understanding that the copyright is assigned to the Journal. The completed copyright transfer form should be submitted together with the manuscript to the Editor. We regret that manuscripts without the copyright transfer from will not be considered for publication.

TRANSFER OF COPYRIGHT AGREEMENT

The author(s) agree that upon acceptance for publication, copyright (including the right to authorise photocopying and reproduction in all media, whether separately or as a part of a journal issue or otherwise) in any manuscript submitted, including its modifications thereafter, is transferred to the *ASEAN Journal on Science and Technology for Development*.

The author(s) agree that the Editors (including its Editorial Advisory Committee and its Board Members) of the *ASEAN Journal on Science and Technology for Development* will have world-wide rights, perpetually, to the manuscript (and the final published article with all its amendments), including the right to distribute the article in whatever form deemed appropriate in the information dissemination process (including the use of internet and WWW). This transfer includes the right to adapt the manuscript/article for use in computer systems and programme, including reproduction in machine readable form and incorporation in retrieval systems.

The author(s) retain the rights to:

i. Any intellectual property rights to any process of procedure described in the manuscript.

ii. Photocopy or make copies of the published article for their own personal use or use by colleagues, including for classroom teaching purposes, provided the copies are not offered for sale and are not distributed in a systematic way outside their employing institution; and

iii. Compile the article into their own collection of printed works.

The author(s) should however, include an indication that the copyright ownership of article rests with the *ASEAN Journal on Science and Technology for Development*, and provide a full citation of the Journal source.

Warranties and Copyright Transfer

The author(s) warrant that the article is the author's original work that has not been published elsewhere. The author(s) warrant that the article contains no material that infringes the rights of other or are of a libelous nature. The author(s) warrant that if excerpts from copyrighted works are included, permission of the relevant copyright owners have been obtained and due acknowledgement given in the article.

If the article is prepared jointly with other author(s), the signing author has informed the co-authors of this copyright transfer and has obtained their permission to sign on their behalf. If copyright is held by the employer, the employer or an authorised representative of the employer must sign. If this assignment is signed by the author, it is taken that the author has the authorisation of the employer and that the terms and conditions of this transfer are with the acceptance of the employer.

Signature of copyright owner(s) : _____
(Please indicate if signing on behalf of all co-authors) YES/NO (Delete as appropriate)

Full name (Please print) : _____

Name and designation if employer representative : _____

Company or institution : _____

Date : _____

PLEASE RETURN AN **ORIGINAL** COPY OF THIS COMPLETED FORM, together with the relevant manuscript to the Editor-in-Chief. We regret that manuscripts without the copyright transfer form will not be considered for publication.

ASEAN JOURNAL ON SCIENCE AND TECHNOLOGY FOR DEVELOPMENT
(*ASEAN J. Sc. Technol. Dev.*)

SUBSCRIPTION FORM

The annual subscription rates for four issues per volume are as follows:

ASEAN countries: USD40.00
Outside ASEAN: USD120.00

Note that the above rate does not include the air mail charge. The air mail charge will be available individually for each subscriber upon request.

Please use the following form, to be returned together with the bank draft or send separately if you pay through bank:

I wish to subscribe to the ASEAN Journal on Science and Technology for Development.

Name of Subscriber: _____

Name of Contact Person: _____

Telephone No.: _____ Fax No.: _____

E-mail Address: _____

Mailing Address: _____

Cheque/Bank Draft No.: _____ Amount: _____

Signature: _____

Date: _____

All subscription correspondence should be addressed to:

Emeritus Prof Md Ikram Mohd Said
Editor-in-Chief
School of Chemical Sciences and Food Technology
Faculty of Science and Technology, Universiti Kebangsaan Malaysia
43600 UKM Bangi, Selangor D.E.
Tel: +603 8921 5445
Fax: +603 8921 5410

Or
You can send information through e-mail:
(e-mail:kiamco65@gmail.com; kiam@ukm.my)

ADVERTISEMENTS

(a) Scientific conferences/Seminars/Training courses
(b) Books/Publications
(c) Scientific instruments/Company/Industrial products
(d) Technologies for licensing/research collaboration
(e) Vacancies and appointments
(f) General publicity on science and technology matters of interest to the scientific community.

The terms and conditions for advertising are as follows:

(a) All advertisements will be in black and white.
(b) The advertisement will be interspersed within the various pages of the Journal and will be charged at a flat rate of USD1000 per B5-sized page for two (2) issues or USD1800 for four (4) issues on a running basis.
(c) Acceptance of advertisements will be on a first-come-first-served basis.
(d) All advertisers will receive two (2) copies of each issue of the Journal free of charge for the duration of the advertisement.
(e) Requests for advertisements should be accompanied with the following information:
    - Name of Advertiser
    - Contact Person
    - Tel. No., Fax No. and e-mail of contact person
    - Mailing address
    - Bank draft/cheque number of relevant amount made payable to the ASEAN Journal on Science and Technology for Development.

The Advertiser shall provide the copy in print ready form, in electronic copy using a common publishing software, together with a hard copy sample of the expected final print form. Advertisements will be published on an "as-is" basis using the material submitted by the Advertiser. No proofs will be given.

The Editor reserves the right to accept or reject requests for advertisements to ensure that the scholarly intent of the Journal is upkept.

All advertising and business correspondences should be addressed to:

Emeritus Prof Md Ikram Mohd Said
Editor-in-Chief
School of Chemical Sciences and Food Technology
Faculty of Science and Technology, Universiti Kebangsaan Malaysia
43600 UKM Bangi, Selangor D.E.
Tel: +603 8921 5445
Fax: +603 8921 5410
(e-mail:kiamco65@gmail.com; kiam@ukm.my)

ASEAN JOURNAL ON SCIENCE & TECHNOLOGY FOR DEVELOPMENT

Contents

ASEAN J. Sc. Technol. Dev.
Volume 29(1), 2012